Potentiating the oncolytic efficacy of poxviruses

By

Monica Komar

A thesis submitted in partial fulfillment of the
requirements for the degree of Master of Science
specialization in Biochemistry

University of Ottawa

Faculty of Medicine

May 25, 2012

Supervisor: Dr. John Bell

Abstract

Several wild-type poxviruses have emerged as potential oncolytic viruses (OVs), including orf virus (OrfV), and vaccinia virus (VV). Oncolytic VVs have been modified to include attenuating mutations that enhance their tumour selective nature, but these mutations also reduce overall viral fitness in cancer cells. Previous studies have shown that a VV (Western Reserve) with its E3L gene replaced with the E3L homologue from, OrfV (designated VV-E3L^{OrfV}), maintained its ability to infect cells *in vitro*, but was attenuated compared to its parental VV *in vivo*. Our goal was to determine the safety and oncolytic potential VV-E3L^{OrfV}, compared to wild type VV and other attenuated recombinants. VV-E3L^{OrfV}, was unable to replicate to the same titers and was sensitive to IFN compared to its parental virus and other attenuated VVs in normal human fibroblast cells. The virus was also less pathogenic when administered *in vivo*. Viral replication, spread and cell killing, as measures of oncolytic potential *in vitro*, along with *in vivo* efficacy, were also observed..

The *Parapoxvirus,* OrfV has been shown to have a unique immune-stimulation profile, inducing a number of pro-inflammatory cytokines, as well as potently recruiting and activating a number of immune cells. Despite this unique profile, OrfV is limited in its ability to replicate and spread in human cancer cells. Various strategies were employed to enhance the oncolytic efficacy of wild-type OrfV. A transient transfection/infection screen was created to determine if any of the VV host-range genes (C7L, K1L, E3L or K3L) would augment OrfV oncolysis. Combination therapy, including the use of microtubule targeting agents, Viral Sensitizer (VSe) compounds and the addition of soluble VV B18R gene product were employed to see if they also enhance OrfV efficacy. Unfortunately, none of the strategies mentioned were able to enhance OrfV.

Acknowledgements

I would like to thank Dr. Bell and the entire Bell lab for all their technical and moral support both in the lab and outside of the lab. I especially want to thank Julia Rintoul, Chantal Lemay, Dr. Carolina Ilkow and Dr. Fabrice Le Boeuf for helping me design experiments and troubleshoot when things went wrong, as well as being sounding boards for all my ideas. I would also like to recognize my TAC committee members Drs. Jonathan Angel and Robin Parks.

I would like to thank my mother, Elizabeth, for always being there for me and supporting and encouraging me through all my life decisions, academic and personal.

I would like to thank my friends for encouraging me and cheering me on, all along this journey.

Table of Contents

List of Abbreviations

2’5’ OAS	2’5’ oligoadenylate synthetase
CMC	carboxymethylcellulose
CNS	central nervous system
CPE	cytopathic effect
CEV	cellular enveloped virus
DMEM	Dulbecco’s modified eagles medium
EC50	half maximal effective concentration
EEV	extracellular enveloped virus
EGFR	epidermal growth factor receptor
eIF2α	eukaryotic initiation factor 2
FADD	fas-associated death domain
FCS	fetal calf serum
FDA	Food and Drug Administration (U.S.A)
fLuc	firefly luciferase
GFP	green fluorescent protein
GM-CSF	granulocyte-macrophage colony-stimulating factor
HDFn	human neonatal dermal fibroblasts
hIFNβ	human interferon-β
HBV	Hepatitis B virus
HCV	Hepatitis C virus
HPV	Human Papilloma virus
HSV	Herpes Simplex virus
IC	intracranial
IN	intranasal
IT	intratumoral
IV	intravenous
IEV	intracellular enveloped virus
IFN	interferon
IκB	inhibitor of NF-κB
IKK	IκB kinase
IMV	intracellular mature virus
IL	Interleukin
JNK pathway	c-Jun amino-terminal kinase
MOI	multiplicity of infection
MTD	maximum tolerated dose
NSCLC	non-small cell lung cancer
OrfV	Orf virus
OV	oncolytic virus
PBS	phosphate buffered saline
pfu	plaque forming units
PKR	dsRNA-dependent protein kinase
PP2A	phosphoprotein phosphatase 2A
PUMA	p53 upregulated modifier of apoptosis
SAHA	suberoylanilide hydroxamic acid

SFM	serum free media
SIM	SUMO-interacting motif
SQ	subcutaneous
SUMO	small ubiquitin-modifier
sup	supernatant
TK	thymidine kinase
TSA	trichostatin A
TTP	thymidine triphosphate
YFP	yellow fluorescent protein
VGF	vaccinia growth factor
VIG	vaccinia immune globulin
VSe	virus sensitizer
VSV	vesicular stomatitis virus
VV	vaccinia virus
VV-COP	vaccinia virus Copenhagen strain
VVdd	vaccinia virus double deleted
WR	Western Reserve
WT	wild-type

List of Figures

List of Tables

Chapter 1 – Introduction

1.1 Cancer

Cancer is one of the leading causes of death among Canadians. It is estimated that in 2012, an average of 500 individuals will be diagnosed with cancer and 200 will die of the disease, every day (21). Numerous risk factors are associated with cancer development, including age, lifestyle (e.g. smoking and alcohol use), chronic infection (e.g. Human Papilloma virus (HPV), Hepatitis B virus (HBV) and Hepatitis C virus (HCV)) and exposure to carcinogens (natural, chemical or radiation). Additionally, certain genetic factors can predispose an individual to the development of cancer, including mutations in BRCA1 and BRCA2 genes, for breast and ovarian cancer (73). After exposure to any of the risk factors mentioned above, carcinogenesis can take decades. The development of malignant cells from normal cells occurs through complex, multi-step processes involving the initiation of transformation of normal cells due to genetic and/or epigenetic mutations, promotion of these initial cancer cells that have acquired a growth advantage and finally progression from a benign tumor to a neoplasm to malignancy (89). Hanahan and Weinberg outlined six accepted hallmarks of cancer cells, which include: self-sustaining proliferative signals, inhibition of growth suppressor signals, uncontrollable proliferation, evasion of apoptosis, angiogenesis and the ability to metastasize (43). While there has been progress in efficacious treatments of cancer, no method is 100% effective. The appearance of drug resistance after systemic therapy—chemotherapy, radiation and/or in combination with a targeted inhibitor—is expected and is a frequent hurdle in treatment. Drug resistance is currently the most common factor in tumor reoccurrence and a contributor to cancer mortality (3), requiring more potent and efficacious treatments.

1.2 Oncolytic viruses

Oncolytic viruses (OV) by definition selectively target and kill cancer cells while leaving normal cells unharmed (85, 110). The knowledge that certain viruses are able to kill cancer cells has existed since the mid 19th century, but only in the last two decades has this technology advanced sufficiently for therapeutic application (85, 89, 110). Since this time, a number of viruses have shown oncolytic potential in preclinical and clinical studies (see ref (89) for a detailed list of all current OV candidates). These viruses—either naturally-occurring or genetically-engineered—preferentially undergo their lytic cycle within cancer cells due to inherent factors, including deficient interferon responses, genetic mutations and/or aberrant signaling pathways (89, 110). OV therapy has multiple advantages over current cancer treatments. These include the ability to attenuate or genetically modify these viruses to selectively target cancer cells, insert various transgenes, such as suicide genes (1, 32), immune-stimulatory genes (e.g. granulocyte-macrophage colony-stimulating factor (GM-CSF)) (19, 23, 109) or enzymes to sensitize infected cancer cells to conventional therapies (9, 10). Additionally, for certain OV candidates, such as VV, they can be administered systemically enabling both primary tumor sites and distant metastases to be targeted (12). Lastly, these viruses are self-replicating which means once at the tumor site, they are able to self-amplify. Unfortunately, there are still barriers to OV treatment. Systemic delivery exposes the virus to the risk of recognition by the host innate immune system. Once recognized, the virus is marked as a foreign pathogen and an immune response is mounted to clear it, potentially prior to the virus reaching the tumor site, as well as decreasing the efficacy of any future doses.

1.3 Vesicular stomatitis virus

Vesicular stomatitis virus (VSV) is a negative-stranded RNA virus and member of the *Rhabdoviridae* family (5, 105). VSV replicates solely within the cytoplasm of infected cells. As WT VSV is neurotoxic in certain mouse strains, a deletion in its matrix (M) protein gene (known as VSVΔM51) was created to attenuate the virus (105). The attenuation restricts the viral replication to cells which have a defective interferon response, specifically cancer cells (67, 105), as the M protein is a virulence factor that is capable of dampening or blocking the expression of host IFN gene expression (5, 105). Recent studies have shown that by altering tumor cell IFN gene expression, one can increase the efficacy of oncolytic VSV (61, 81).

1.4 Vaccinia virus

Vaccinia virus (VV) is a large, linear double-stranded DNA virus from the *Orthopoxvirus* genus in the *Poxvirdae* family. It contains 200 genes which are encoded along its approximate 200 kilobase (kB) pair genome (35). Due to the large size of the VV genome, an additional 50 kB of DNA can be inserted, providing the opportunity to insert a number of therapeutic or imaging genes (60, 77, 78). Additionally, VV was used as a live vaccine during the eradication of smallpox campaign (31) and its safety profile in humans is well established.

Like all poxviruses, VV is capable of infecting many vertebrate animal species, as it has a wide host-range (71) and replicates solely in the cytoplasm of infected cells. Two distinct forms of infectious particles—the intracellular mature virus (IMV) and the extracellular enveloped virus (EEV)—are able to initiate infection (66, 111). These particles are able to ubiquitously enter cells (47) and, in permissive cells, viral replication is

characterized by three waves (early, intermediate and late) of viral mRNA and protein synthesis, followed by morphogenesis of viral particles (71, 76). During the early wave many intracellular modulators, including genes important for apoptosis inhibition, antiviral state blockade, signaling modulators and host-range genes are expressed (71). Their expression is required to allow VV to go through the later stages of replication. Through the morphogenesis stage, IMV particles are transported via microtubules and wrapped with Golgi-derived membrane to become intracellular enveloped virus (IEV) (63). The IEV particles can then fuse to the cell surface membrane to form cell-associated enveloped virus (CEV) which is then released away from the cell by actin-tail polymerization (101, 102) or the IEV particles can be released to form free EEV (103). Upon cell lysis, IMV particles are also released (71). EEV particles have few exposed viral proteins allowing these particles, to not be recognized by the host innate immune system and therefore allow for long-range dissemination (103).

VV has been explored as a vaccine and OV candidate due to its many ideal features. Oncolytic VV has shown promise in preclinical tumor models (13, 84) and in clinical trials (14, 54). The current clinical candidate JX-594 has undergone a number of Phase I and II clinical trials, showing its safety and efficacy in treating both melanoma and advanced liver cancers (12, 48, 64, 86). Importantly, it was recently published that IV administered virus was able to reach and infect the primary tumor site (12). These data indicated that VV is a promising clinical candidate, but as some cancers are still resistant to VV infection, novel VV recombinants are required.

Chapter 2 – Materials and Methods

2.1 Cell culture

The cell lines: U2OS, HeLa, 786O, ACHN, HT29, SW620, HCT116, HCT15, MCF7, T47D, MDA-MB-435, UACC-257, SKRB3, NCI-H226, NCI-H23, HOP-92, A549, OVCAR8, SNB75, OA3.Ts, MRC5, 4T1, MC38, wild-type (WT) CT26, CT26LacZ (CT26.CL25) and BHK21 were purchased from ATCC (Manassas, Virginia). GM38 and HDFn were purchased from the National Institute of General Medical Sciences Mutant Cell Repository (Camden, New Jersey) and Cascade Biologics (Burlington, Ontario), respectively. B16F10LacZ cells were obtained from Dr. Ann Chambers (LRCP, London, Ontario) (55). Cell lines used in the glioma panel (DBT IRE, BT4C, CNS1, AST11.9.2, CT2A, G26, SF767, U87, U118 and U251) were obtained from Dr. Markus Vähä-Koskela (OHRI, Ottawa, Ontario).

Most cell lines, with the exception of the HOP-92, A549 and CNS1 cells which were grown in RPMI (HyClone, Logan, Utah), were maintained in Dulbecco's modified Eagle's medium (DMEM; HyClone) supplemented with 10% fetal calf serum (FCS, complete media; PAA Laboratories, Etobicoke, Ontario).

2.2 Viruses

WT OrfV strain NZ2 was obtained from Dr. Andrew Mercer (University of Otago, Dunedin, New Zealand). Viral stocks were prepared by the infection of confluent OA3.Ts at a multiplicity of infection (MOI) of 0.05. Cells and supernatants were harvested following a 5-7 day infection at 37°C, 5% CO_2 by gentle cell scraping, as described previously (95). Briefly, cell lysates were collected by centrifugation, and resuspended in 1 mM TRIS pH 9.0 and subjected to three freeze–thaw cycles. Cell debris was removed by centrifugation and

lysates dounce homogenized before sucrose cushion purification in a JS-13.1 rotor at 11,500 rpm for 1.5 hours at 4°C. Virus stocks were resuspended in PBS. Stock titers were determined by titration (see 2.3).

VV-E3L^{OrfV} was obtained from Dr. Bertram Jacobs (Arizona State University, Tempe, Arizona). Western Reserve (WR) strain was purchased from ATCC. VVdd-mCherry (VVdd), WR2loxpyfp (WRΔTK) and WRflucΔVGF (WRΔVGF) were previously generated in our lab. All viral stocks were prepared by the infection of 85-95% confluent HeLa rollerbottles at MOI 0.01. Cells were harvested following a 72 hour infection at 37°C. Cell lysates were collected by centrifugation, and resuspended in 1 mM TRIS pH 9.0, and subjected to three freeze–thaw cycles. Cell debris was removed by centrifugation, followed by sucrose cushion purification as described above.

Additionally, VSVΔM51-eGFP and WT VV Copenhagen (VV-COP) strain were used as positive controls in the B18R study and confirmation of C7L^{VV} and E3L^{VV} protein expression study, respectively.

2.3 Titration of viral stocks and samples

OrfV and VV stocks and samples were titered on OA3.Ts and U2OS cells, respectively. Samples (cells and supernatants) underwent three freeze-thaw cycles prior to titering. For both viral stocks and samples 10-fold or half-log serial dilutions were performed and 150 µL of each dilution were put on confluent cells for 1 hour at 37°C, 5% CO_2. After the incubation, the inoculum was removed and an overlay solution (1:1 ratio of 3% CMC:2X DMEM+20%FCS) was added. Plaques were visualized after 72 hour or 7 day incubation at at 37°C, 5% CO_2 for VV or OrfV, respectively, by removal of overlay and staining with 0.1% crystal violent, in 80% methanol.

2.4 Cloning

Vaccinia virus host-range genes C7L, K1L, E3L and K3L cDNA (Appendix I) were PCR amplified from purified virus stocks using primer sets listed (Table 1). The gene cDNAs were then subcloned into the pT7blue.3 expression vector (Novagen, Mississauga, Ontario) and transformed into Nova Blue competent cells (Novagen). Clones were amplified and DNA was extracted to allow for sequencing of clones, to confirm proper orientation using SeqMan (DNASTAR, Madison, Wisconsin). pT7blue.3 clones which sequenced successfully were digested out of the subcloning vector and DNA isolated by gel extraction. The fragments were then cloned into either pcDNA3.1(-) (Invitrogen, Burlington, Ontario) or pV41 (generously provided by Dr. Andrew Mercer) vectors and transformed into Nova Blue competent cells, amplified and DNA extracted.

Table 1. Primer list for VV host-range cDNA amplification.

Gene	VV strain cDNA	Forward Primer	Reverse Primer
$C7L^{VV}$	COP	GGAGATCTCATGACAATTTCCGAAGATGG	CCTCTAGATTACTATTAACGCCGTCGGTATT
$E3L^{VV}$	WR	CCTCTAGAGAAACGACGAACCACCAGAG	GGCCAGATCTTCAGAATCTAATGATGAC
$K1L^{VV}$	COP	GGTCTAGAATGTTAACAAAAATGTGGGAG	ACTCGAGTATACACTAATTAGCGTCTCG
$K3L^{VV}$	WR	GGCCAGATCTTTATTGATGTCTACACATCC	GGCCTCTAGAATGCTTGCATTTTGTTATTC

2.5 Western blotting

To confirm $C7L^{VV}$ and $E3L^{VV}$ expression in pcDNA constructs, subconfluent monolayers of HeLa cells in 60 mm dishes were transfected using 15 µL/sample Lipofectamine2000 (Invitrogen) plus 8 µg DNA (pe-yfp-c1, pcDNA-$C7L^{VV}$ or pcDNA-$E3L^{VV}$) for 3 hours at 37°C, 5% CO_2. Transfection inoculum was then removed and complete medium (DMEM+10% FCS) was added. Additionally, HeLa cells were infected with VV Copenhagen (VV-COP) strain at MOI 0.5 as a positive control. Proteins were harvested at 6 and 12 hours post transfection or infection using 1% NP40 (50 mM Tris-Cl pH 7.5, 150 mM NaCl, 1% NP40, 1 mM EDTA) lysis buffer containing protease inhibitor

(Roche Diagnostics). After collection and centrifugation at 10,000xg for 10 minutes at 4°C, cleared supernatant was collected and protein concentration was quantified by BCA protein assay (Pierce Biotechnology, Ottawa, Ontario). Protein (40 μg) was separated by SDS-PAGE and transfered onto PVDF membrane. The membrane was blocked with 5% milk in TBST for 1 hour at room temperature and then probed with either mouse monoclonal antibodies anti-C7L (1:3; generously provided by Dr. Gerd Sutter, Paul-Ehrich-Institute, Langen, Germany) or anti-E3L (1:500; generously provided by Dr. Stuart Isaacs, Penn State University, State College, Pennsylvania) overnight (16 hours) at 4°C or anti-β-tubulin (1:3,000; Abcam) for 1 hour at room temperature in 5% milk. Proteins were detected by incubation with anti-mouse (against C7L and E3L antibodies) or anti-goat (against β-tubulin antibody) horseradish peroxidase-conjugated secondary antibodies diluted 1:3,000 for 1 hour at room temperature followed by brief incubation with chemiluminescent reagent (Pierce Biotechnology) and exposure on film.

To confirm $C7L^{VV}$ in pV41-$C7L^{VV}$ a transient transfection (pV41-$C7L^{VV}$)/infection (with OrfV at MOI 1) was performed and proteins extracted for western blotting as described above with the difference that, prior to blocking with milk, PVDF membranes were exposed to Amido Black (Sigma, Oakville, Ontario) to confirm equal loading of samples.

2.6 Rescuing OrfV recombinant viruses

pV41-$C7L^{VV}$ vector was linearized with XhoI (Invitrogen). 293T cells were infected at an MOI of 5, 0.5, 1 and 0.1 with OrfV and subsequently transfected with either 1.6 μg or 3 μg linearlized pV41-$C7L^{VV}$ vector using Lipofectamine 2000. Orf-$C7L^{VV}$ was selected for by using the X-Gluc (β-glucuronidase) GUS reporter system (Cedarlane, Burlington,

Ontario) and was plaque purified on OA3.Ts cells. The recombinant plaques were filtered through a 0.22 μM pore to eliminate any wild type-recombinant aggregates. DNA from round 5 plaques was isolated using a DNeasy Kit (Qiagen, Mississauga, Ontario). Standard PCR protocol using $C7L^{VV}$ primers listed in Table 1 was performed.

2.7 *In vitro* assays

2.7.1 Microscopy

Phase-contrast and fluorescence microscopy was performed using a Zeiss Axiovert S 100 microscope. All images are shown at 10X magnification.

2.7.2 Growth curves

Single-step growth curves were conducted to assess virus replication in human and murine tumor cells. Confluent monolayers of cells were infected at MOI 3 in a minimal volume for 1 hour at 37°C and 5% CO_2. Viral inoculum was then removed, and replaced with complete media. Cells and supernatants were harvested at 0, 4, 8, 12, 24 and 48 hours post infection. Samples were titered as described in 2.3.

Multi-step growth curves were conducted to assess virus replication and spread in human and murine tumor cells. Confluent monolayers of cells were infected at MOI 0.3 or MOI 0.1 for OrfV or indicated VV's, respectively, in a minimal volume for 1 hour at 37°C and 5% CO_2. Cells and supernatants were harvested at 12, 24, 36, 48, 72 and 96 hours post infection. Samples were titered as described in 2.3.

2.7.3 Cytotoxicity assays

Confluent monolayers of cells in 96-well dishes were directly infected with viruses at indicated MOIs. 72 hours post infection cytotoxicity was assessed using a 1 in 5 dilution of

alamarBlue (AbD Serotec, Raleigh, North Carolina) to complete media. After incubation at 37°C and 5% CO_2 for 1-2 hours, plates were read using a spectrophotometer at excitation 530 nm, emission 590 nm.

2.7.4 Drug Screen

Cells were plated in 96-well dishes in complete media in the presence of 30mM HEPES pH 7.4 buffer. Confluent monolayers of cells were pretreated with 2-fold dilutions of drugs directly into the media (see Table 2 for drug concentrations used). Following a 4 hour incubation at 37°C and 5% CO_2 , cells were either mock infected or infected at MOI 0.1 or 0.01 for OrfV or VV-E3L^{OrfV}, respectively. Cells were then incubated for 72 hours at 37°C and 5% CO_2, at which point cytotoxicity was assessed as described in 2.7.3. Data were normalized to each conditions, with respect to controls.

To assess if VSe1 enhanced viral yields of VV-E3L^{OrfV}, HeLa cells were plated in 6-well dishes. The next day, cells were either pretreated with VSe1 at 19.5 μM or mock treated for 4 hours at 37°C and 5% CO_2 and then infected with VV-E3L^{OrfV} at MOI 0.01 directly into the media. Cell lysates and supernatants were harvested separately, to mirror the process of virus stock production, subjected to 3 freeze-thaw cycles and then titered.

Table 2. Drug compounds and concentrations used in the drug screen.

Drug	Lowest concentration (μM)	Highest concentration (μM)
VSe1	3.75	30
VSe6	0.078125	5
VSe7	0.46825	30
VSe11	0.15625	10
TSA	0.05	0.4
Colchicine	0.00625	0.4
Paclitaxel	0.00625	0.4

2.7.5 Safety assays

Human normal fibroblast GM38 and MRC5 cells were plated at $1.3x10^5$ cells/well in 24-well dishes. Once attached to the tissue culture plastic, cells were pretreated with 0, 50 or 500 IU/mL of human IFN-α (Intron A from Schering, Kenilworth, New Jersey) or 0, 100, or 1000 IU/mL or human IFN-β (Betaseron from Bayer, Montville, New Jersey) overnight (16 hours) and then mock infected or infected with either WR or VV-E3L^{OrfV} at MOI 0.001 directly into the media. Phase-contrast images were collected at 24, 48 and 72 hours post infection and samples were harvested at 72 hours post infection for titering.

Human normal HDFn cells were plated at $1x10^4$ cells/well in 96-well dishes with complete media in the presence of 30mM HEPES pH 7.4 buffer. The next day, cells were either mock infected or infected with indicated VV's at MOI 0.001, 0.01 and 0.1 directly into the media. 72 hours post-infection cytotoxicity was assessed as described above and plates frozen for titering.

2.7.6 B18R studies

Confluent U2OS cells in 6-well dishes were infected with VVdd-mCherry at MOI 0.1 or mock infected in a minimal volume for 1 hour at 37°C, 5% CO_2. Complete media was then added to the cells and infection was allowed to persist for 24 hours at 37°C, 5% CO_2. Fluorescence microscopy was then performed to confirm productive VVdd-mCherry infection. Supernatants from mock and VVdd-mCherry infected cells were harvested and filtered through 0.22 μM filter directly into naïve 786O, CT26 or HT29 cells. Cells were incubated for 2 hours 37°C, 5% CO_2 and then infected with OrfV at MOI 0.1 directly. As a positive control, 786-O cells were infected with VSVΔM51-eGFP at MOI 0.1 in the

presence or absence of VVdd-mCherry supernatant. 48 hours post infection phase-contrast microscopy was performed to visualize any enhancement of virus infection.

2.7.7 Spreading assay

Confluent monolayers of cells were covered with an agarose overlay (1% agarose in dH_20:2X DMEM+20% FCS). Once agarose overlay had solidified holes were created in the center of each well using a Pasteur pipette. 5000 plaque forming units (pfu) of virus or PBS was added to the holes. Cells were incubated for 72 hours at 37°C, 5% CO_2. To visualize cell death induced by viral spread, cells were fixed using 3:1 ratio of methanol to acetic acid, followed by Coomassie blue staining. Plates were scanned using Epson Perfection 4990 photo scanner and relative area was quantified using image analysis software ImageJ (NIH).

2.7.8 Transient transfection/infection pcDNA screen

Subconfluent monolayers of HeLa cells were transfected using 1 μL/sample Lipofectamine2000 (Invitrogen) plus or minus 1.6 μg DNA (pe-yfp-c1, pcDNA-C7L^{VV}, pcDNA-E3L^{VV}, pcDNA-K1L^{VV} or pcDNA-K3L^{VV}) or mock transfected for 2.5 hours at 37°C, 5% CO_2. Transfection inoculum was then removed and complete media was added. 24 hours post transfection, efficiency was confirmed by detection of GFP positive cells in the pe-yfp-c1 transfected cells. Cells were then either mock infected or infected with OrfV at MOI 0.1 directly into media. Viability was quantified 48 hours post infection by trypan blue exclusion using the ViCell XR cell viability analyzer (Beckman Coulter).

2.8 *In vivo* studies

2.8.1 Animals

Female 6-8 week old Balb/c, C57Bl/6 or CD-1 nude mice were supplied by Charles River Canada (St Constant, Quebec) and housed in a level 2 biocontainment facility at the Animal Care and Veterinary Services within the University of Ottawa.

2.8.2 Intranasal maximum tolerated dose

To determine maximum tolerated dose (MTD) C57Bl/6 mice were given escalating doses of WR ($5x10^3$ to $5x10^5$ pfu/dose) or VV-E3L^{OrfV} ($5x10^4$ to $5x10^6$ pfu/dose) through an 10 μL intranasal injection once placed under isoflurane anaesthetic. Mice were followed for signs of illness for 16 days, examining physical changes such as weight loss, general appearance, lesion formation, and respiratory distress.

2.8.3 WT CT26 SQ tumor model

Balb/c mice received $3x10^5$ WT CT26 cells in 100 μL PBS subcutaneously (SQ) in the right flank. On days 15 and 18 after tumor implantation, mice received either 50 μL PBS or $1x10^7$ pfu of VV-E3L^{OrfV} or VVdd intratumorally (IT). Tumor size was measured using digital calipers and tumor volume ($(L \times W^2)/2$, where L = tumor length and W = tumor width) was calculated. Once mice reached endpoint (tumor volume ≥1500 mm^3), animals were euthanized and tumors resected, homogenized and VV viral titers were determined.

2.8.4 B16F10LacZ lung model

C57Bl/6 mice received $3x10^5$ B16F10LacZ cells in 100 μL PBS intravenously (IV) through tail vein injection. On day 5 post tumor implantation, mice received one dose of either 100 μL PBS or $5x10^6$ pfu VV-E3L^{OrfV} or WR IV. Mice were monitored daily for signs

of distress or changes in weight. Mice were sacrificed on day 14 and lungs were harvested and stained with β-galactosidase solution, as previously described (55, 104). Total number of lung metastases was determined by separation of the lobes and counting of surface metastases under a dissection microscope (Leica, Richmond Hill, Ontario).

2.8.5 HT-29 xenograft model

CD-1 nude mice received $1x10^6$ HT29 cells in 100 µL SQ in the right flank. On days 9, 11, 14 and 16 mice received either 50 µL PBS or $1x10^7$ pfu of VV-E3L^{OrfV} or VVdd IT. Tumor size was measured using digital calipers and tumor volume was calculated. Once mice reached endpoint, either due to tumor size or when in distress, animals were euthanized. Tumors and organs were harvested from the VV-E3L^{OrfV} treated mice for titering.

2.9 Statistical analyses

All statistical analyses were performed using Graphpad Prism 4.0 (GraphPad Software, La Jolla, California). Data are presented as Mean ± SEM, unless otherwise indicated. For EC50 curves, cytotoxicity data were analyzed using a non-linear regression equation: Y=Bottom + (Top-Bottom)/1+10^((LogEC50-X)*HillSlope)), with HillSlope shared between a data set (all viruses/cell line). In the B16F10LacZ lung model, a two-way ANOVA with Bonferroni multiple comparisons test was used to compare group weights. A log-rank test was performed for Kaplan Meier survival curves. All other analyses were performed using an unpaired, two-tail t-test with Welch's correction.

Chapter 3 – Characterizing VV-E3L^{OrfV}, a novel oncolytic virus candidate

3.1 Introduction

3.1.1 E3L^{VV} function

E3L is an early host-range VV gene that plays a role in innate immune evasion (22, 58). E3L sequesters dsRNA, inhibiting activation of PKR and the 2'5'OAS signaling pathways, thus inhibiting the blockade of translation in infected cells and enabling viral replication (Figure 1) (22, 26, 58, 65, 97, 99). Signaling pathways involving PKR are described in Figure 2. At late times post VV infection, the E3L^{VV} product is thought to bind and mask virtually all the dsRNA synthesized by the virus (58). E3L has been shown to antagonize both PKR-dependent and PKR-independent pathways to regulate cytokine expression, suppressing the host innate immune response (59, 79). Furthermore, E3L is known to impair phosphorylation and activation of IFN regulatory factor 3 (IRF-3), an important antiviral innate immune response element (118).

E3L encodes a 190 amino-acid protein with two domains that play a role in immune evasion. The C-terminal domain contains a consensus dsRNA-binding domain which is necessary and sufficient for IFN resistance and wide host-range *in vitro* (57, 113). Its N-terminal contains a Z-DNA binding domain which is not required for IFN resistance, but is required for VV virulence *in vivo* (11, 57, 113). Through the Z-DNA binding domain, E3L has been shown to modulate cellular genes at the transcriptional level and inhibit apoptosis (56). Additionally, this domain was recently shown to inhibit the IFN response specifically through the actions of PKR *in vivo* (115).

Figure 1. VV E3L inhibition of IFN antiviral pathways. E3L sequesters dsRNA, inhibiting activation of PKR and the 2'5'OAS signaling pathways, thus inhibiting the block of translation and degradation of cellular and viral RNAs, respectively, in infected cells. K3L encodes a homolog of the eIF2α subunit, antagonizing PKR's function to phosphorylate eIF2α. Additionally, VV encodes soluble IFN receptors B8R and B18R which prevent IFN from binding its cellular receptor. Taken from (51), license number 2954830850440.

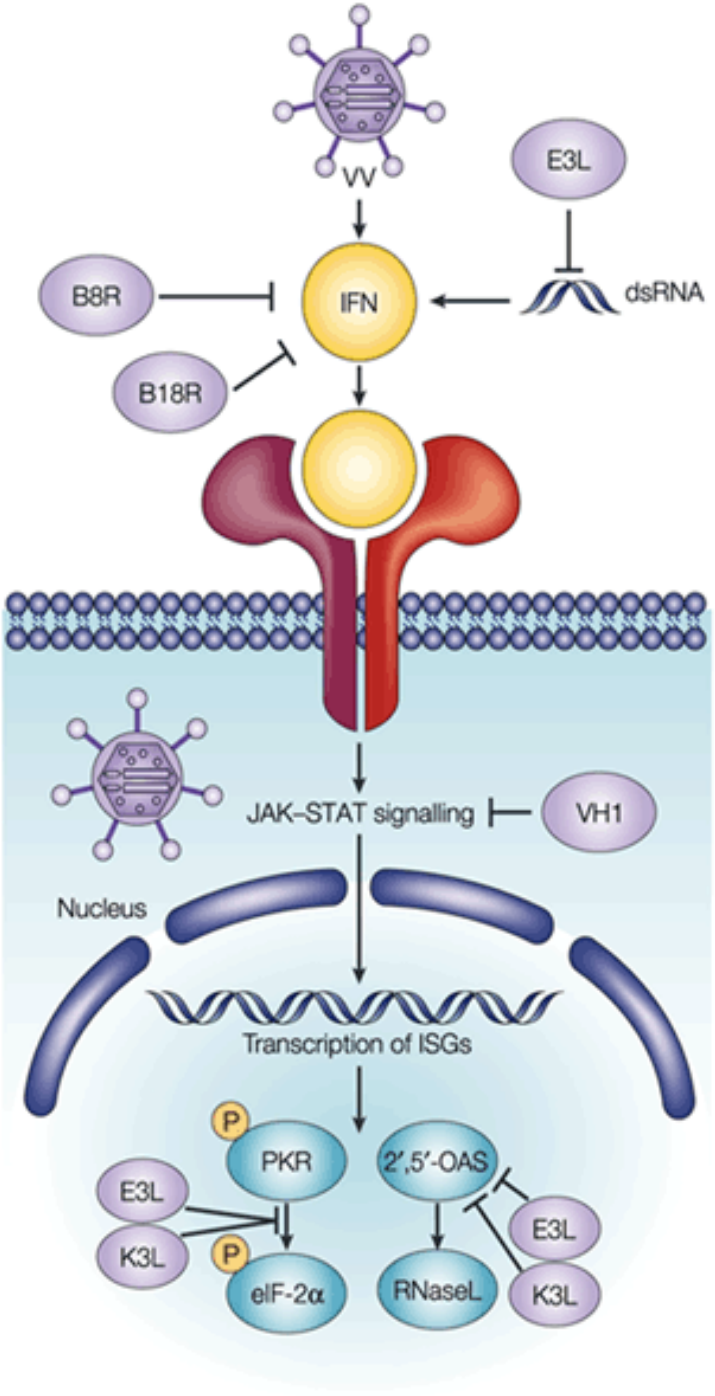

Nature Reviews | Immunology

Figure 2. PKR-dependent signaling pathways. The presence of dsRNA during DNA virus replication occurs as a product of overlapping transcription from their compact genomes. The dsRNA activated PKR, causing a dimerization, autophosphorylation and activation of its kinase activity. PKR can then phosphorylate several substrates including more PKR monomers, eIF2α and the regulatory subunit of protein phosphatase 2A (PP2A). Phosphorylation of eIF2α inhibits most translational initiation, but some messenger RNAs are selectively transcribed. Additionally, autophagy can be initiated through unknown mechanisms. PKR activation can also activate FAS-associated death domain (FADD) initiating the apoptosis, NF-κB, p38 and c-Jun amino-terminal kinase (JNK) pathways causing transcriptional effects through mechanisms which do not require eIF2α phosphorylation. IκB, inhibitor of NF-κB; IKK, IκB inhibitor. Taken from (53), license number 2954831062147.

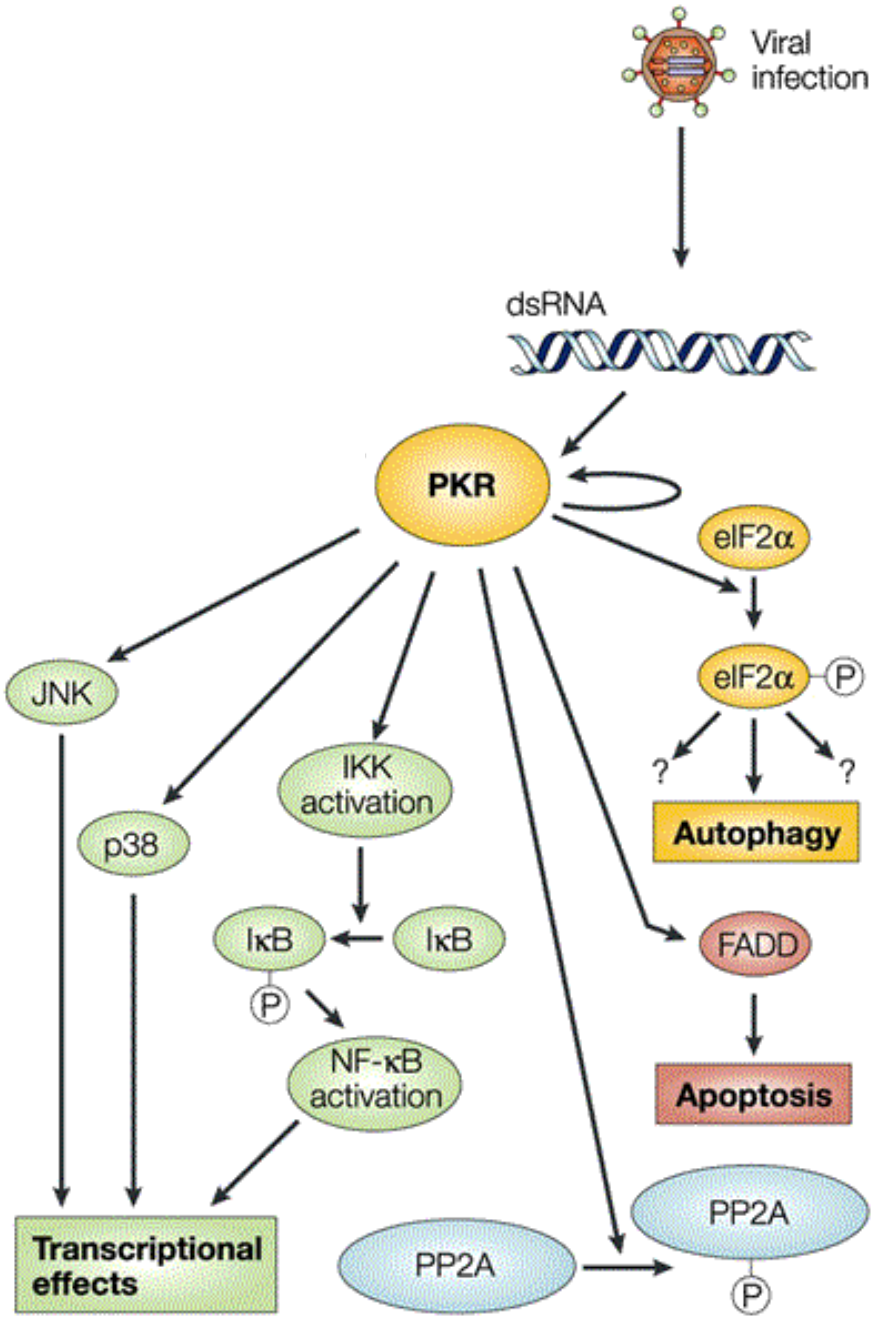
Viral infection
dsRNA
PKR
eIF2α
eIF2α
P
JNK
IKK activation
p38
?
?
Autophagy
IκB
IκB
P
FADD
NF-κB activation
Apoptosis
Transcriptional effects
PP2A
PP2A
P
Nature Reviews | Microbiology

Recently, it has been discovered that E3L interacts with small ubiquitin-like modifier protein 1 (SUMO1) through a SUMO-interacting motif (SIM) (36). Gonzalez-Santamaria et al. (2011) showed that the integrity of the SIM motif was important for maintaining the stability of the E3L protein and for covalent conjugation with SUMO1 (36). This modification was shown to have a negative effect on E3L transcriptional transactivation of the p53-upregulated modulator of apoptosis (PUMA) and APAF-1 genes (36). Furthermore, E3L was shown to be ubiquinated, a posttranslational modification that does not destabilize the WT protein (36).

3.1.2 E3L^{OrfV} function

The OrfV homologue (OV20.0L) shares 31% amino acid identity (57% similarity) with E3L^{VV} gene (41, 72, 113). While E3L^{OrfV} function has not been fully elucidated, previous data have shown that it is involved in IFN resistance in ovine cells and was able to inhibit the autophosphorylation of PKR in sheep cells (72). Vijaysri et al. (2003) were able to show that *in vivo* the E3L^{OrfV} homologue is able to complement E3L^{VV} N-terminus, but not the C-terminal (113). Interestingly, E3L^{OrfV} C-terminal dsRNA binding domain shares only 37% amino acid identity to that of E3L^{VV} (113). The authors postulate that an alanine-to-cysteine change at position 175 affects E3L^{OrfV} dsRNA binding affinity, thereby having a negative effect for function (113).

3.1.3 Previous data on VV-E3L^{OrfV}

VV-E3L^{OrfV} is of Western Reserve (WR) backbone. The VV E3L gene is replaced by the *Parapoxvirus* OrfV E3L homologue. Importantly, this virus still contains its thymidine kinase (TK) and vaccinia growth factor (VGF) genes. Vijaysri et al. (2003) showed that just

like parental WR, VV-E3L^{OrfV} was IFN resistant in RK-13 cells in the presence of rabbit IFN-β (113). Additionally, VV-E3L^{OrfV} was 1,000-fold and 100,000-fold safer in C57Bl/6 mice by IN and IC injections, respectively (113). Unfortunately, in SCID mice, VV-E3L^{OrfV} was almost as pathogenic as WR when given through IN injection (112).

3.1.4 WR and its attenuated recombinants

WR strain is a WT mouse neuroadapted VV derivative. Like all other WT poxviruses it has a broad host-range and therefore is thought not to be tumor selective. Interestingly, Thorne et al. (2007) found that WR displayed inherently superior replication in tumor cells relative to normal cells compared to a panel of WT and vaccine strain VVs (109). Genetic engineering of WR has resulted in multiple OV clinical candidates by limiting virus replication to rapidly dividing cells. VV TK is encoded by an early promoter and once translated can quickly increase the pool of nucleotide precursors for DNA replication (69). The deletion of viral TK resulted in preferential replication in dividing cells, as the virus now requires high nucleotide pools of cellular deoxythymidine triphosphate (dTTP) for DNA synthesis (18). Constitutively higher levels of TK, have been reported in tumor cells compared to normal cells (44, 45). The resulting WRΔTK virus showed preference for tumors, but was still found in normal tissues, requiring further improvements to increase tumor selectivity (92). VGF is a secreted protein expressed early after infection, binding to the epidermal growth factor receptor (EGFR) priming adjacent cells for viral infection (17, 70). Deletion of VGF resulted in a virus that was attenuated in resting cells and 1000-fold safer than parental WR after IC injection (16). WRΔVGF was also dependent on an activated EGFR pathway, which is found activated in over 90% of human solid tumors (84). To further increase tumor selectivity, VV TK and VGF genes were deleted from WR virus

creating a double-deleted mutant VV (known as VVdd) (70). It was found that VVdd was significantly less pathogenic than WT and single-deleted viruses *in vivo*, while maintaining the parental virus potent ability to infect tumors (70, 109).

3.1.5 Rationale

Oncolytic VVs have been modified to include attenuating mutations that enhance their tumour selective nature. Although these mutations offer tumour selectivity, they also reduce the overall fitness of the virus, in cancer cells. We aimed to explore a new strategy for generating tumour selective VVs without comprising the fitness of the virus, in cancer cells, by increasing VV IFN sensitivity. VV deleted of its E3L gene is interferon-sensitive, but at an extreme cost to viral fitness. Previous studies have shown that a VV with its E3L gene replaced with the E3L homologue from the parapoxvirus, OrfV (designated VV-E3L^{OrfV}), maintained its ability to infect cells *in vitro*, but was attenuated compared to its parental VV *in vivo* (113).

3.1.6 Hypothesis

VV-E3L^{OrfV} will be (a) safer, but as potent of an oncolytic as its parental WR virus and (b) will have a different oncolytic profile when compared to the WR attenuated recombinants.

3.1.7 Objectives

1. To determine the safety profile of VV-E3L^{OrfV} *in vitro* and *in vivo*
2. To compare the oncolytic properties of VV-E3L^{OrfV} to WR and its attenuated recombinants *in vitro*
3. To determine the *in vivo* efficacy of VV-E3L^{OrfV}

3.2 Results

3.2.1 VV-E3L^{OrfV} infection is attenuated and sensitive to the addition of IFN in normal human fibroblast cells.

As VV-E3L^{OrfV} is a novel OV candidate, its safety profile both *in vitro* and *in vivo* must be established. *In vitro,* we are able to use a number of normal human cell lines, including adult GM38, HDFn and MRC5 fibroblast cells. Additionally, we are able to add exogenous type I IFNs (IFNβ or Intron A (IFNα)) to stimulate an "anti-viral" response and observe if the virus is able or unable to overcome this. A successful OV candidate must either be unable to infect normal cells naturally or be sensitive to the effects of IFNs. With these characteristics in mind for a safe OV GM38, HDFn and MRC5 cells were tested. In the absence of added IFN, both VV-E3L^{OrfV} and WR are able to infect GM38 cells to similar titers (Figure 3B, D). The addition of 1000U human IFNβ significantly decreased VV-E3L^{OrfV} titers compared to WR ($p=0.01$; Figure 3B). While not statistically significant, a similar trend was observed when 500U of IFNα was added when comparing VV-E3L^{OrfV} titers to WR ($p=0.09$; Figure 3D).

In contrast to GM38 cells, VV-E3L^{OrfV} infection is attenuated compared to WR in the absence of IFN in HDFn cells. VV-E3L^{OrfV} titers were significantly lower than WR, VVdd, WRΔVGF ($p\leq0.01$) and WRΔTK ($p=0.02$) at MOI 0.1 (Figure 3E). Even at 100-fold less virus VV-E3L^{OrfV} titers were significantly lower than VVdd ($p=0.01$) and trending towards significance for WR ($p=0.06$; Figure 3F).

This attenuation was also observed in MRC5 cells in the absence of IFN ($p<0.0001$; Figure 4B, D). Additionally, VV-E3L^{OrfV} was sensitive to the addition of 100U or 1000U of human IFNβ, as there is a 100-fold decrease in viral titer compared to a 10-fold decrease for

WR, the differences between viruses was trending towards significance (p=0.09; Figure 4B). Phase-contrast images showed that cytopathic effect (CPE) was present in WR-infected cells even in the presence of IFNα, while there is less CPE present in VV-E3L^{OrfV}-infected cells (Figure 4A and C). The addition of IFNα at 50U and 500U, significantly decreased VV-E3L^{OrfV} viral titers compared to WR (p=0.01 and p=0.009, respectively; Figure 4D).

In addition to comparing viral titers in normal fibroblast cell lines of VV-E3L^{OrfV}, WR and VVdd, we wanted to visualize the ability of these viruses to spread through a monolayer of cells. Confluent monolayers of MRC5 cells were overlaid with an agarose overlay. 5000 pfu of either PBS, VV-E3L^{OrfV}, WR or VVdd directly added into the holes created in the center of agarose overlaid cells. 72 hours post infection cells were fixed and stained with Coomassie Blue. Plates were then scanned (Figure 4E) and relative area of cell death as a measure of spread was calculated. While there were no statistically significant differences in relative area of cell death, there was a trend that WR spread the most throughout the MRC5 monolayer followed by VV-E3L^{OrfV} and lastly VVdd (Figure 4F).

3.2.2 VV-E3L^{OrfV} is 10-fold safer than WR when administered through IN injection.

VV-E3L^{OrfV} safety has been previously published by Vijaysri et al. (2003) in both an IN MTD and IC MTD (113). A 100-fold and 100,000-fold safety profile was seen between VV-E3L^{OrfV} and WR (113). We wanted to confirm the IN safety profile in our hands. C57Bl/6 mice were given escalating doses of VV-E3L^{OrfV} or WR IN and wellness was monitored (Figure 5A). We found a 10-fold safety profile between VV-E3L^{OrfV} and WR, at $5x10^5$ or $5x10^6$ pfu, respectively (p=0.03; Figure 5B). Additionally, those mice which succumbed to WR showed dramatic weight loss (Figure 5C), while VV-E3L^{OrfV}-treated mice maintained their weight throughout the experiment (Figure 5D).

Figure 3. VV-E3L^{OrfV} is sensitive to hIFNβ and IFNα in normal human GM38 fibroblast cells and its infection is attenuated in normal human HDFn cells. GM38 were either treated with human IFNβ (0U or 100U) or IFNα (0U or 500U) 16 hours prior to infection. Cells were then directly infected with either VV-E3L^{OrfV} or WR at MOI 0.001. Phase-contrast images were taken at 72 hours post infection (A, C) and cells were harvested for viral titering (B, *p=0.01; D, ns =0.09; n=3). Virus-induced replication and spread was analyzed in HDFn cells infected at MOI 0.1 (E; *p=0.02, **p≤0.01) and 0.001 (F; ns=0.06, *p=0.01) 72 hours post infection (n=4).

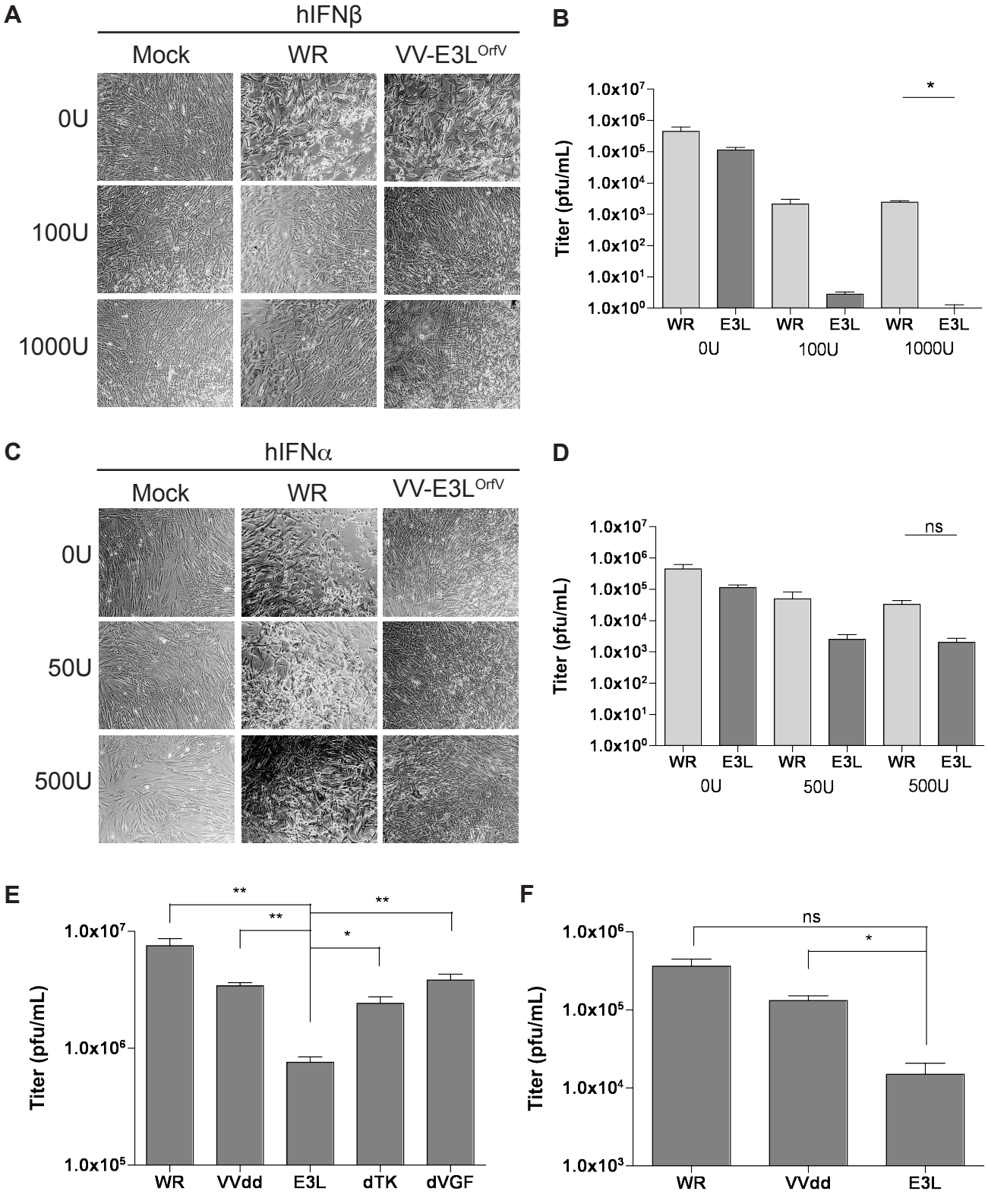
A
hIFNβ
Mock
WR
VV-E3L OrfV
0U
100U
1000U
B
Titer (pfu/mL)
1.0x10^7
1.0x10^6
1.0x10^5
1.0x10^4
1.0x10^3
1.0x10^2
1.0x10^1
1.0x10^0
*
WR
E3L
WR
E3L
WR
E3L
0U
100U
1000U
C
hIFNα
Mock
WR
VV-E3L OrfV
0U
50U
500U
D
Titer (pfu/mL)
ns
WR
E3L
WR
E3L
WR
E3L
0U
50U
500U
E
Titer (pfu/mL)
**
**
**
*
1.0x10^7
1.0x10^6
1.0x10^5
WR
VVdd
E3L
dTK
dVGF
F
Titer (pfu/mL)
ns
*
1.0x10^6
1.0x10^5
1.0x10^4
1.0x10^3
WR
VVdd
E3L

Figure 4. VV-E3L^{OrfV} is sensitive to hIFNβ and IFNα in normal human MRC5 fibroblast cells. MRC5 cells were either treated with human IFN-β (0U or 100U) or IFNα (0U or 500U) 16 hours prior to infection. Cells were then infected with either VV-E3L^{OrfV} or WR at MOI 0.001. Phase-contrast images were taken at 72 hours post infection (A, C) and cells were harvested for viral titering (B, ***$p<0.0001$, ns=0.09; D, ***$p<0.0001$, *$p=0.01$, **$p=0.009$; n=3). To see if virus is able to spread, confluent monolayers of MRC5 cells were covered with an agarose overlay. Once agarose solidified, holes were created in the center of each well. 5000 pfu of virus or PBS was then added directly in the holes. 72 hours post infection cells were fixed and stained with Coomassie Blue. Plates were then scanned (E) and relative area of cell death was calculated using ImageJ software (F; n=3).

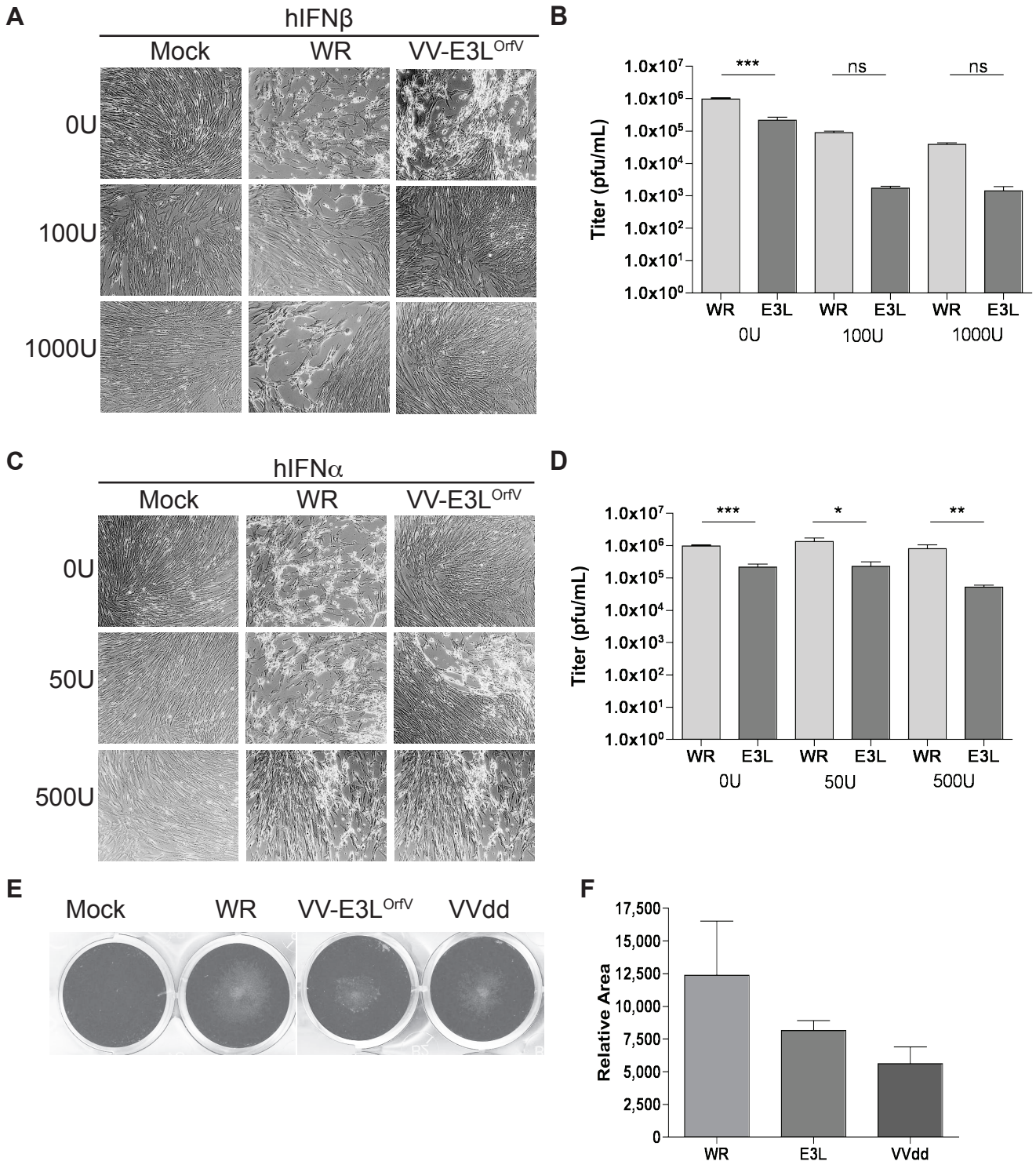
A
hIFNβ
Mock
WR
VV-E3L OrfV
0U
100U
1000U
B
Titer (pfu/mL)
1.0x10^7
1.0x10^6
1.0x10^5
1.0x10^4
1.0x10^3
1.0x10^2
1.0x10^1
1.0x10^0
***
ns
ns
WR
E3L
WR
E3L
WR
E3L
0U
100U
1000U
C
hIFNα
Mock
WR
VV-E3L OrfV
0U
50U
500U
D
Titer (pfu/mL)
1.0x10^7
1.0x10^6
1.0x10^5
1.0x10^4
1.0x10^3
1.0x10^2
1.0x10^1
1.0x10^0
***
*
**
WR
E3L
WR
E3L
WR
E3L
0U
50U
500U
E
Mock
WR
VV-E3L OrfV
VVdd
F
Relative Area
17,500
15,000
12,500
10,000
7,500
5,000
2,500
0
WR
E3L
VVdd

Figure 5. VV-E3L^{OrfV} is 10-fold safer than WR when administered through intranasal injection. C57BL/6 mice were treated by intranasal (IN) injection of escalating doses of WR and VV-E3L^{OrfV} and monitored for survival. Experimental design (A). VV-E3LOrfV ($5x10^6$ pfu; n=5) was 10-fold less pathogenic than WR ($5x10^5$ pfu; n=6; *p = 0.03; B). Only two out of six WR treated mice (C) were able to regain their weight, while VV-E3L^{OrfV} treated mice (D) maintained their body weight.

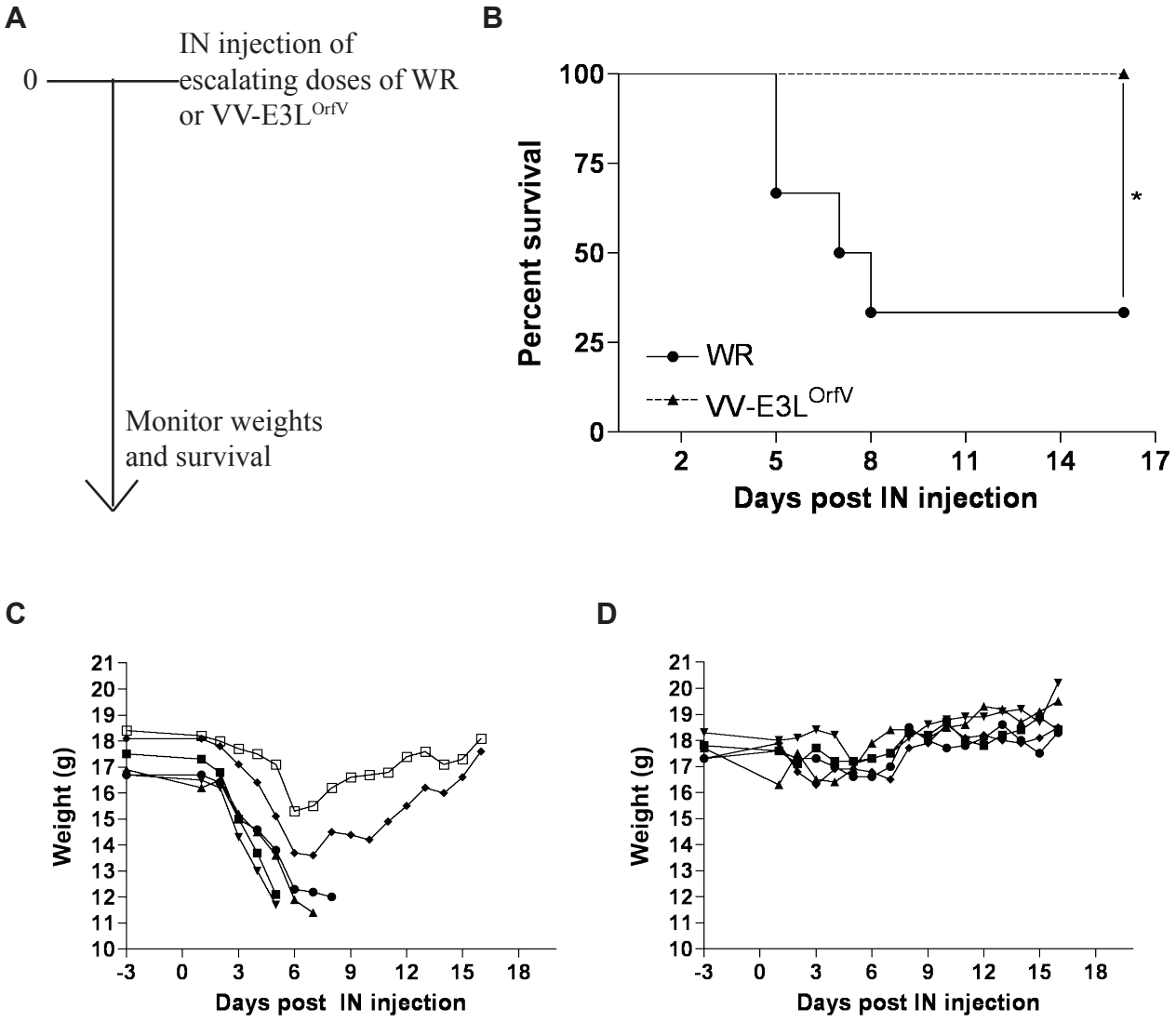
A
0
IN injection of
escalating doses of WR
or VV-E3L OrfV
Monitor weights
and survival
B
Percent survival
100
75
50
25
0
WR
VV-E3L OrfV
*
2
5
8
11
14
17
Days post IN injection
C
Weight (g)
21
20
19
18
17
16
15
14
13
12
11
10
-3
0
3
6
9
12
15
18
Days post IN injection
D
Weight (g)
Days post IN injection

3.2.3 VV-E3L^{OrfV} is at least as oncolytic as WR and its attenuated recombinants *in vitro*.

3.2.3.1 VV-E3L^{OrfV} is, at least as cytotoxic as, WR and its attenuated recombinants in a panel of murine and human cancer cell lines.

With VV-E3L^{OrfV} safety profile established both in *in vitro* and *in vivo*, we next wanted to determine its oncolytic properties compared to WR and its attenuated recombinants. A panel of murine and human cancer cell lines was screened. The murine cell lines chosen included B16F10LacZ, CT26LacZ, 4T1 and MC38. HeLa and U2OS cells were chosen due to their use in virus manufacturing and titering, respectively. Lastly, human cancer cell lines were chosen from the NCI60 cancer panel and were from various organ origins including renal, colon, NSCLC, breast, ovarian, melanoma and CNS. Cells were chosen based on their responsiveness to IFN using data previously collected in our lab (105). IFN non-responsive cells included NCI-H23, A549, UACC-257, MDA-MB-435 and MCF7. IFN responsive cells included HOP-92, OVCAR8, 786O, ACHN, HCT116, SW620, HCT15, SNB-75 and T-47D. Additionally, human NCI-H226 and SKRB3 cancer cells were used. To assess oncolytic potential virus-induced cytotoxicity assays were performed. Cells were infected with 10-fold dilutions beginning at MOI 1 to MOI 0.001 for 72 hours, after which alamarBlue was added and cell viability was quantified. Data from MOI 0.1 and 0.01 are shown (Figure 6). One striking observation made, was that WRΔVGF was unable to induce cell death to the same extent as all the other viruses tested. Similar killing ability was observed with VV-E3L^{OrfV} as with WR, WRΔTK and VVdd in many of the cell lines tested. For a select few cell lines, including SNB-75 and HOP-92, VV-E3L^{OrfV} was able to induce the greatest cell death at MOI 0.1, with even greater differences with 10-fold less virus. Interestingly, VVdd-induced cytotoxicity in the majority of cell lines tested was

greater than individual mutant viruses, WRΔTK and WRΔVGF.

Next, EC50 values were calculated for all the viruses and cell lines tested (Table 3). WRΔVGF had the highest EC50 values (20/22), while VV-E3L^{OrfV} had the lowest EC50 values (8/22), with WR and VVdd next (6/22), followed by WRΔTK. For certain cell lines, including HeLa, HCT116 and MCF7, EC50 values for all viruses tested are within 1-log of each other. In contrast, in SNB-75, 786O and OVCAR-8 as examples, there was up to a 3-log difference in EC50 values.

3.2.3.2 VV-E3L^{OrfV} shares similar growth kinetics in HeLa and B16F10LacZ cells as WR and its attenuated recombinants.

Viral growth kinetics were analyzed using HeLa and B16F10LacZ cells. These cell lines were chosen due to the fact we use HeLa cells in virus manufacturing and B16F10LacZ cells due to their use in subsequent *in vivo* studies. VV-E3L^{OrfV} was compared to WR, WRΔTK and WRΔVGF in its ability to either replicate or replicate and spread using single-step and multi-step growth curves, respectively. In HeLa cells, there was a delay in replication for WRΔVGF compared to the other viruses, but by the last time point at 48 hours all viruses were within 1-log of each other (Figure 7A). WRΔVGF replication was also delayed in B16F10LacZ, but at the last time point all viruses reached similar titers (Figure 7B). Additionally, there was a 1-log increase in viral titers in B16F10LacZ cells compared to HeLa cells. Similar observations were seen in HeLa and B16F10LacZ cells in the multi-step growth curves (Figure 7C and D, respectively).

Figure 6. Comparing VV-E3L^{OrfV}-induced cytotoxicity to WR and its attenuated recombinants. Various murine and human cancer cell lines were infected with VV-E3L^{OrfV}, WR, VVdd, WRΔTK (dTK), WRΔVGF (dVGF) and VVdd at MOI 0.1 (A) or 0.01 (B). 72 hours post infection cytotoxicity was assessed by alamarBlue assay (n=6).

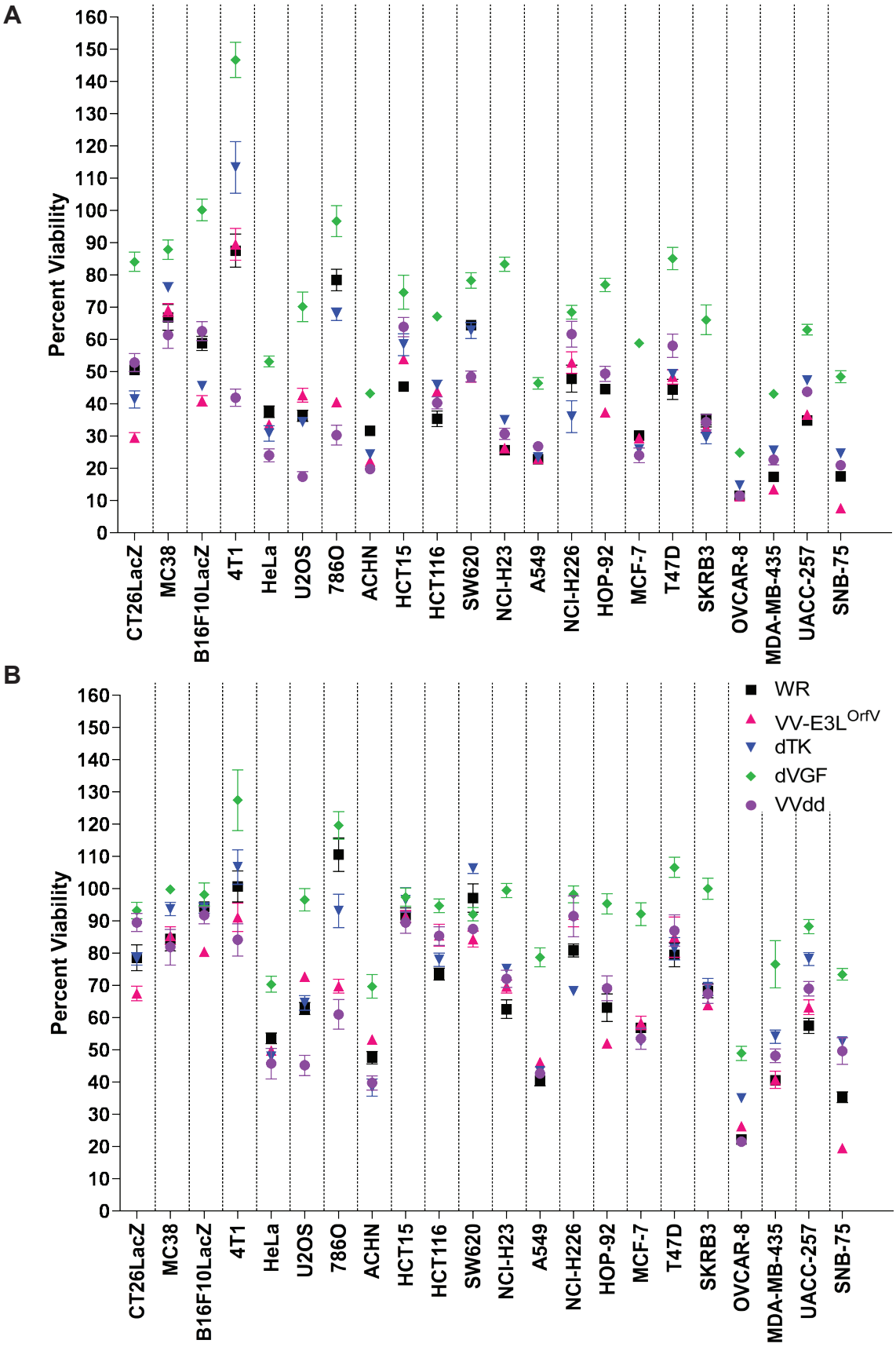
A
B
Percent Viability
0
10
20
30
40
50
60
70
80
90
100
110
120
130
140
150
160
CT26LacZ
MC38
B16F10LacZ
4T1
HeLa
U2OS
786O
ACHN
HCT15
HCT116
SW620
NCI-H23
A549
NCI-H226
HOP-92
MCF-7
T47D
SKRB3
OVCAR-8
MDA-MB-435
UACC-257
SNB-75
WR
VV-E3L^{OrfV}
dTK
dVGF
VVdd

Table 3. EC50 values for VV-E3L^{OrfV} and all WR recombinants in murine and human cancer cells.

Murine		**WR**	**VV-E3L^{OrfV}**	**WRΔTK**	**WRΔVGF**	**VVdd**
CT26LacZ	Colon	0.08763	0.02770	0.05596	2.00300	0.10100
MC38	Colon	0.92730	1.59100	26.65000	27.73000	0.23960
B16F10LacZ	Melanoma	0.08237	0.05098	0.06442	3.76500	0.10170
4T1	Breast	0.14030	1.41000	2.83900	0.05234	0.04084
Human		**WR**	**VV-E3L^{OrfV}**	**WRΔTK**	**WRΔVGF**	**VVdd**
HeLa	Cervical	0.00053	0.00023	0.00015	0.00014	0.00014
U2OS	Osteosarcoma	0.01177	0.01043	0.00632	0.01220	0.00139
786O	Renal	1.64800	0.00001	0.02241	5.92100	0.00027
ACHN	Renal	0.00148	0.00273	0.00376	0.05292	0.00009
HCT15	Colon	0.08131	0.10190	0.13730	0.31830	0.29340
HCT116	Colon	0.03522	0.06223	0.05263	0.17570	0.04847
SW620	Colon	0.17110	0.08798	0.10980	0.42410	0.10990
NCI-H23	NSCLC	0.02141	0.02400	0.02613	0.32740	0.03373
A549	NSCLC	0.00094	0.00137	0.00057	0.02606	0.00035
NCI-H226	NSCLC	0.03096	0.11680	0.01140	0.12300	0.06242
HOP-92	NSCLC	0.03197	0.00511	0.05707	0.18080	0.07898
MCF7	Breast	0.00372	0.00554	0.00495	0.08509	0.00487
T47D	Breast	0.01399	0.00558	0.01684	0.21640	0.03345
SKRB3	Breast	0.00847	0.00682	0.01029	0.09198	0.01479
OVCAR-8	Ovarian	0.00006	0.00044	0.00125	0.00566	0.00008
MDA-MB-435	Melanoma	0.00303	0.00372	0.00747	0.04105	0.00626
UACC-257	Melanoma	0.00488	0.01527	0.01467	0.06200	0.00598
SNB-75	CNS	0.00247	0.00007	0.00867	0.06934	0.00931

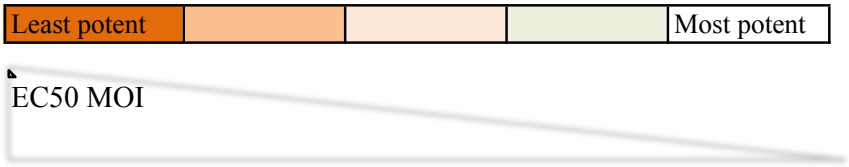

*EC50 values were calculated using Graphpad Prism 4.0. Data was analyzed using non-linear regression equation: Y=Bottom + (Top-Bottom)/1+10^((LogEC50-X)*HillSlope)) where:
X is the logarithm of concentration.
Y is the response. Y starts at Bottom and goes to Top with a sigmoid shape.
HillSlope is shared between each data set (all viruses/each cell line).

Figure 7. Comparing VV-E3L^{OrfV} replication and spread to WR and its attenuated recombinants. Single-step (A, B) and multi-step (C, D) growth curves analysis was performed in HeLa (A, C) B16F10LacZ (B, D) cells. Samples were harvested at indicated time points and titered (n=2).

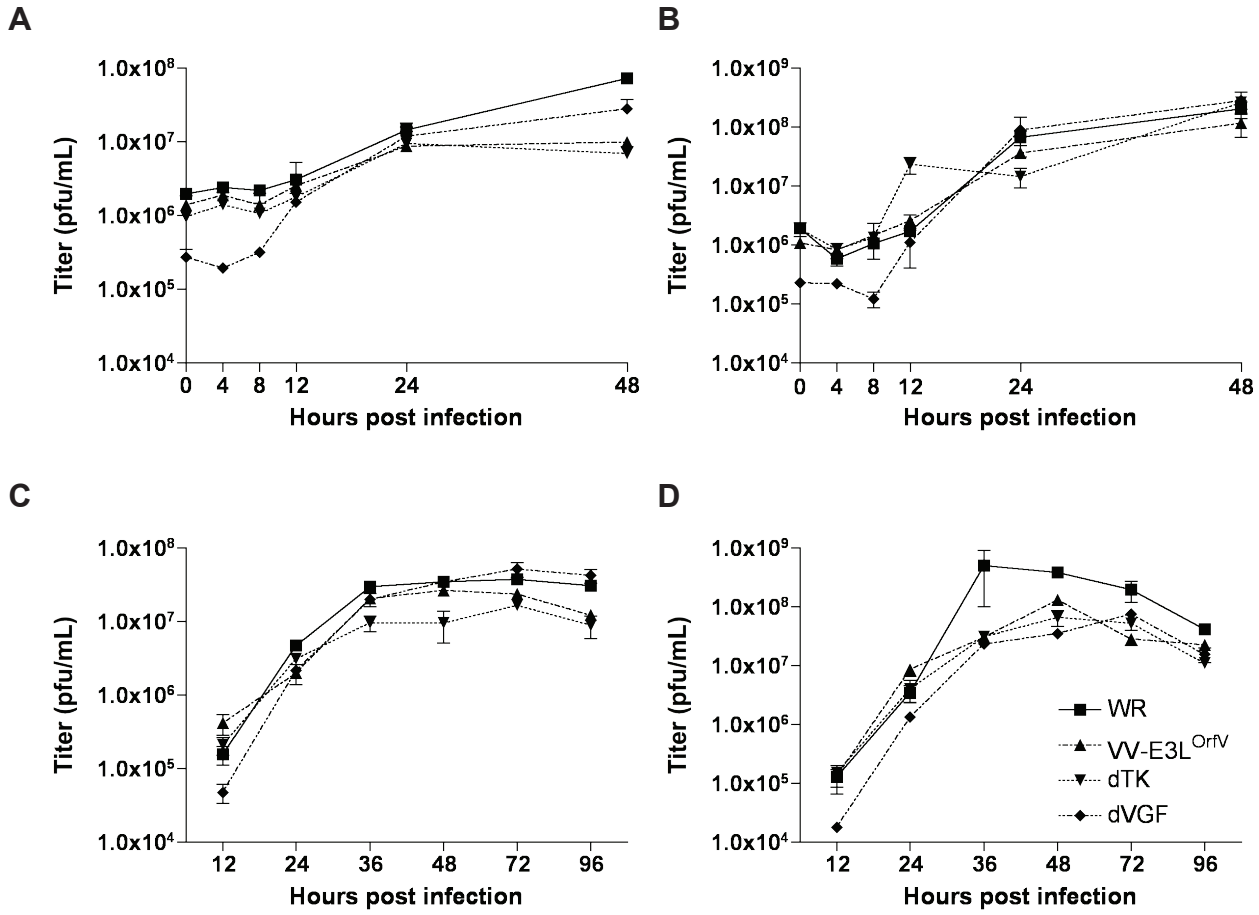
A
B
C
D
Titer (pfu/mL)
Hours post infection
1.0x10^8
1.0x10^7
1.0x10^6
1.0x10^5
1.0x10^4
1.0x10^9
0 4 8 12 24 48
12 24 36 48 72 96
WR
VV-E3L^OrfV
dTK
dVGF

3.2.3.3 VV-E3L^{OrfV} is able to spread as well as or better than WR and its attenuated recombinants.

In addition to comparing virus-induced cytotoxicity and viral titers in a panel of human cancer cell lines by WR, VV-E3L^{OrfV}, VVdd, WRΔTK and WRΔVGF, we wanted to visualize the ability of these viruses to spread through a monolayer of cells. Confluent monolayers of HeLa, OVCAR-8 and 786O cells were covered with an agarose overlay. 5000 pfu of either PBS, VV-E3L^{OrfV}, WR, VVdd, WRΔTK or WRΔVGF directly added into the holes created in the center of agarose overlaid cells. 72 hours post infection, cells were fixed and stained with Coomassie Blue. Plates were then scanned and relative area of cell death as a measure of spread was calculated. VV-E3L^{OrfV}, WR, WRΔTK and WRΔVGF were all able to spread through HeLa cells to a similar extent (Figure 8A, B). A similar observation was made in 786O cells, where VV-E3L^{OrfV}, WR and VVdd spread was comparable (Figure 8E, F). In contrast, VV-E3L^{OrfV} was able to spread through OVCAR-8 cells significantly more than all the other viruses ($p \leq 0.05$; Figure 8C, D).

3.2.3.4 VV-E3L^{OrfV} is a potential treatment for gliomas.

In Figure 6, we were able to show that VV-E3L^{OrfV} was more potent in human CNS SNB-75 cancer cells compared to WR, VVdd, WRΔTK and WRΔVGF. Additionally, it has been previously shown that VV-E3L^{OrfV} is 100,000-fold safer than WR when injected IC (113). We therefore wanted to test a panel of glioma cell lines and compare VV-E3L^{OrfV}'s ability to replicate in and spread to VVdd. WR is known to be highly neurovirulent and as such was not included. Additionally, WRΔTK and WRΔVGF were excluded as the only WR backbone clinical candidate is a modified version of VVdd which contains the immune-stimulatory gene GM-CSF (Jennerex product JX-963). A variety of rodent (rat and mouse)

and human cell lines was tested. Cells were either mock infected or infected with VV-E3L^{OrfV} or VVdd, at MOI 0.05, allowing us to observe both replication and spread ability. 48 hours post infection, phase-contrast images were taken and samples collected for titering. Images of BT4C, CNS1, DBT IRE, SF767 and U87 are shown and in the presence of either virus, CPE is seen compared to mock infected controls (Figure 9A). In murine DBT IRE cells, VV-E3L^{OrfV} viral titers were at least 2-logs greater than VVdd's when compared to inputs. For the majority of other cell lines including, BT4C, CNS1, AST 11.9.2, CT2A, G26, SF767 and U118, VV-E3L^{OrfV} performed as well as VVdd (Figure 9B). In human U87 and U251 cancer cells VVdd performed better than VV-E3L^{OrfV}.

3.2.4 VV-E3L^{OrfV} efficacy *in vivo*.

3.2.4.1 VV-E3L^{OrfV} is able to delay the progression of SQ HT29 tumors.

With VV-E3L^{OrfV} oncolytic ability characterized *in vitro*, we wanted to test its efficacy *in vivo*. Human colon cancer HT29 cells were implanted SQ in CD-1 nude mice. Once tumors were established, mice were treated with either PBS or 1x10^7 pfu VV-E3L^{OrfV} or VVdd IT on days 9, 11, 14 and 16. Tumor volumes were measured every 2 to 3 days and survival was monitored. Experimental design is outlined in Figure 10A. Mice that received VV-E3L^{OrfV} treatment had delayed tumor progression compared to VVdd- and PBS-treated mice (Figure 10B). Unfortunately, the VV-E3L^{OrfV}-treated mice exhibited toxicity due to viremia and were sacrificed once in distress (Figure 10C). The experiment was terminated once the last VV-E3L^{OrfV} mouse was sacrificed. At endpoint, tissues including tumor, lungs, ovaries, spleen and brain, were harvested from VV-E3L^{OrfV}-treated mice for titering. While virus was found in the tumors (5/5), lungs (4/5) and ovaries (1/5), no virus was found in the spleen and brain (Figure 10D).

Figure 8. Comparing VV-E3L^{OrfV} spread to WR and its attenuated recombinants in human cancer cells. Confluent monolayers of HeLa (A), OVCAR8 (C) and 786O (E) cells were covered with an agarose overlay. Once agarose solidified, holes were created in the center of each well. 5000 pfu of virus or PBS was then added directly in the holes. 72 hours post infection cells were fixed and stained with Coomassie Blue. Plates were then scanned and relative area of cell death was calculated using ImageJ software (B, D and E; n=3 or 4; *$p \leq 0.05$).

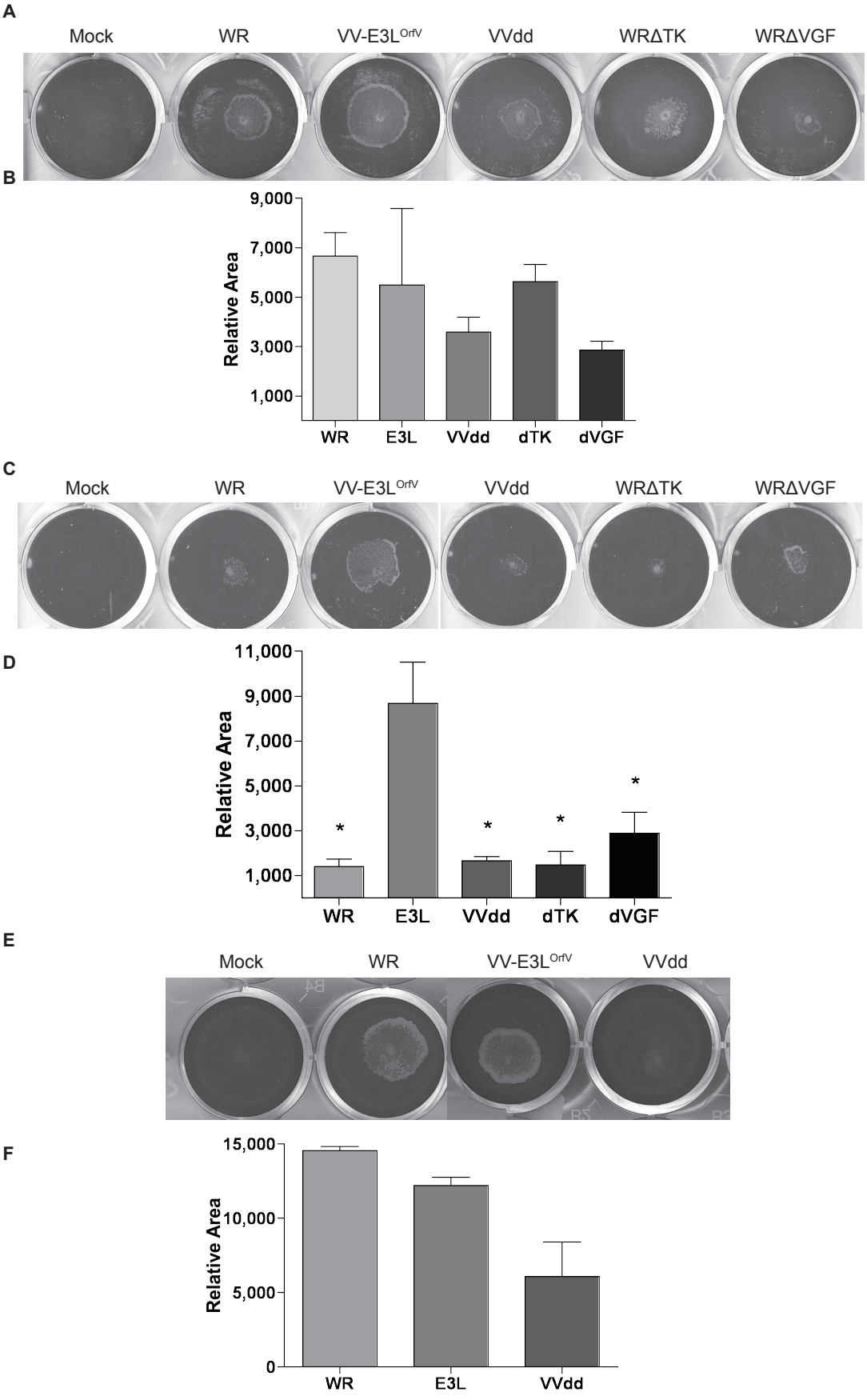
A
Mock
WR
VV-E3L OrfV
VVdd
WRΔTK
WRΔVGF
B
Relative Area
9,000
7,000
5,000
3,000
1,000
WR
E3L
VVdd
dTK
dVGF
C
Mock
WR
VV-E3L OrfV
VVdd
WRΔTK
WRΔVGF
D
Relative Area
11,000
9,000
7,000
5,000
3,000
1,000
*
WR
E3L
VVdd
dTK
dVGF
E
Mock
WR
VV-E3L OrfV
VVdd
F
Relative Area
15,000
10,000
5,000
0
WR
E3L
VVdd

Figure 9. VV-E3L^{OrfV} is able to infect glioma cells, as well as or better than VVdd. Glioma cells BT4C, CNS1, AST 11.9.2, CT2A, DBT IRE, G26 and SF767, U87, U118 and U251 were either mock infected or treated with VV-E3L^{OrfV} or VVdd at a MOI 0.05. Phase-contrast images were taken at 48 hours post infection (A) and cells were harvested for viral titering (B).

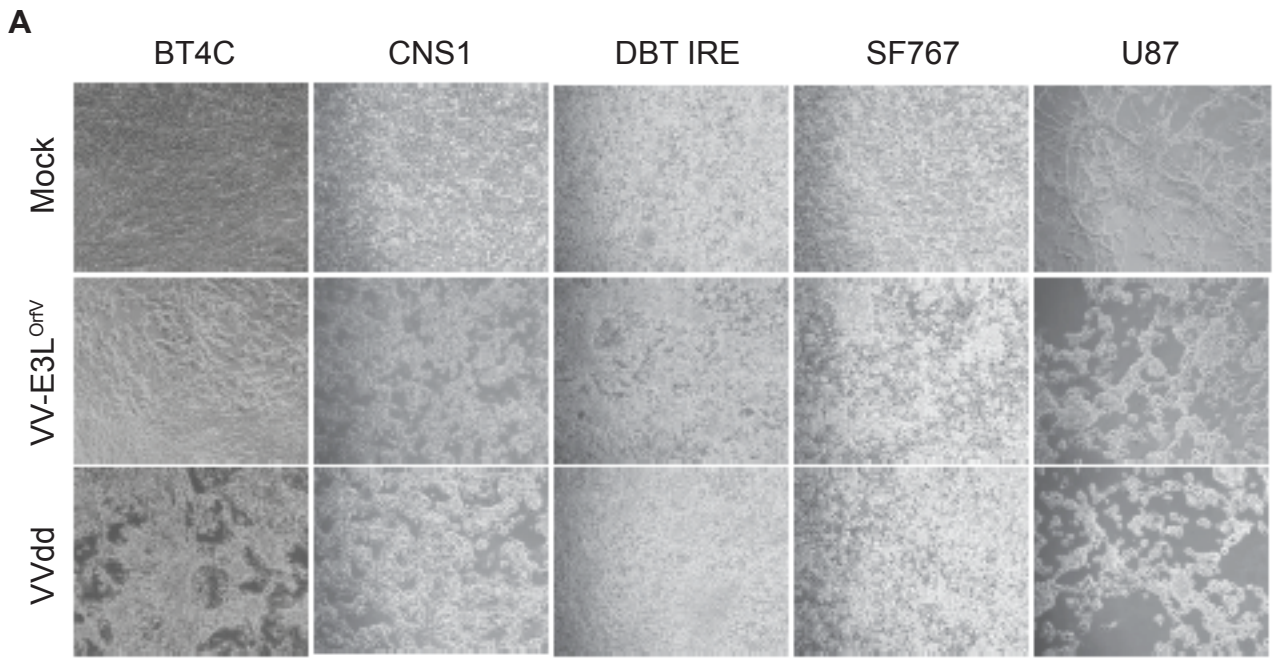
A
BT4C
CNS1
DBT IRE
SF767
U87
Mock
VV-E3L OrfV
VVdd

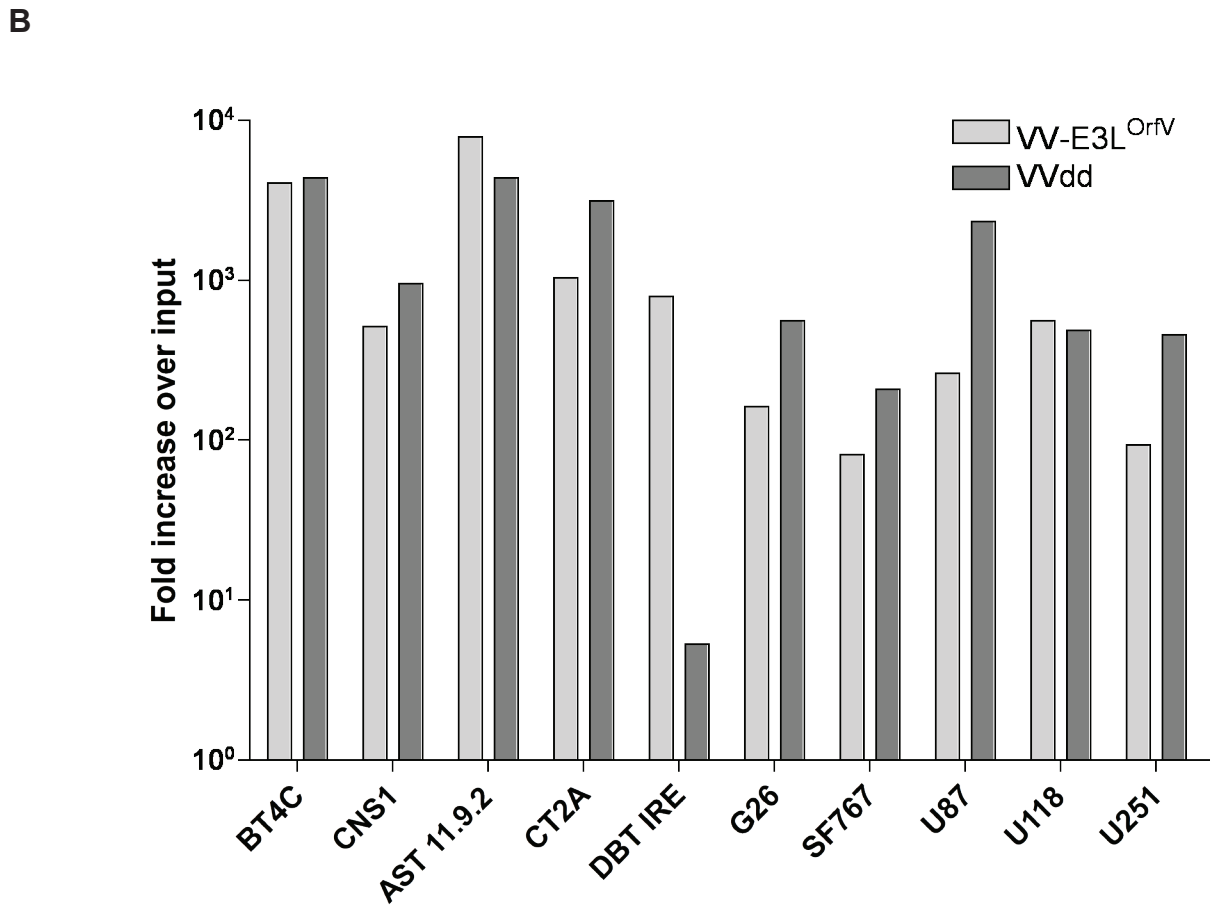
B
Fold increase over input
10^4
10^3
10^2
10^1
10^0
VV-E3L OrfV
VVdd
BT4C
CNS1
AST 11.9.2
CT2A
DBT IRE
G26
SF767
U87
U118
U251

Figure 10. VV-E3L^{OrfV} is able to stabilize HT29 tumor burden in a xenograft tumor model. CD-1 Nude mice received 1x10^6 HT29 human colon carcinoma cells SQ in the right flank. On days 9, 11, 14 and 16 mice received IT injections of either PBS or 1x10^7 pfu VV-E3L^{OrfV} or VVdd (n=5/group; A). Tumor volume was followed (B) and survival followed (C). At endpoint, animals were sacrificed, and VV-E3L^{OrfV} mice had lungs, ovaries, spleen and brain, along with tumors harvested for viral titering (D).

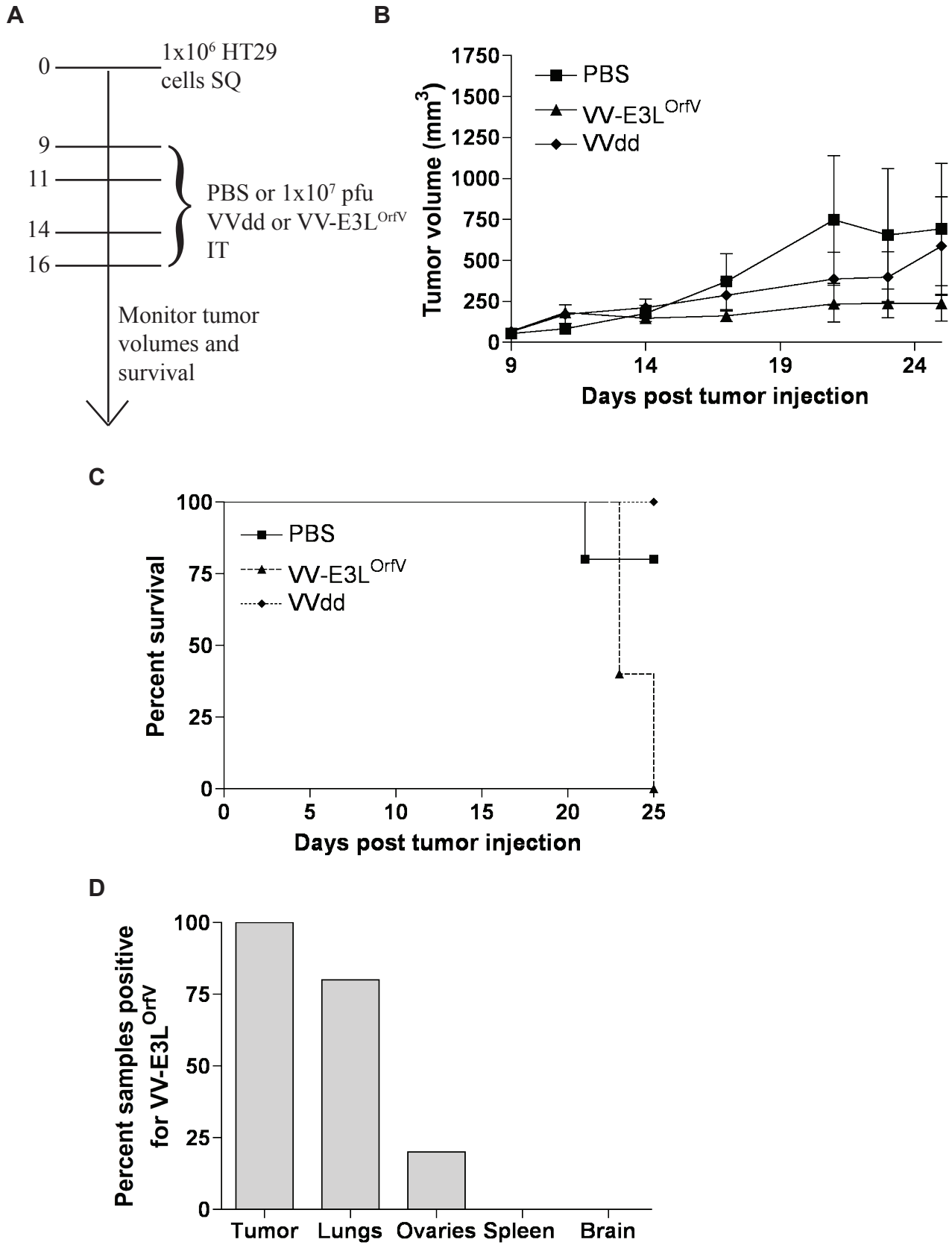
A
0
1x10^6 HT29 cells SQ
9
11
14
16
PBS or 1x10^7 pfu VVdd or VV-E3L^OrfV IT
Monitor tumor volumes and survival
B
Tumor volume (mm^3)
1750
1500
1250
1000
750
500
250
0
PBS
VV-E3L^OrfV
VVdd
9
14
19
24
Days post tumor injection
C
Percent survival
100
75
50
25
0
PBS
VV-E3L^OrfV
VVdd
0
5
10
15
20
25
Days post tumor injection
D
Percent samples positive for VV-E3L^OrfV
100
75
50
25
0
Tumor
Lungs
Ovaries
Spleen
Brain

3.2.4.2 VV-E3L^{OrfV} is not efficacious in an immunocompetent WT CT26 SQ tumor model.

Immunocompetent Balb/c mice received syngeneic WT CT26 colon cancer cells SQ in the right flank. On days 15 and 18 post tumor implantation mice were treated with either PBS or 1x10^7 pfu VV-E3L^{OrfV} or VVdd IT. Tumor volumes were measured every 2 to 3 days and survival was monitored. Experimental design is outlined in Figure 11A. There were no significant differences in tumor volumes, VVdd-treated mice had the greatest tumor burden (Figure 11B). At the end of the experiment 33.3% of PBS mice and 20% of VV-E3L^{OrfV} mice survived compared to 0% of VVdd mice (Figure 11C). At endpoint, tumors were harvested from VV-E3L^{OrfV}- and VVdd-treated mice for titering. While not statistically significant, more virus was recovered from VV-E3L^{OrfV}-treated tumors compared to VVdd (pfu/g p=0.19; pfu/mL p=0.23; Figure 11D).

3.2.4.3 VV-E3L^{OrfV} is as efficacious and better tolerated than WR in the B16F10LacZ lung tumor model.

Immunocompetent C57Bl/6 mice received syngeneic B16F10LacZ melanoma cells IV through tail vein injection. On day 5, mice received either PBS or 5x10^6 pfu of VV-E3L^{OrfV} or WR IV. On day 14 mice were sacrificed, lungs harvested and stained for β-galactosidase to visualize lung metastases. Additionally, throughout the experiment, mice weights were followed. Experimental design is outlined in Figure 12A. Compared to PBS-treated mice both WR and VV-E3L^{OrfV} significantly reduced tumor burden (p=0.01). There was no difference in efficacy between VV-E3L^{OrfV} and WR (Figure 12B). In contrast, VV-E3L^{OrfV} was better tolerated than WR, as indicated by the weight lost by WR-treated mice (p<0.0001; Figure 12C).

Figure 11. VV-E3L^{OrfV} is not efficacious in the WT CT26 colon carcinoma SQ tumor model. Balb/c mice received 3x10^5 WT CT26 murine colon carcinoma cells SQ in the right flank. On days 15 and 18 after tumor implantation, mice received either PBS (n=5) or 1x10^7 pfu of VV-E3L^{OrfV} (n=5) or VVdd IT (n=5; A). Tumor size was measured (B) and survival followed (C). Once mice reached endpoint (tumor volume ≥1500 mm3) or when experiment was ended due to the endpoint of all VVdd mice, animals were sacrificed, and tumors resected, homogenized and VV viral titers were determined (D).

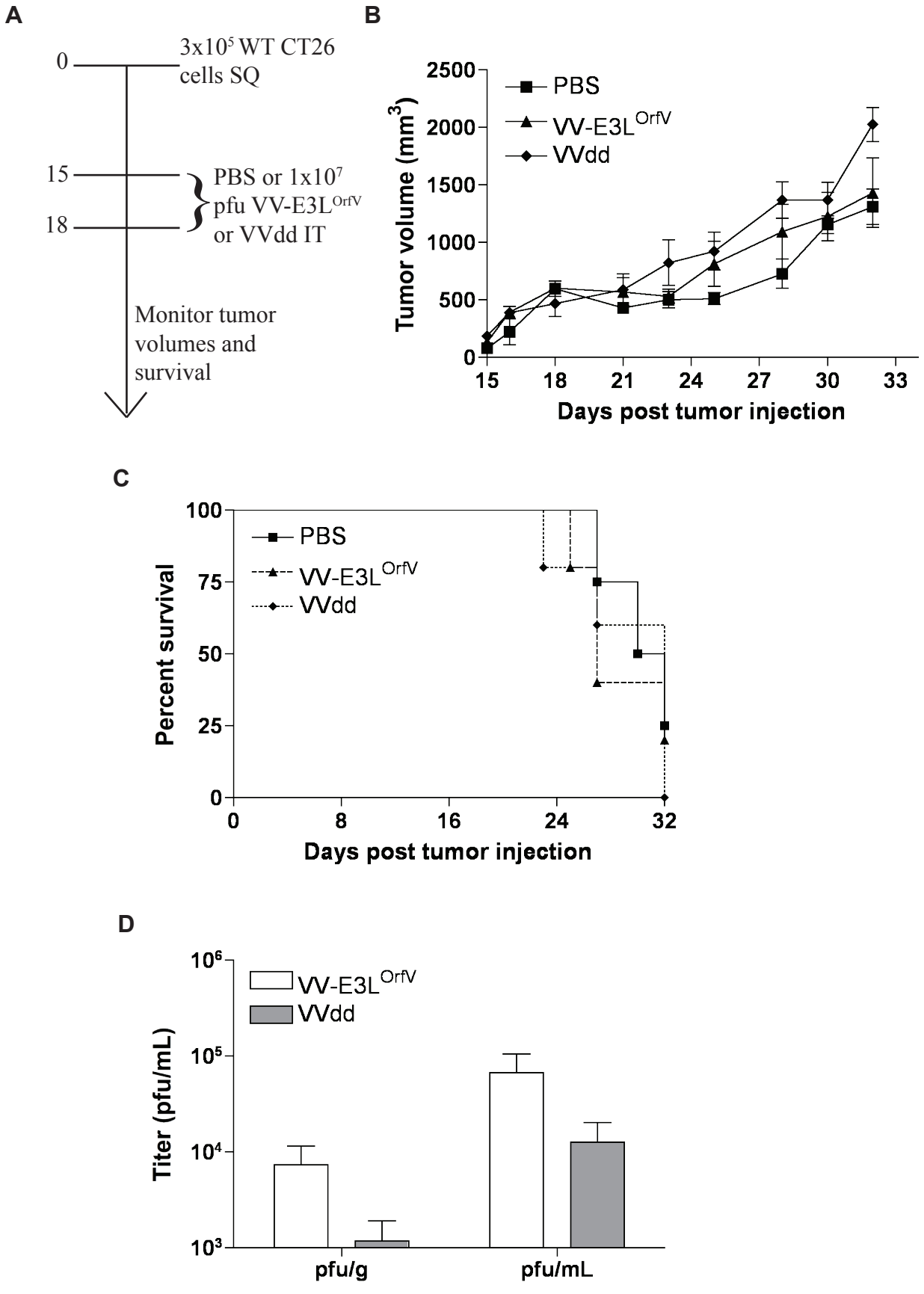
A
0
3x10^5 WT CT26 cells SQ
15
18
PBS or 1x10^7 pfu VV-E3L^OrfV or VVdd IT
Monitor tumor volumes and survival
B
Tumor volume (mm^3)
2500
2000
1500
1000
500
0
PBS
VV-E3L^OrfV
VVdd
15
18
21
24
27
30
33
Days post tumor injection
C
Percent survival
100
75
50
25
0
PBS
VV-E3L^OrfV
VVdd
0
8
16
24
32
Days post tumor injection
D
Titer (pfu/mL)
10^6
10^5
10^4
10^3
VV-E3L^OrfV
VVdd
pfu/g
pfu/mL

Figure 12. VV-E3L^{OrfV} is as efficacious as WR, but better tolerated in a B16F10LacZ lung tumor model. C57Bl/6 mice received 3x10^5 B16F10LacZ murine melanoma cells IV through the tail vein. On day 5 mice received either PBS (n=5) or 5x10^6 pfu VV-E3L^{OrfV} (n=6) or WR (n=5) IV. Mice were then sacrificed on day 14 and lungs were harvested for β-galactosidase to visualize lung metastases (A). VV-E3L^{OrfV} and WR treated mice had a significantly lower lung tumor burden than PBS treated mice (*p=0.01). WR treated mice lost a significant amount of weight (***p<0.001) compared to PBS and VV-E3L^{OrfV} groups on days 10 to 12 (C).

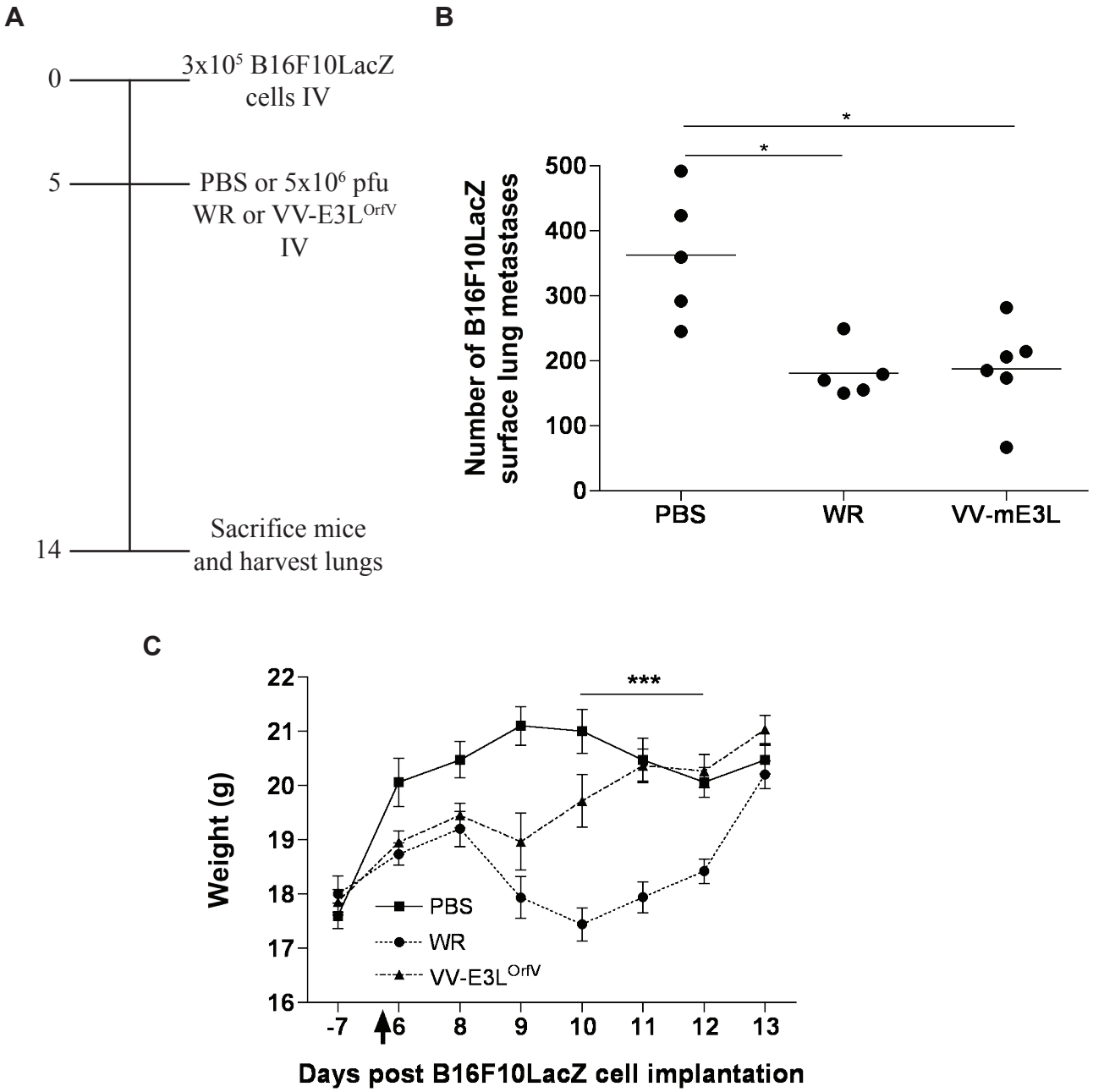
A
0
3x10^5 B16F10LacZ cells IV
5
PBS or 5x10^6 pfu WR or VV-E3L^OrfV IV
14
Sacrifice mice and harvest lungs
B
Number of B16F10LacZ surface lung metastases
500
400
300
200
100
0
*
*
PBS
WR
VV-mE3L
C
Weight (g)
22
21
20
19
18
17
16
***
PBS
WR
VV-E3L^OrfV
-7
6
8
9
10
11
12
13
Days post B16F10LacZ cell implantation

3.3 Discussion

3.3.1 VV-E3L^{OrfV} is attenuated both *in vitro* and *in vivo*.

We have characterized VV-E3L^{OrfV} safety profile in this study. It has been previously reported that while attenuated *in vivo*, VV-E3L^{OrfV} was interferon-resistant in RK13 cells, just like its parental WR virus (113). In contrast, we found VV-E3L^{OrfV} was attenuated in normal human cells *in vitro* (Figures 3 and 4). The addition of exogenous IFN-β and IFN-α (IFNα) either showed trends towards significance or was significantly attenuating VV-E3L^{OrfV} infection compared to WR in GM38 and MRC5 cells. Additionally, we have shown that VV-E3L^{OrfV} infection is attenuated in MRC5 and HDFn cells in the absence of IFNs compared with not only WR but also the attenuated recombinants (Figure 3E). The discrepancy between our results and those previously published could be due to the cell lines, rabbit RK13 and human fibroblast cells, in previous studies and our study, respectively.

We also confirmed that VV-E3L^{OrfV} is attenuated *in vivo*. Previously published reports observed that the IN MTD for WR was $4x10^3$ pfu (93), while in our hands we saw the MTD at $5x10^5$ pfu (Figure 5). This 100-fold difference may be attributed to the difference in age of mice used, as younger mice are more susceptible to virus. Additionally, the stocks of WR used between our study and the others are not the same, so it is possible that our WR stock came from a different clone. To complete VV-E3L^{OrfV} safety profile, a biodistribution assay must be performed to compare where WR and VV-E3L^{OrfV} are found 1 day and 5 days post IV virus injection in tumor-bearing mice. It is expected that WR would be found in the brain even at 5 days, while VV-E3L^{OrfV} should not be found in the brain at either time point. It would be expected that both viruses would be found in the SQ tumors,

hopefully at both time points. It would also be expected that virus would be present in the lungs and ovaries at least on day 1, but cleared by day 5, as VV is commonly found within the ovaries as it is a site of increased vascular permeability, as well as high cell turnover within the ovarian follicle (70, 94).

As previously mentioned, $E3L^{OrfV}$ is unable to complement $E3L^{VV}$ C-terminus, which plays a key role in inhibiting PKR activation (113). We can hypothesize that the $E3L^{OrfV}$ is unable to bind and mask dsRNA as efficiently as $E3L^{VV}$, therefore decreasing its ability to inhibit PKR activation and subsequent antiviral gene expression. Whether this impacts PKR-dependent and PKR-independent activation of cytokines increasing the innate immune response towards the virus, eIF2α-induced translation inhibition, apoptosis, autophagy and various other functions has yet to elucidated. Microarray analysis between gene expression profiles comparing WR and VV-$E3L^{OrfV}$ infection would provide valuable insights. Nevertheless, VV-$E3L^{OrfV}$ fulfills the premier requirement for any OV, safety in human cells and *in vivo*.

3.3.2 VV-$E3L^{OrfV}$ is at least as oncolytic as WR and its attenuated recombinants *in vitro*.

We have shown that VV-$E3L^{OrfV}$ is able to kill, replicate and spread in a large panel of human and murine cancer cell lines *in vitro* (Figure 6). Virus-induced cytotoxicity was used as the main measure of oncolytic potential. One potential caveat in using cytotoxicity as a readout of oncolytic potential for poxviruses, is that they are known to induce death *in vitro* independent of viral replication (particularly at very high MOI) due to their ubiquitous ability to enter cells and initiate early gene transcription and stimulate death programs (30). The data collected within this study can be used to selectively chose cell lines to further

compare virus replication and spread between VV-E3L^{OrfV} and the WR attenuated recombinants. It is interesting to note that WRΔVGF infection induced the least cytotoxicity, but was able to replicate and spread to similar levels as the other viruses. Only once a more complete data set is collected, will we be able to postulate if VV-E3L^{OrfV} occupies a novel cancer niche compared with current clinical candidates.

Interestingly, while VV-E3L^{OrfV} is sensitive to IFN in normal cells, it does not seem to be sensitive to IFN by producing/responsive cancer cells. Human renal 786O and ovarian OVCAR8 cancer cells are readily infected by VV-E3L^{OrfV}, while other IFN sensitive OVs, including VSVΔM51, have been shown to be unable to replicate and spread (105). As VV has evolved multiple mechanisms to ensure inhibition of the IFN-induced anti-viral response, we can postulate that these genes, in particular B18R, are able to inhibit the host anti-viral response. Additionally, the presence of exogenous B18R or creation of a VSVΔM51 virus expressing B18R renders the virus capable of infecting 786O cells (61). To test the hypothesis that B18R is playing a key role in VV-E3L^{OrfV} ability to infect IFN producing/responsive cancer cells, a B18R knock-out VV-E3L^{OrfV} should be created. One would expect that this virus would become extremely sensitive to IFN, both in normal and cancer cells. It is also possible to postulate, that since VV-E3L^{OrfV} still contains its TK and VGF genes, their functions are able to complement any defects intrinsic to the virus. It is interesting to note that VVdd induced more cytotoxicity than either single-deleted WR virus in both 786O and OVCAR8 cells (Figure 8). It would be interesting to see if there was any additional synergy with VVdd if the E3L^{OrfV} substitution was included. The creation of these novel recombinant viruses would provide further insight into VV biology.

Finally, one promising observation made is VV-E3L^{OrfV} ability to infect CNS and glioma cancer cells *in vitro* (Figure 6 and 9). It is promising that, when injected directly in the brain, VV-E3L^{OrfV} is 100,000-fold safer than WR (113), but it would be important to be able to make a comparison with current clinical candidates. More detailed *in vitro* and *in vivo* studies would need to be performed to confirm this observation, but if true, this would provide a novel OV therapy for glioma patients.

3.3.3 VV-E3L^{OrfV} is efficacious in the B16F10LacZ lung model and is able to delay the progression of disease in the xenograft HT29 model.

In the WT CT26 SQ model no efficacy was seen, but no conclusions can be made as the tumors were not treated until day 15, which was approximately a week later than these tumors are generally treated. It is important to note that virus was recovered from the tumors up to 15 days after the last injection and it would be interesting to see if the virus is able to persist for longer, as this has been observed in patients treated with oncolytic VV (JX-594; (12)). To draw conclusions, this experiment would have to be repeated, taking into account the date of first treatment, which should occur around day 7 or 8, and also that the PBS-treated mice show the proper trend once treatments have started.

In the HT29 SQ model while VV-E3L^{OrfV} showed a trend to delay disease progression, the viremia (pox lesions and severe weight loss) that occurred after four IT injections indicated that too much virus was given, in too short period of time (Figure 10). Additionally, during the IT injections, it was observed that after the first VV-E3L^{OrfV} treatment, tumors had become pus-filled and seemed to implode. Subsequent treatments were injected at the tumor site, but it is possible that virus administered was delivered to SQ normal tissue rather than into tumor tissue. To prevent the reoccurrence of viremia, a lower

dose of virus should be administered, as well as limiting the number of doses or allowing a greater period of time between injections to allow mice a period of recovery. Nevertheless, the data collected were invaluable as they provide insight to how the virus functions within an immunodeficient host. In a clinical setting, many cancer patients are immunosuppressed due to standard of care therapies, it will be important to characterize VV-E3L^{OrfV} within this setting. Fortunately, there are FDA approved compounds, including vaccinia immune globulins (VIG) (117) and Cidofovir (27), that are able to be administered to treat serious adverse effects caused by VV infection. Lastly, the data collected from the B16F10LacZ lung model in immunocompetent mice shows that VV-E3L^{OrfV} is not pathogenic compared to WR when a functional immune system is present (Figure 12). Comparison of VV-E3L^{OrfV} with a current oncolytic candidate (i.e. VVdd) in this model and in other xenograft models will be important experiments to perform to further delineate its oncolytic potential.

Chapter 4 – Increasing the oncolytic efficacy of OrfV

4.1 Introduction

4.1.1 Orf virus

The prototypic *Parapoxvirus* OrfV, has a narrow host-range, in contrast to VV. It is only capable of infecting ruminants (goats and sheep) and shows limited pathogenicity in humans (38). OrfV infection causes cutaneous lesions with no systemic spread (42, 98). These lesions are characterized by extensive vascular proliferation and dilation of wounded epidermal cells, caused by the expression of vascular endothelial growth factor (VEGF) by the virus alongside host production (98). Both VV and OrfV are platforms for antiviral therapeutics due to the inherent nature of immune-stimulation (80, 114). Importantly, when compared to other poxviruses, it has been shown that OrfV has a unique immune-stimulation profile in a number of animal models, inducing a number of cytokines, such as interleukin-1β (IL-1β), IL-8, GM-CSF, IL-2 and IFN-γ (20, 40, 114) and accumulation of both innate and adaptive immune cells, such as natural killer cells, neutrophils, B cells and dendritic cells (39, 96). When compared with VV, OrfV has been shown to be more potent in the recruitment and activation of T cells, an intrinsic property of the viral particle itself (106). Lastly, while neutralizing antibodies are a limiting factor in oncolytic VSV and VV infection (90, 91), the presence of these antibodies against OrfV are rare (15, 42) and anti-OrfV immunity appears be short-lived (25, 42). Harnessing this unique profile, our lab has recently shown that OrfV is capable of inducing a potent antitumor immune response in syngeneic models of cancer and of its oncolytic potential in an A549 xenograft model of cancer (96). Nevertheless, OrfV has limited replication ability in a majority of mammalian

cancer cell lines which leaves the potential and possibility to increase OrfV's oncolytic potential.

4.1.2 Host-range genes

As mentioned in Chapter 1, VV has a very broad host-range. This in part is attributed to its host-range genes C7L, E3L, K1L and K3L (34, 82, 87, 88). VV mutants deleted of E3L or both C7L and K1L undergo abortive infection and express only a subset of viral genes (6, 7, 75, 87). OrfV contains a homologue of $E3L^{VV}$, whose importance and function was extensively covered in 3.1.1 and 3.1.2. Notably, OrfV does not contain homologues of C7L or K1L (74) and it is unknown if it contains a K3L homologue.

C7L is present or a functional homologue is present in almost all mammalian poxviruses, with the exception of Molluscum Contagiosum virus and *Parapoxvirus* genus (74). It is hypothesized that the C7L-like host-range gene may represent an adaptation of mammalian poxviruses to mammalian hosts (74). While its exact molecular function is still unknown, it has been shown that it is required for sustaining E3L expression in HeLa cells and thereby indirectly affecting PKR phosphorylation by affecting E3L expression (4, 74). Additionally, it is thought to have a role in inhibiting cellular apoptosis in response to VV infection (75). Recently, it has been shown that the reintroduction of $C7L^{VV}$ into the highly attenuated VV vaccine strain, NYVAC, which expresses four HIV-1 antigens from clade B (Env, Gag, Pol and Nef) has restored the capacity of the virus to replicate in mammalian cells while maintaining an attenuated phenotype in mice (80).

In contrast to C7L, K1L is present in only a few orthopoxviruses. It consists entirely of multiple ankyrin repeats, where it functions through novel ankyrin interaction surfaces for protein-ligand interactions (62, 75). It has been shown that K1L prevents the degradation of

IκBα, thereby inhibiting NF-κB (75, 100) in RK13 cells. Additionally, K1L is necessary to inhibit virus induced eIF2α phosphorylation in RK13 and HeLa cells (116). Importantly, either K1L or C7L can complement replication deficiency in ΔC7LΔK1L mutants even though these two genes share no sequence homology (87, 107) and both antagonize type I IFN pathway through a novel mechanism that does not involve directly inhibiting IFN signaling or PKR activation (75).

Two VV host-range genes, E3L and K3L, inhibit the activation of PKR and subsequent anti-viral cascade. E3L was covered in depth in 3.1.1 and Figure 1. The K3L gene product encodes a homolog of eIF2α subunit which acts to interfere with PKR's function to phosphorylate eIF2α (7, 8, 26). It has been recently shown that K3L may not be the only substrate for PKR and that it may play a role in virus dissemination *in vivo* (95).

4.1.3 Combination therapy

The use of combination therapeutics is a common strategy to circumvent the occurrence of multi-drug resistance and/or treatment failure. These additional agents can be FDA approved and/or novel agents whose exact mechanism of actions is unknown. In recent years there have been a number of publications involving the combination of radiation therapy, chemotherapeutics or biologic therapeutics and OVs (46, 83). The synergistic effect of these combinations allows for the reduction of drug concentrations thereby reducing the severity of adverse effects. In this study microtubule targeting agents, histone deacetylase inhibitors (HDACi), VSe's and other OVs were used in combination with OrfV.

There are two classes of microtubule targeting agents. Microtubule stabilizers, such as the anticancer therapy Paclitaxel (Taxol), function by stabilizing the microtubule polymer protecting it from disassembly, thereby blocking the progression of mitosis (49, 50). In

contrast, microtubule destabilizers, such as colchicine which was an anti-cancer therapy and currently is used to treat gout and familial Mediterranean disease, function by inhibiting microtubule polymerization by binding to tubulin, thereby inhibiting mitosis (49, 50). Our lab has shown that there is synergy of these agents in combination with oncolytic VSV, increasing viral spread, replication and virus-induced cytotoxicity (personal communication, Dr. J-S Diallo).

HDACi are small molecule compounds which have been found to have potent anti-cancer properties, as well as dampen cellular innate immune responses by preventing the transcription of antiviral genes after IFN stimulation of virus infection (37, 52, 68). Our lab and others have shown that HDACi Trichostatin A (TSA) and Suberoylanilide hydroxamic acid (SAHA/Vornistat) selectively and effectively increase oncolytic VSV and VV replication and spread in cancer cells while maintaining their safety profile (28, 68, 81).

VSe (1-15) compounds were found through a high-throughput screening method looking at the compounds ability to increase oncolytic VSV oncolysis (28). These compounds have been shown to enhance efficacy, while maintaining safety in normal tissues (29). While the mechanism of actions of most of the VSe compounds is still being elucidated, it was found that VSe1 functions by disrupting IFN-induced antiviral responses (29). Additionally, VSe7 has been shown to enhance the infection of both oncolytic VV and the attenuated MVA vaccine strain (personal communication with Drs. J-S Diallo and F. Le Boeuf). As more becomes known about VSes, this may be a strategy to increase OV oncolysis without genetically modifying the viruses and potentially altering their tropism.

With an arsenal of different OVs at our disposal, our lab has recently shown that there can be synergistic interaction between oncolytic VSV and VV (61). Oncolytic VSV is

extremely sensitive to the effects of type I IFNs (105) but the addition of oncolytic VV (VVdd) or filtered supernatants from a VVdd infection were able to abrogate this sensitivity, thereby increasing VSV oncolysis (61). This abrogation of IFN sensitivity can be attributed to the VV B18R soluble interferon receptor antagonist (2, 24, 108). Moreover, this phenomenon has also been observed with HSV (personal communication with Dr. F. Le Bouef). The presence of a B18R homolog in OrfV has yet to be established (72).

4.1.4 Rationale

OrfV has strong immune-stimulatory effects, but limited oncolytic potential. In contrast VV is a potent oncolytic virus with *some* immune-stimulatory effects. By combining the best attributes of both viruses and strategies used to increase efficacy of other OVs, OrfV can become another OV clinical candidate.

4.1.5 Hypothesis

The addition of VV host-range genes and/or combination therapy, will result in a safe and more potent OrfV oncolytic candidate.

4.1.6 Objectives

1. To select and characterize the best OrfV candidate for future studies, *in vitro*
2. To determine if the addition of VV host-range genes enhances OrfV oncolysis
3. To determine if combination therapy enhances OrfV oncolysis

4.2 Results

4.2.1 OrfV oncolytic properties.

Our lab has recently shown that OrfV has oncolytic properties (96). We have also observed that high passage OrfV (passage >6) is attenuated compared to low passage OrfV (passage=3) and making low passage OrfV the best candidate to work with. Therefore, prior to attempting to increase the oncolytic properties of OrfV we characterized the best candidates ability to replicate, spread and induce cytotoxicity in a number of human and murine cancer cell lines. A number of cell lines were permissive to virus replication and spread, including HeLa (Figure 13A) and A549 (Figure 13B) with greater than 100-fold increase in viral titers from the initial time points. For WT CT26 (Figure 13Ci) and OVCAR8 (Figure 13Di) there was a delay in virus replication by about 12 hours compared with HeLa and A549 cells. Additionally, OrfV was unable to spread in these cells. In MCF7 (Figure 13E) and 786O (Figure 13F) cells OrfV was unable to replicate or spread. In contrast to the differences between virus replication and spread among the cell lines tested, all the cell lines are resistant to OrfV-induced cytotoxicity at 72 hours post infection, as all cell lines required greater than MOI 1 to reach 50% cell death (Figure 13iii).

4.2.2 VV host-range genes are unable to increase OrfV oncolysis.

Host-range genes play an important role in VVs broad tropism. In contrast, OrfV has a very narrow tropism and importantly is from one of the few genera from the P*oxviridae* family not to contain homologues for all the VV host-range genes. This lead us to hypothesize that the addition of VV host-range genes—C7L, E3L, K1L or K3L—would increase OrfVs tropism and therefore enhance its oncolytic potential. Before being able to test the genes, they first needed to be amplified and cloned into a plasmid containing a

mammalian promoter. $C7L^{VV}$ and $K1L^{VV}$ cDNA were amplified from VV-COP DNA and $E3L^{VV}$ and $K3L^{VV}$ cDNA were amplified from VV-WR DNA. The genes were next cloned into pcDNA3.1(-). To confirm that the host-range pcDNA constructs were expressing the genes, western blot analysis was performed on pcDNA-$C7L^{VV}$ or pcDNA-$E3L^{VV}$ constructs transfected into HeLa cells, as there are no antibodies against K1L or K3L available. As a positive control, VV-COP infection was used, while HeLa protein lysate and pe-yfp plasmid served as negative controls, as well as pe-yfp served as a read-out of transfection efficiency (Figure 14A). Expression of $C7L^{VV}$ and $E3L^{VV}$ by pcDNA-$C7L^{VV}$ and pcDNA-$E3L^{VV}$, respectively began 6 hours post transfection, while the expression of these genes did not appear until 12 hours post infection with VV-COP (Figure 14B).

A pcDNA-VV host-range gene transient transfection/infection screen was created to test each genes ability to increase OrfV cytotoxicity. HeLa cells were transiently transfected with either pe-yfp-c1, pcDNA-$C7L^{VV}$, pcDNA-$E3L^{VV}$, pcDNA-$K1L^{VV}$ or pcDNA-$K3L^{VV}$ for 24 hours prior to infection with either OrfV at MOI 0.1 or mock infection. Transfection efficiency was confirmed through fluorescence microscopy of the pe-yfp transfected well (Figure 14C). 48 hours post OrfV infection cell viability was quantified by trypan blue exclusion. Cell viability of transiently transfected HeLa cells that were mock infected was not significantly altered compared to the mock transfected control (Figure 14D). The only exception was the pcDNA-$K3L^{VV}$ that significantly increased cell viability ($p=0.03$). OrfV infection of HeLa cells decreased cell viability compared with uninfected cells, but there was no statistically significant difference between the transiently transfected, OrfV infected cells compared to the mock transfected, OrfV infected control (Figure 14D).

Figure 13. Oncolytic potential of OrfV in a number of human and murine cancer cell lines. To assess OrfV viral replication and spread, single-step (i) and multi-step (ii) growth curves were performed, respectively, in HeLa (A), A549 (B), WT CT26 (C), OVCAR8 (D), MCF7 (E) and 786O (F) cells. Additionally, OrfV-induced cytotoxicity at 72 hours post infection (iii; n=6) was analyzed.

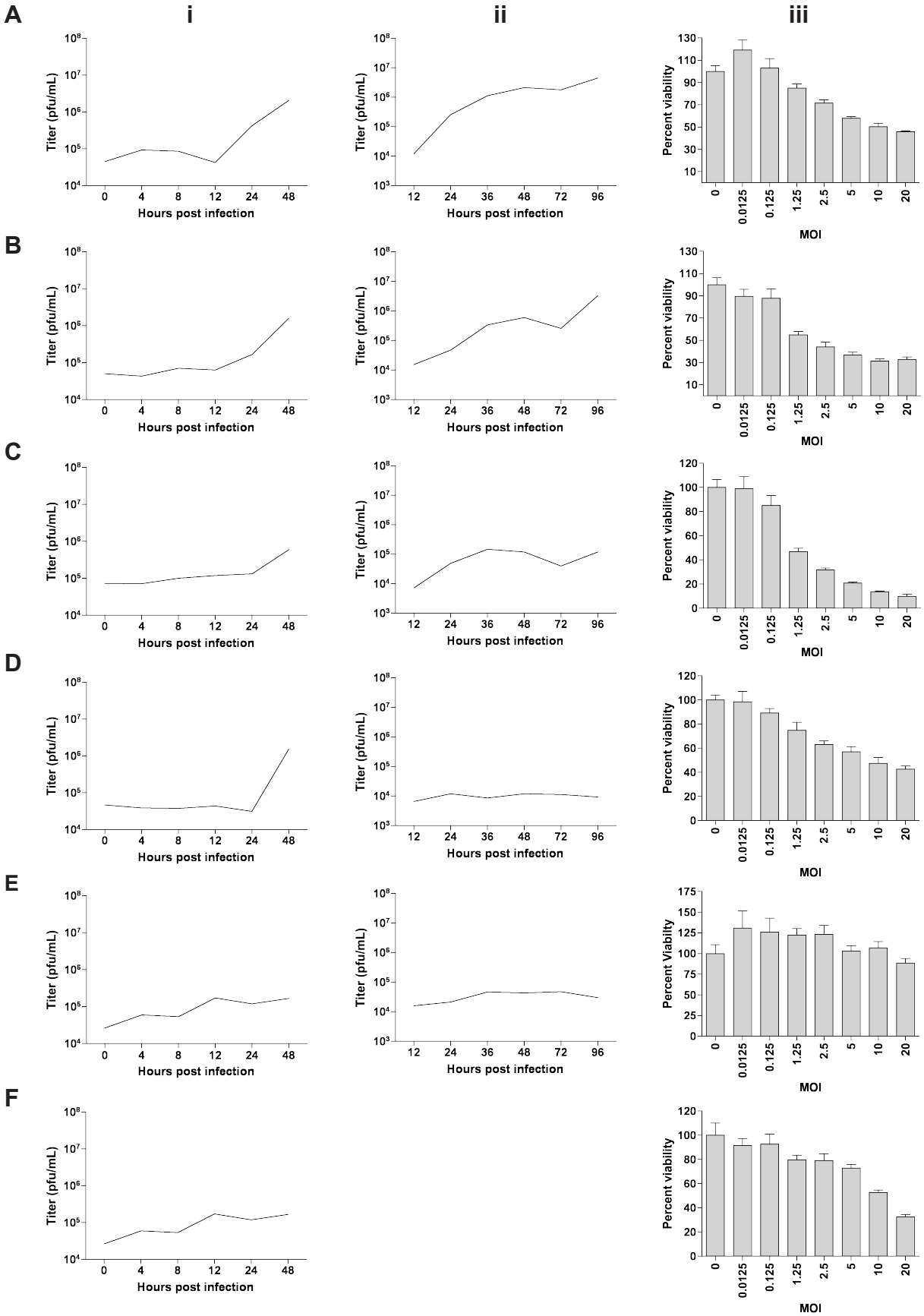
A
i
ii
iii
B
C
D
E
F
Titer (pfu/mL)
Hours post infection
Percent viability
Percent Viabilty
MOI
0
0.0125
0.125
1.25
2.5
5
10
20

Figure 14. Vaccinia virus host-range genes are unable to enhance OrfV-induced HeLa cell killing. To confirm expression of $C7L^{VV}$ and $E3L^{VV}$ proteins in their respective pcDNA3.1 constructs, subconfluent monolayers of HeLa cells were transfected using pe-yfp, pcDNA-$C7L^{VV}$ or pcDNA-$E3L^{VV}$ for 3 hours. Additionally, cells were infected with VV-COP at MOI 0.5 as a positive control. Transfection efficiency was confirmed by presence of YFP positive cells in the pe-yfp transfected cells (A). Western blotting was then performed to confirm expression of $C7L^{VV}$ and $E3L^{VV}$ in transfected cells and in HeLa cells infected with VV-COP at 6 and 12 hours post infection (B). Next, to determine if VV host-range genes enhance OrfV-induced cell killing, HeLa cells were mock transfected or transfected with pe-yfp, pcDNA-$C7L^{VV}$, pcDNA-$E3L^{VV}$, pcDNA-$K1L^{VV}$ or pcDNA-$K3L^{VV}$. 24 hours post transfection, efficiency was confirmed by presence of YFP positive cells in the pe-yfp transfected cells (C; inset). Cells were then either mock infected (B; *p=0.03) or infected with OrfV at MOI 0.1 (D) directly into media. Viability was quantified 48 hours post infection by trypan blue exclusion (n=3).

A

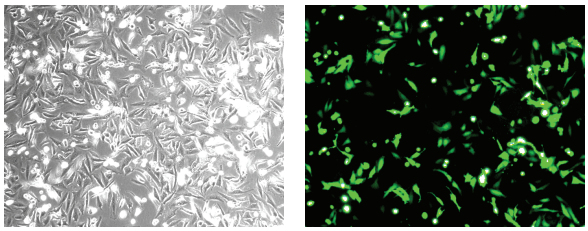

B

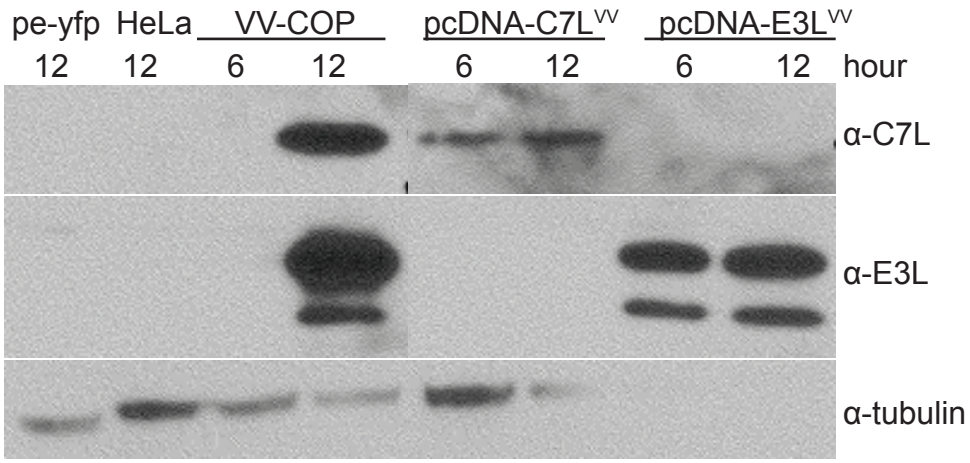
pe-yfp HeLa VV-COP pcDNA-C7L^VV pcDNA-E3L^VV
12 12 6 12 6 12 6 12 hour
α-C7L
α-E3L
α-tubulin

C

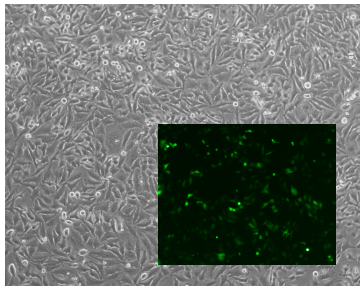

D

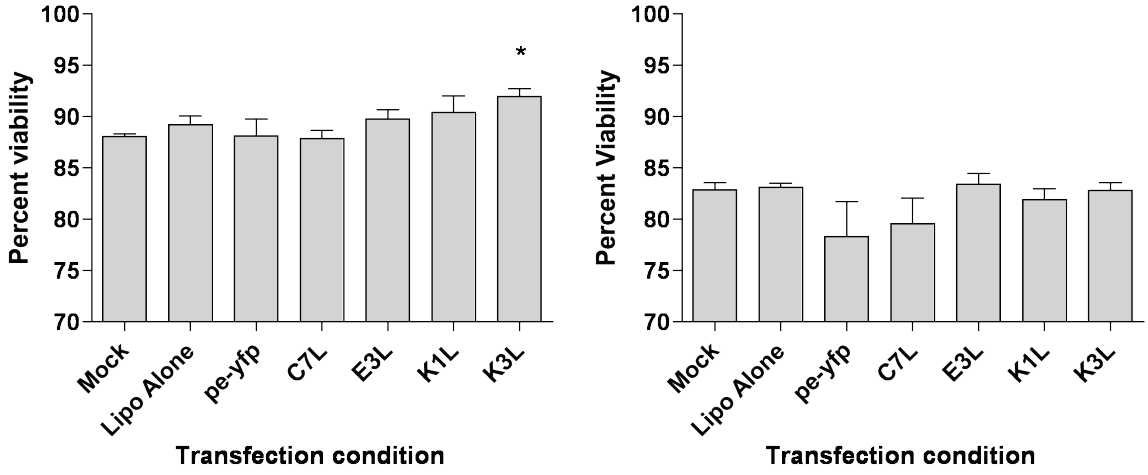
Percent viability
100
95
90
85
80
75
70
*
Mock
Lipo Alone
pe-yfp
C7L
E3L
K1L
K3L
Transfection condition
Percent Viability
100
95
90
85
80
75
70
Mock
Lipo Alone
pe-yfp
C7L
E3L
K1L
K3L
Transfection condition

4.2.3 Microtubule targeting and VSe agents are unable to increase OrfV oncolysis.

Combination therapy is a strategy commonly used in cancer treatment to attack the tumor and/or metastases at as many fronts as possible. Our lab has found that there are many VSe compounds and FDA approved drugs that enhance oncolytic VSV, HSV and VV therapy. With this knowledge we asked if any of the microtubule targeting agents or VSe compounds would be able to enhance OrfV infection. Human 786O, HT29 and MCF7 cancer cells, along with murine 4T1 cancer cells were tested. Cells were plated in 96-well dishes. Once confluent, cells were pretreated with two-fold dilutions of drug for 4 hours. Cells were then either mock infected or infected with OrfV at MOI 0.1 for 72 hours. Cytotoxicity was then quantified by alamarBlue assay. The microtubule targeting agents alone were quite cytotoxic, especially at the highest doses in the human cancer cell lines tested (Figure 15A, B, C and D). In contrast, VSe11, VSe7 and VSe6 showed little toxicity alone (Figure 16A, B, C and D). Nevertheless, neither colchicine nor Paclitaxel were able to enhance OrfV-induced cytotoxicity in any of the cell lines tested (Figure 15). While there looks to be enhancement of OrfV-induced cytotoxicity with both drugs in 4T1 cells at the lowest dose given, the two-fold higher concentration was not enhanced and may be an artifact of the assay (Figure 15D). No enhancement was observed with the addition of VSe compounds in all cell lines tested (Figure 16).

4.2.4 VV soluble interferon receptor B18R is unable to increase OrfV oncolysis.

The use of exogenous B18R has previously been shown to enhance oncolytic VSVΔM51 infection in cancer cells, while maintaining its safety profile (61). This observation lead us to postulate that exogenous $B18R^{VV}$ would also enhance OrfV infection.

While previous studies were able to visualize virus enhancement by increased expression of fluorescence,

OrfV does not contain a fluorescent tag, therefore visualization of virus enhancement would have to be by phase-contrast microscopy and enhancement of CPE. As $B18R^{VV}$ is a soluble factor that is secreted throughout the VV replication cycle (2), U2OS cells were infected with VVdd-mCherry at a low MOI. 24 hours post infection, the supernatant was filtered through a 0.22 μM to remove any infectious viral particles, leaving only the soluble factors secreted during VV infection, including B18R (Figure 17A). As a control, supernatants from uninfected cells was also filtered. The filtered supernatant was then added to confluent monolayers of 786O, HT29 and WT CT26 cells for 2 hours. Cells were then infected for 48 hours. As a positive control, 786O cells were also infected with VSVΔM51-eGFP. The addition of $B18R^{VV}$ supernatant enhanced VSVΔ5M1-eGFP infection (Figure 17B top panel) compared with the addition of control supernatant. In contrast, there was no increase in CPE in OrfV infected cells in the presence of $B18R^{VV}$ (Figure 17B).

Figure 15. Microtubule destabilizing and stabilizing agents, Colchicine and Paclitaxel, respectively, are unable to enhance OrfV oncolysis. Dose-response curves of decreasing concentrations of drugs in the absence (black square) or presence (blue triangle) of OrfV at MOI 0.1 was performed in HT29 (A), MCF7 (B), 786O (C) and WT CT26 (D) cells (n=3).

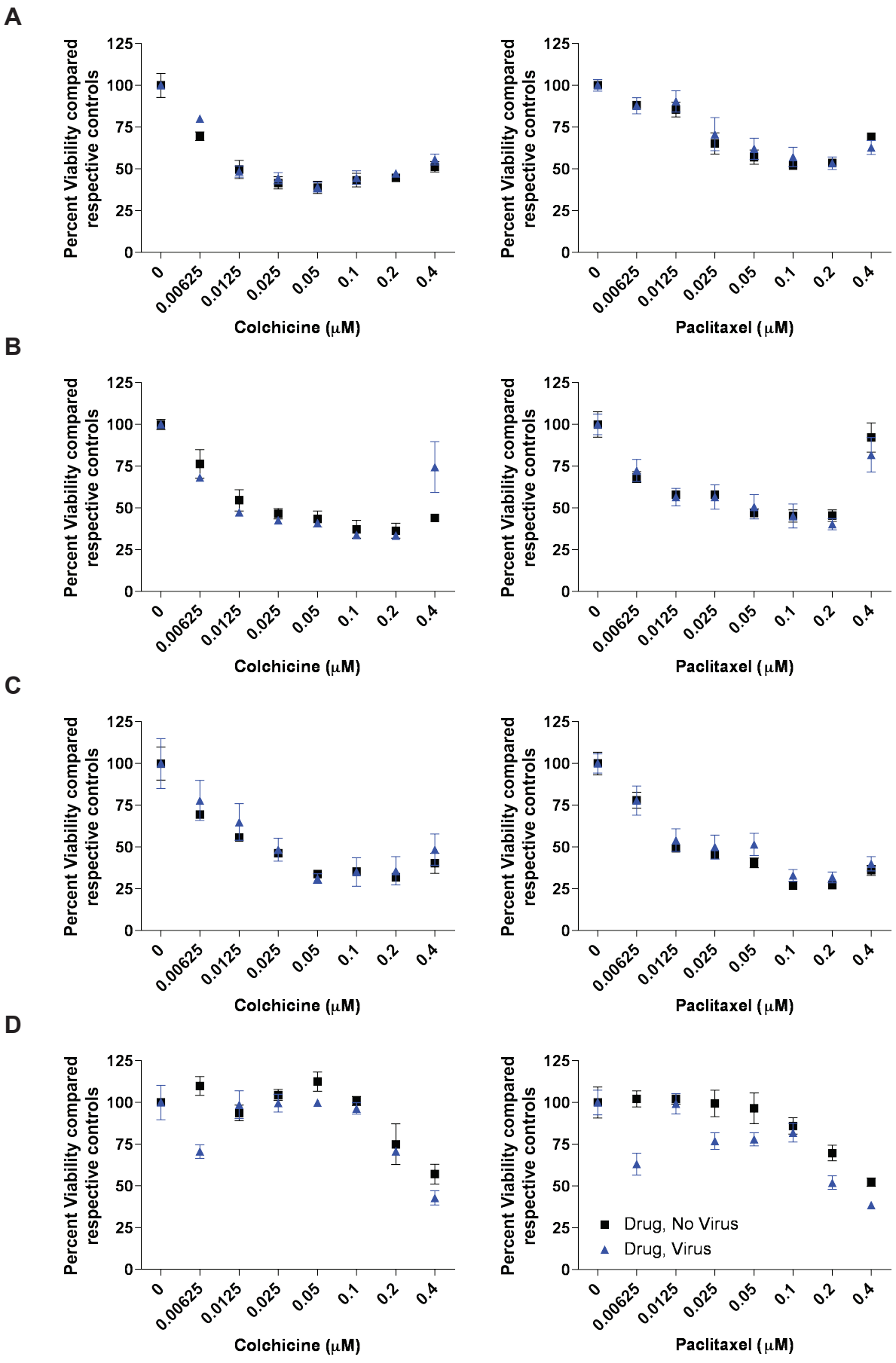
A
B
C
D
Percent Viability compared respective controls
125
100
75
50
25
0
0
0.00625
0.0125
0.025
0.05
0.1
0.2
0.4
Colchicine (μM)
Paclitaxel (μM)
Drug, No Virus
Drug, Virus

Figure 16. Viral sensitizing agents VSe11, VSe7 and VSe6 are unable to enhance OrfV oncolysis. Dose-response curves of decreasing concentrations of drugs in the absence (black square) or presence (blue triangle) of OrfV at MOI 0.1 was performed in (A) HT29 (B) MCF7 (C) 786O (D) WT CT26 cells (n=3).

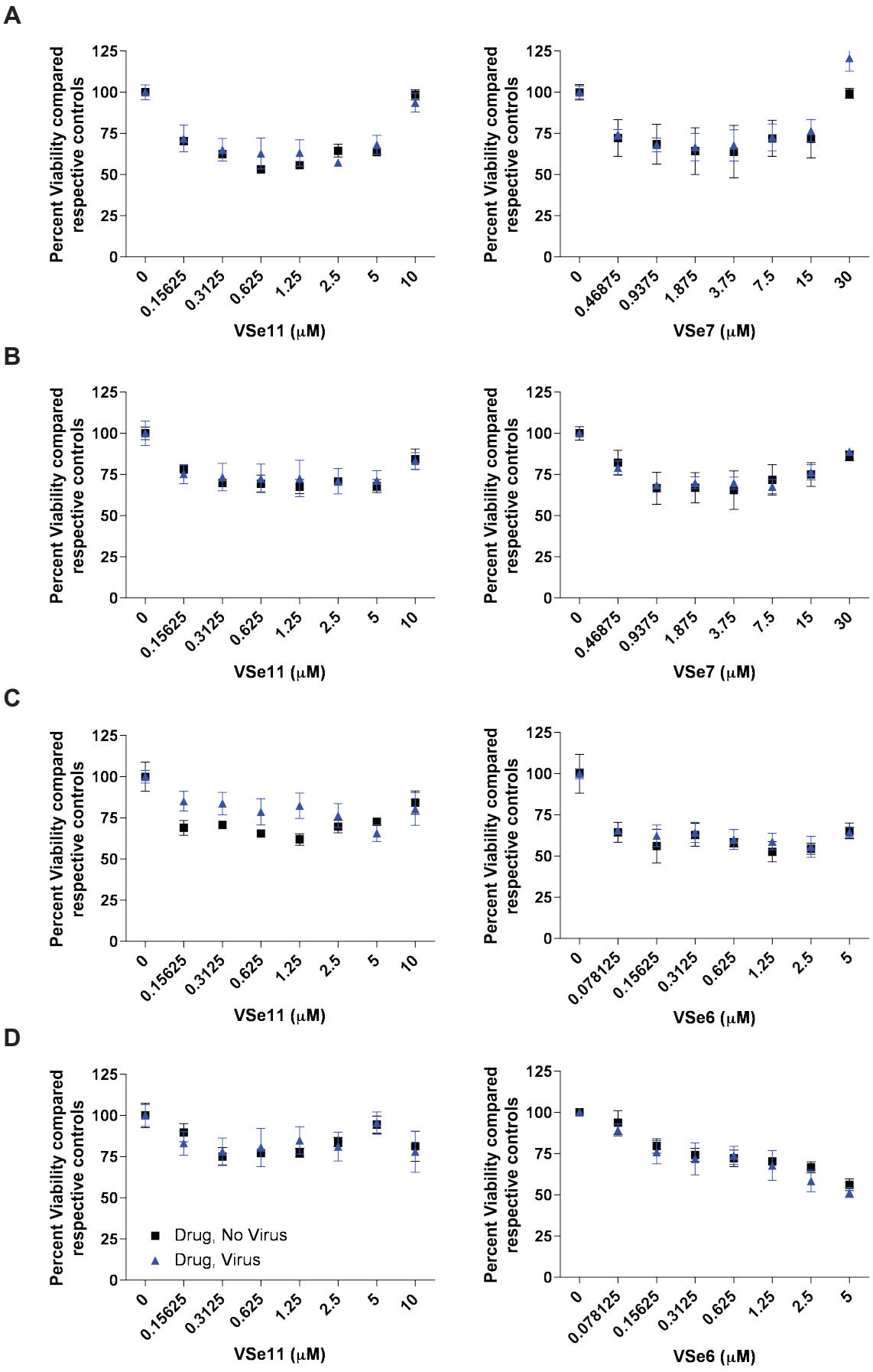
A
B
C
D
Percent Viability compared respective controls
125
100
75
50
25
0
0
0.15625
0.3125
0.625
1.25
2.5
5
10
VSe11 (μM)
0
0.46875
0.9375
1.875
3.75
7.5
15
30
VSe7 (μM)
0
0.078125
0.15625
0.3125
0.625
1.25
2.5
5
VSe6 (μM)
Drug, No Virus
Drug, Virus

Figure 17. Vaccinia virus soluble interferon receptor B18R is unable to enhance OrfV infection. U2OS cells were infected with VVdd-mCherry at MOI 0.1 or mock infected in a minimal volume for 1 hour. Complete media was then added to the cells and infection was allowed to persist for 24 hours. Fluorescence microscopy was then performed to confirm productive VVdd-mCherry infection (A). Supernatants from mock and VVdd-mCherry infected cells were harvested and filtered through 0.22 μM filter directly into naïve 786O, CT26 or HT29 cells. Cells were incubated for 2 hours and then infected with OrfV at MOI 0.1 directly. As a positive control, 786-O cells were infected with VSVΔM51-eGFP at MOI 0.1 in the presence or absence of VVdd-mCherry supernatant. 48 hours post infection phase-contrast microscopy was performed to visualize any enhancement of virus infection (B).

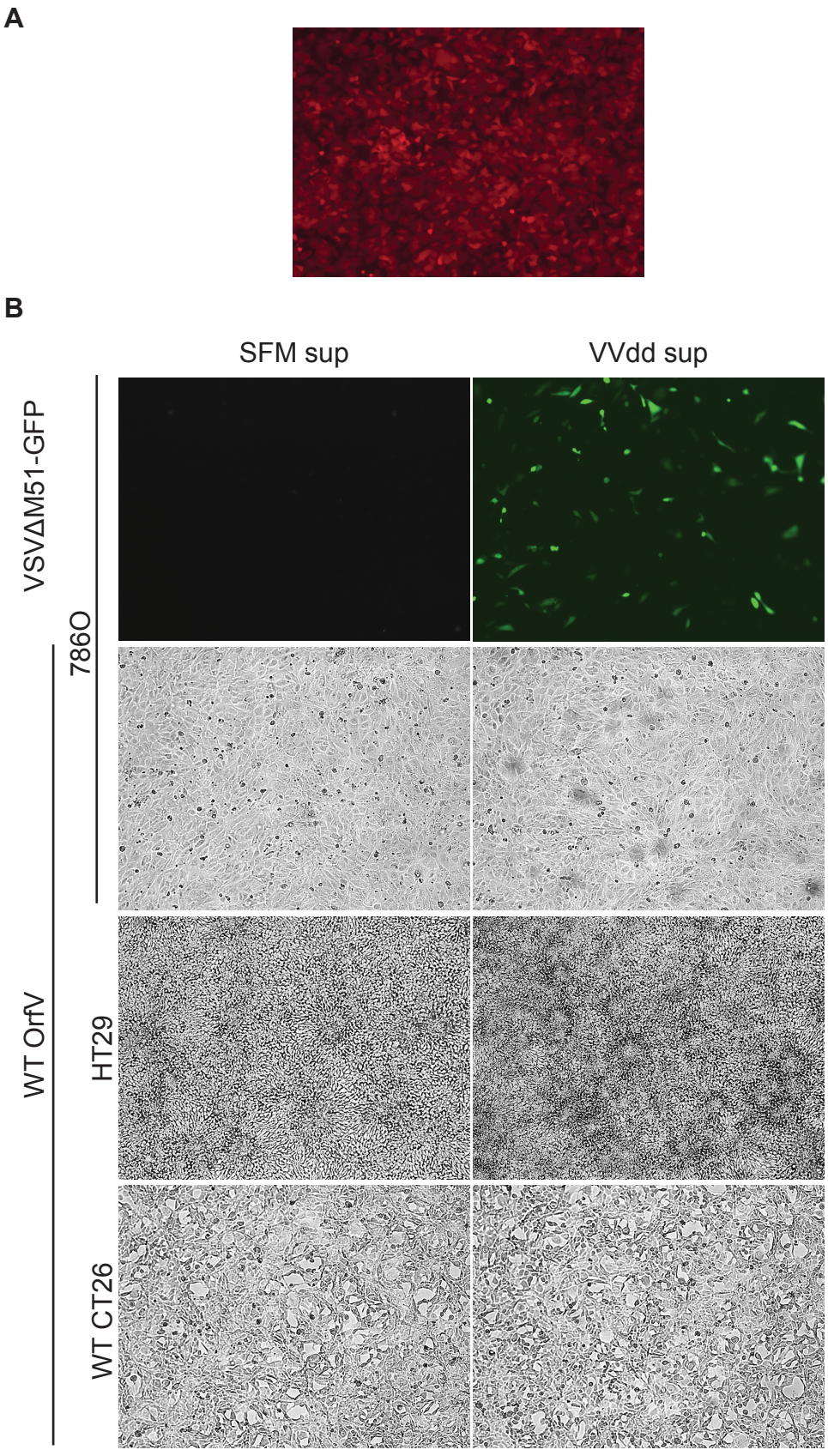
A
B
SFM sup
VVdd sup
VSVΔM51-GFP
786O
WT OrfV
HT29
WT CT26

4.3 Discussion

4.3.1 OrfV has potential to become a potent OV

OrfV has been previously shown to productively infect a number of human and murine cancer cell lines, but this ability is limited compared to current clinical OV candidates (96). Cell lines were chosen to represent those which OrfV readily infects and also those which are resistant to infection (Figure 13). One common feature shared between permissive and resistant cell lines was the inability of OrfV to induce cytotoxicity at low MOIs (<1) compared with other oncolytic candidates including VV and VSV. There are many possible reasons for this disparity including the differences in viral host-ranges, life cycles and host anti-viral responses. Both VV and VSV have broad host-ranges allowing these viruses, as genetically different as they are, to infect a large subset of mammalian cells. In contrast, OrfV has a narrow host-range restricting its ability to infect many mammalian cells. Compared to poxviruses, VSV has a short and rapid viral life cycle, nevertheless, VV is still able to induce significant oncolysis compared to OrfV. Using the differences between the various efficacious OVs and the baseline data of OrfVs oncolytic potential we can apply various strategies to alter its host-range and/or enhance its anti-viral mechanisms.

4.3.2 VV host-range genes are unable to enhance OrfV

The insertion of VV host-range genes, notably C7L into super attenuated VV vaccine strain NYVAC, has resulted in the viruses increased ability to replicate in mammalian cells while maintaining their safety profiles (33). This strategy therefore seemed to be a promising avenue to pursue, especially in light of the fact that OrfV did not contain homologues of C7L and K1L and it is unknown if it contains a K3L homologue (74). While the strategy of a transient transfection/infection that was used to screen the VV host-range genes was

unsuccessful in increasing OrfV oncolysis it may be worthwhile to continue to pursue these genes. Prior to any further studies, the pcDNA-VV host-range constructs must be shown to function when transfected into cells. As all these genes have a function in inhibiting the activation of PKR and its subsequent anti-viral properties, the phosphorylation status of PKR could be a read-out of functionality. Once their function has been established, the timing of transfection and OrfV infection will need to be determined. We may have to better mimic the timing that occurs during a VV infection to see efficacy. As the average time for initial expression of VV host-range is between 6 and 8 hours post infection (4) and expression of the pcDNA constructs begins at 6 hours post transfection (Figure 14), transfection and infection concurrently may be the best way to determine whether or not their presence will augment OrfV. Lastly, OrfV-induced cytotoxicity should not be the only read-out as the VV host-range genes may enhance another aspect of oncolytic OrfV such as viral titers.

In concert with creating the pcDNA-C7L^{VV} construct, C7L^{VV} was also cloned into the OrfV pV41 plasmid allowing for the insertion of our gene of interest into an intergenic region of OrfV through homologous recombination. OrfV plaques positive for the C7L^{VV} insertion were selected for their expression of β-glucuronidase for five successive rounds. C7L^{VV} PCR confirmation was performed during the fifth round (Appendix II). Expression of β-glucuronidase was rapidly lost in the following rounds of purification and further attempts to rescue the virus were unsuccessful. There are a few potential reasons why the rescue of OrfV-C7L^{VV} recombinants failed. We can postulate that the insertion of C7L^{VV} resulted in genetic instability of the virus. As OrfV is one of the only poxviruses not to contain a C7L homologue, there may have been an evolutionary selection for an OrfV clone that had a narrow host-range allowing for its ability to infect ungulates (42). As the exact function of

$C7L^{VV}$ is still unknown, it is also possible to hypothesize that the cloned C7L cDNA is missing an important component for its proper function.

4.3.3 Combination therapy is unsuccessful in increasing OrfV oncolysis.

Whereas the addition of microtubule targeting agents, VSe compounds and B18R has enhanced the effect of many oncolytic candidates including VSVΔM51, HSV and VV, this strategy did not have an impact on OrfV oncolysis (Figures 14, 15 and 16). The mechanism of action of all of these therapies seems to hinge on the host cell anti-viral response (personal communication, J-S Diallo) (68, 81). As OrfV has a unique immune-stimulatory profile we can postulate that the addition of these compounds may negatively impact this profile. Using the previously established OrfV efficacy in the *in vivo* lung models we could hypothesize that addition of these compounds negatively impacts OrfV-induced immune stimulation and decreases its efficacy. Additionally, looking only at the drug effects on OrfV-induced cytotoxicity may have also prevented us from observing any other changes, to OrfV infection. It is also possible, that combination therapy just does not have any positive or negative effects on OrfV. Lastly, for combination therapy to work we may have to use more than one compound in combination, each targeting a different mechanism to see efficacy.

Chapter 5 – Conclusions

VV-E3L^{OrfV} is a novel OV where the attenuation by substitution of the E3L host-range gene from VV to that of the OrfV homologue resulted in a potent oncolytic, while not reducing the viruses overall fitness, in cancer cells. We found that VV-E3L^{OrfV} was sensitive to IFN in human normal fibroblast cells and additionally its infection was attenuated in normal HDFn cells compared to parental WR and its attenuated recombinants. The virus was also less pathogenic when administered *in vivo*. VV-E3L^{OrfV} was at least as oncolytic as WR and its attenuated recombinants *in vitro*, in both murine and human cancer cell lines. Additionally, VV-E3L^{OrfV} showed efficacy in the B16F10LacZ lung model. While there are still experiments that need to be performed, we propose that further clinical evaluation of OV's which retain their viral efficacy is merited.

OrfV is able to mount a potent anti-tumor response that is NK cell-mediated. Nevertheless, OrfVs oncolytic potential is still quite weak. The strategies we employed to increase the oncolytic efficacy of OrfV, including the use of VV host-range genes or combination therapy—using microtubule targeting agents, VSe compounds or VV B18R—did not work. It is possible, as technologies advance and more information is known about OrfV, that these strategies may work in the future. The question is not if, but when will it be possible to increase the oncolytic efficacy of OrfV. Once available, viral oncolysis combined with its unique immune-stimulatory properties, OrfV can be powerful weapon to use in our war against cancer.

References

1. **Ahn, M., S. J. Lee, X. Li, J. A. Jimenez, Y. P. Zhang, K. H. Bae, Y. Mohammadi, C. Kao, and T. A. Gardner.** 2009. Enhanced combined tumor-specific oncolysis and suicide gene therapy for prostate cancer using M6 promoter. Cancer gene therapy **16:**73-82.

2. **Alcami, A., J. A. Symons, and G. L. Smith.** 2000. The vaccinia virus soluble alpha/beta interferon (IFN) receptor binds to the cell surface and protects cells from the antiviral effects of IFN. Journal of virology **74:**11230-11239.

3. **Allen, K. E., and G. J. Weiss.** 2010. Resistance may not be futile: microRNA biomarkers for chemoresistance and potential therapeutics. Molecular cancer therapeutics **9:**3126-3136.

4. **Backes, S., K. M. Sperling, J. Zwilling, G. Gasteiger, H. Ludwig, E. Kremmer, A. Schwantes, C. Staib, and G. Sutter.** 2010. Viral host-range factor C7 or K1 is essential for modified vaccinia virus Ankara late gene expression in human and murine cells, irrespective of their capacity to inhibit protein kinase R-mediated phosphorylation of eukaryotic translation initiation factor 2alpha. The Journal of general virology **91:**470-482.

5. **Barber, G. N.** 2005. VSV-tumor selective replication and protein translation. Oncogene **24:**7710-7719.

6. **Beattie, E., E. B. Kauffman, H. Martinez, M. E. Perkus, B. L. Jacobs, E. Paoletti, and J. Tartaglia.** 1996. Host-range restriction of vaccinia virus E3L-specific deletion mutants. Virus genes **12:**89-94.

7. **Beattie, E., E. Paoletti, and J. Tartaglia.** 1995. Distinct patterns of IFN sensitivity observed in cells infected with vaccinia K3L- and E3L- mutant viruses. Virology **210:**254-263.

8. **Beattie, E., J. Tartaglia, and E. Paoletti.** 1991. Vaccinia virus-encoded eIF-2 alpha homolog abrogates the antiviral effect of interferon. Virology **183:**419-422.

9. **Bossow, S., C. Grossardt, A. Temme, M. F. Leber, S. Sawall, E. P. Rieber, R. Cattaneo, C. von Kalle, and G. Ungerechts.** 2011. Armed and targeted measles virus for chemovirotherapy of pancreatic cancer. Cancer gene therapy **18:**598-608.

10. **Braidwood, L., P. D. Dunn, S. Hardy, T. R. Evans, and S. M. Brown.** 2009. Antitumor activity of a selectively replication competent herpes simplex virus (HSV) with enzyme prodrug therapy. Anticancer research **29:**2159-2166.

11. **Brandt, T., M. C. Heck, S. Vijaysri, G. M. Jentarra, J. M. Cameron, and B. L. Jacobs.** 2005. The N-terminal domain of the vaccinia virus E3L-protein is required

for neurovirulence, but not induction of a protective immune response. Virology **333:**263-270.

12. **Breitbach, C. J., J. Burke, D. Jonker, J. Stephenson, A. R. Haas, L. Q. Chow, J. Nieva, T. H. Hwang, A. Moon, R. Patt, A. Pelusio, F. Le Boeuf, J. Burns, L. Evgin, N. De Silva, S. Cvancic, T. Robertson, J. E. Je, Y. S. Lee, K. Parato, J. S. Diallo, A. Fenster, M. Daneshmand, J. C. Bell, and D. H. Kirn.** 2011. Intravenous delivery of a multi-mechanistic cancer-targeted oncolytic poxvirus in humans. Nature **477:**99-102.

13. **Breitbach, C. J., N. S. De Silva, T. J. Falls, U. Aladl, L. Evgin, J. Paterson, Y. Y. Sun, D. G. Roy, J. L. Rintoul, M. Daneshmand, K. Parato, M. M. Stanford, B. D. Lichty, A. Fenster, D. Kirn, H. Atkins, and J. C. Bell.** 2011. Targeting tumor vasculature with an oncolytic virus. Molecular therapy : the journal of the American Society of Gene Therapy **19:**886-894.

14. **Breitbach, C. J., T. Reid, J. Burke, J. C. Bell, and D. H. Kirn.** 2010. Navigating the clinical development landscape for oncolytic viruses and other cancer therapeutics: no shortcuts on the road to approval. Cytokine & growth factor reviews **21:**85-89.

15. **Buddle, B. M., R. W. Dellers, and G. G. Schurig.** 1984. Contagious ecthyma virus-vaccination failures. American journal of veterinary research **45:**263-266.

16. **Buller, R. M., S. Chakrabarti, J. A. Cooper, D. R. Twardzik, and B. Moss.** 1988. Deletion of the vaccinia virus growth factor gene reduces virus virulence. Journal of virology **62:**866-874.

17. **Buller, R. M., S. Chakrabarti, B. Moss, and T. Fredrickson.** 1988. Cell proliferative response to vaccinia virus is mediated by VGF. Virology **164:**182-192.

18. **Buller, R. M., G. L. Smith, K. Cremer, A. L. Notkins, and B. Moss.** 1985. Decreased virulence of recombinant vaccinia virus expression vectors is associated with a thymidine kinase-negative phenotype. Nature **317:**813-815.

19. **Burke, J. M.** 2010. GM-CSF-armed, replication-competent viruses for cancer. Cytokine & growth factor reviews **21:**149-151.

20. **Buttner, M., C. P. Czerny, K. H. Lehner, and K. Wertz.** 1995. Interferon induction in peripheral blood mononuclear leukocytes of man and farm animals by poxvirus vector candidates and some poxvirus constructs. Veterinary immunology and immunopathology **46:**237-250.

21. **Canadian Cancer Society/National Cancer Institute of Canada**. Canadian Cancer Statistics 2012, Toronto, Canada.

22. **Chang, H. W., J. C. Watson, and B. L. Jacobs.** 1992. The E3L gene of vaccinia virus encodes an inhibitor of the interferon-induced, double-stranded RNA-dependent protein kinase. Proceedings of the National Academy of Sciences of the United States of America **89:**4825-4829.

23. **Choi, K. J., J. H. Kim, Y. S. Lee, J. Kim, B. S. Suh, H. Kim, S. Cho, J. H. Sohn, G. E. Kim, and C. O. Yun.** 2006. Concurrent delivery of GM-CSF and B7-1 using an oncolytic adenovirus elicits potent antitumor effect. Gene therapy **13:**1010-1020.

24. **Colamonici, O. R., P. Domanski, S. M. Sweitzer, A. Larner, and R. M. Buller.** 1995. Vaccinia virus B18R gene encodes a type I interferon-binding protein that blocks interferon alpha transmembrane signaling. The Journal of biological chemistry **270:**15974-15978.

25. **Czerny, C. P., C. Zeller-Lue, A. M. Eis-Hubinger, O. R. Kaaden, and H. Meyer.** 1997. Characterization of a cowpox-like orthopox virus which had caused a lethal infection in man. Archives of virology. Supplementum **13:**13-24.

26. **Davies, M. V., H. W. Chang, B. L. Jacobs, and R. J. Kaufman.** 1993. The E3L and K3L vaccinia virus gene products stimulate translation through inhibition of the double-stranded RNA-dependent protein kinase by different mechanisms. Journal of virology **67:**1688-1692.

27. **De Clercq, E.** 2002. Cidofovir in the treatment of poxvirus infections. Antiviral research **55:**1-13.

28. **Diallo, J. S., F. Le Boeuf, F. Lai, J. Cox, M. Vaha-Koskela, H. Abdelbary, H. MacTavish, K. Waite, T. Falls, J. Wang, R. Brown, J. E. Blanchard, E. D. Brown, D. H. Kirn, J. Hiscott, H. Atkins, B. D. Lichty, and J. C. Bell.** 2010. A high-throughput pharmacoviral approach identifies novel oncolytic virus sensitizers. Molecular therapy : the journal of the American Society of Gene Therapy **18:**1123-1129.

29. **Diallo, J. S., D. Roy, H. Abdelbary, N. De Silva, and J. C. Bell.** 2011. Ex vivo infection of live tissue with oncolytic viruses. Journal of visualized experiments : JoVE.

30. **Evgin, L., M. Vaha-Koskela, J. Rintoul, T. Falls, F. Le Boeuf, J. W. Barrett, J. C. Bell, and M. M. Stanford.** 2010. Potent oncolytic activity of raccoonpox virus in the absence of natural pathogenicity. Molecular therapy : the journal of the American Society of Gene Therapy **18:**896-902.

31. **Fenner, F.** 1982. A successful eradication campaign. Global eradication of smallpox. Reviews of infectious diseases **4:**916-930.

32. **Foloppe, J., J. Kintz, N. Futin, A. Findeli, P. Cordier, Y. Schlesinger, C. Hoffmann, C. Tosch, J. M. Balloul, and P. Erbs.** 2008. Targeted delivery of a suicide gene to human colorectal tumors by a conditionally replicating vaccinia virus. Gene therapy **15:**1361-1371.

33. **Garcia-Arriaza, J., J. L. Najera, C. E. Gomez, N. Tewabe, C. O. Sorzano, T. Calandra, T. Roger, and M. Esteban.** 2011. A candidate HIV/AIDS vaccine (MVA-B) lacking vaccinia virus gene C6L enhances memory HIV-1-specific T-cell responses. PloS one **6:**e24244.

34. **Gillard, S., D. Spehner, R. Drillien, and A. Kirn.** 1986. Localization and sequence of a vaccinia virus gene required for multiplication in human cells. Proceedings of the National Academy of Sciences of the United States of America **83:**5573-5577.

35. **Goebel, S. J., G. P. Johnson, M. E. Perkus, S. W. Davis, J. P. Winslow, and E. Paoletti.** 1990. The complete DNA sequence of vaccinia virus. Virology **179:**247-266, 517-263.

36. **Gonzalez-Santamaria, J., M. Campagna, M. A. Garcia, L. Marcos-Villar, D. Gonzalez, P. Gallego, F. Lopitz-Otsoa, S. Guerra, M. S. Rodriguez, M. Esteban, and C. Rivas.** 2011. Regulation of vaccinia virus E3 protein by small ubiquitin-like modifier proteins. Journal of virology **85:**12890-12900.

37. **Gu, W., I. Nusinzon, R. D. Smith, Jr., C. M. Horvath, and R. B. Silverman.** 2006. Carbonyl- and sulfur-containing analogs of suberoylanilide hydroxamic acid: Potent inhibition of histone deacetylases. Bioorganic & medicinal chemistry **14:**3320-3329.

38. **Haig, D., C. McInnes, D. Deane, A. Lear, N. Myatt, H. Reid, J. Rothel, H. F. Seow, P. Wood, D. Lyttle, and A. Mercer.** 1996. Cytokines and their inhibitors in orf virus infection. Veterinary immunology and immunopathology **54:**261-267.

39. **Haig, D. M., D. L. Deane, N. Myatt, J. Thomson, G. Entrican, J. Rothel, and H. W. Reid.** 1996. The activation status of ovine CD45R+ and CD45R- efferent lymph T cells after orf virus reinfection. Journal of comparative pathology **115:**163-174.

40. **Haig, D. M., and C. J. McInnes.** 2002. Immunity and counter-immunity during infection with the parapoxvirus orf virus. Virus research **88:**3-16.

41. **Haig, D. M., C. J. McInnes, J. Thomson, A. Wood, K. Bunyan, and A. Mercer.** 1998. The orf virus OV20.0L gene product is involved in interferon resistance and inhibits an interferon-inducible, double-stranded RNA-dependent kinase. Immunology **93:**335-340.

42. **Haig, D. M., and A. A. Mercer.** 1998. Ovine diseases. Orf. Veterinary research **29:**311-326.

43. **Hanahan, D., and R. A. Weinberg.** 2011. Hallmarks of cancer: the next generation. Cell **144:**646-674.

44. **Hengstschlager, M., M. Knofler, E. W. Mullner, E. Ogris, E. Wintersberger, and E. Wawra.** 1994. Different regulation of thymidine kinase during the cell cycle of normal versus DNA tumor virus-transformed cells. The Journal of biological chemistry **269:**13836-13842.

45. **Hengstschlager, M., E. Mullner, and E. Wawra.** 1994. Thymidine kinase is expressed differently in transformed versus normal-cells - a novel test for malignancy. International journal of oncology **4:**207-210.

46. **Heo, J., C. J. Breitbach, A. Moon, C. W. Kim, R. Patt, M. K. Kim, Y. K. Lee, S. Y. Oh, H. Y. Woo, K. Parato, J. Rintoul, T. Falls, T. Hickman, B. G. Rhee, J. C. Bell, D. H. Kirn, and T. H. Hwang.** 2011. Sequential therapy with JX-594, a targeted oncolytic poxvirus, followed by sorafenib in hepatocellular carcinoma: preclinical and clinical demonstration of combination efficacy. Molecular therapy : the journal of the American Society of Gene Therapy **19:**1170-1179.

47. **Hsiao, J. C., C. S. Chung, and W. Chang.** 1999. Vaccinia virus envelope D8L protein binds to cell surface chondroitin sulfate and mediates the adsorption of intracellular mature virions to cells. Journal of virology **73:**8750-8761.

48. **Hwang, T. H., A. Moon, J. Burke, A. Ribas, J. Stephenson, C. J. Breitbach, M. Daneshmand, N. De Silva, K. Parato, J. S. Diallo, Y. S. Lee, T. C. Liu, J. C. Bell, and D. H. Kirn.** 2011. A mechanistic proof-of-concept clinical trial with JX-594, a targeted multi-mechanistic oncolytic poxvirus, in patients with metastatic melanoma. Molecular therapy : the journal of the American Society of Gene Therapy **19:**1913-1922.

49. **Jordan, M. A., and L. Wilson.** 1998. Microtubules and actin filaments: dynamic targets for cancer chemotherapy. Current opinion in cell biology **10:**123-130.

50. **Jordan, M. A., and L. Wilson.** 2004. Microtubules as a target for anticancer drugs. Nature reviews. Cancer **4:**253-265.

51. **Katze, M. G., Y. He, and M. Gale, Jr.** 2002. Viruses and interferon: a fight for supremacy. Nature reviews. Immunology **2:**675-687.

52. **Kelly, W. K., and P. A. Marks.** 2005. Drug insight: Histone deacetylase inhibitors--development of the new targeted anticancer agent suberoylanilide hydroxamic acid. Nature clinical practice. Oncology **2:**150-157.

53. **Kirkegaard, K., M. P. Taylor, and W. T. Jackson.** 2004. Cellular autophagy: surrender, avoidance and subversion by microorganisms. Nature reviews. Microbiology **2:**301-314.

54. **Kirn, D. H., and S. H. Thorne.** 2009. Targeted and armed oncolytic poxviruses: a novel multi-mechanistic therapeutic class for cancer. Nature reviews. Cancer **9:**64-71.

55. **Kirstein, J. M., K. C. Graham, L. T. Mackenzie, D. E. Johnston, L. J. Martin, A. B. Tuck, I. C. MacDonald, and A. F. Chambers.** 2009. Effect of anti-fibrinolytic therapy on experimental melanoma metastasis. Clinical & experimental metastasis **26:**121-131.

56. **Kwon, J. A., and A. Rich.** 2005. Biological function of the vaccinia virus Z-DNA-binding protein E3L: gene transactivation and antiapoptotic activity in HeLa cells. Proceedings of the National Academy of Sciences of the United States of America **102:**12759-12764.

57. **Langland, J. O., and B. L. Jacobs.** 2004. Inhibition of PKR by vaccinia virus: role of the N- and C-terminal domains of E3L. Virology **324:**419-429.

58. **Langland, J. O., and B. L. Jacobs.** 2002. The role of the PKR-inhibitory genes, E3L and K3L, in determining vaccinia virus host range. Virology **299:**133-141.

59. **Langland, J. O., J. C. Kash, V. Carter, M. J. Thomas, M. G. Katze, and B. L. Jacobs.** 2006. Suppression of proinflammatory signal transduction and gene expression by the dual nucleic acid binding domains of the vaccinia virus E3L proteins. Journal of virology **80:**10083-10095.

60. **Le Boeuf, F., and J. C. Bell.** 2010. United virus: the oncolytic tag-team against cancer! Cytokine & growth factor reviews **21:**205-211.

61. **Le Boeuf, F., J. S. Diallo, J. A. McCart, S. Thorne, T. Falls, M. Stanford, F. Kanji, R. Auer, C. W. Brown, B. D. Lichty, K. Parato, H. Atkins, D. Kirn, and J. C. Bell.** 2010. Synergistic interaction between oncolytic viruses augments tumor killing. Molecular therapy : the journal of the American Society of Gene Therapy **18:**888-895.

62. **Li, Y., X. Meng, Y. Xiang, and J. Deng.** 2010. Structure function studies of vaccinia virus host range protein k1 reveal a novel functional surface for ankyrin repeat proteins. Journal of virology **84:**3331-3338.

63. **Lin, C. L., C. S. Chung, H. G. Heine, and W. Chang.** 2000. Vaccinia virus envelope H3L protein binds to cell surface heparan sulfate and is important for intracellular mature virion morphogenesis and virus infection in vitro and a. Journal of virology **74:**3353-3365.

64. **Liu, T. C., T. Hwang, B. H. Park, J. Bell, and D. H. Kirn.** 2008. The targeted oncolytic poxvirus JX-594 demonstrates antitumoral, antivascular, and anti-HBV

activities in patients with hepatocellular carcinoma. Molecular therapy : the journal of the American Society of Gene Therapy **16:**1637-1642.

65. **Liu, Y., K. C. Wolff, B. L. Jacobs, and C. E. Samuel.** 2001. Vaccinia virus E3L interferon resistance protein inhibits the interferon-induced adenosine deaminase A-to-I editing activity. Virology **289:**378-387.

66. **Locker, J. K., A. Kuehn, S. Schleich, G. Rutter, H. Hohenberg, R. Wepf, and G. Griffiths.** 2000. Entry of the two infectious forms of vaccinia virus at the plasma membane is signaling-dependent for the IMV but not the EEV. Molecular biology of the cell **11:**2497-2511.

67. **Lun, X., D. L. Senger, T. Alain, A. Oprea, K. Parato, D. Stojdl, B. Lichty, A. Power, R. N. Johnston, M. Hamilton, I. Parney, J. C. Bell, and P. A. Forsyth.** 2006. Effects of intravenously administered recombinant vesicular stomatitis virus (VSV(deltaM51)) on multifocal and invasive gliomas. Journal of the National Cancer Institute **98:**1546-1557.

68. **MacTavish, H., J. S. Diallo, B. Huang, M. Stanford, F. Le Boeuf, N. De Silva, J. Cox, J. G. Simmons, T. Guimond, T. Falls, J. A. McCart, H. Atkins, C. Breitbach, D. Kirn, S. Thorne, and J. C. Bell.** 2010. Enhancement of vaccinia virus based oncolysis with histone deacetylase inhibitors. PloS one **5:**e14462.

69. **McAuslan, B. R.** 1963. The Induction and Repression of Thymidine Kinase in the Poxvirus-Infected Hela Cell. Virology **21:**383-389.

70. **McCart, J. A., J. M. Ward, J. Lee, Y. Hu, H. R. Alexander, S. K. Libutti, B. Moss, and D. L. Bartlett.** 2001. Systemic cancer therapy with a tumor-selective vaccinia virus mutant lacking thymidine kinase and vaccinia growth factor genes. Cancer research **61:**8751-8757.

71. **McFadden, G.** 2005. Poxvirus tropism. Nature reviews. Microbiology **3:**201-213.

72. **McInnes, C. J., A. R. Wood, and A. A. Mercer.** 1998. Orf virus encodes a homolog of the vaccinia virus interferon-resistance gene E3L. Virus genes **17:**107-115.

73. **McLaughlin, J. R., H. A. Risch, J. Lubinski, P. Moller, P. Ghadirian, H. Lynch, B. Karlan, D. Fishman, B. Rosen, S. L. Neuhausen, K. Offit, N. Kauff, S. Domchek, N. Tung, E. Friedman, W. Foulkes, P. Sun, and S. A. Narod.** 2007. Reproductive risk factors for ovarian cancer in carriers of BRCA1 or BRCA2 mutations: a case-control study. The lancet oncology **8:**26-34.

74. **Meng, X., J. Chao, and Y. Xiang.** 2008. Identification from diverse mammalian poxviruses of host-range regulatory genes functioning equivalently to vaccinia virus C7L. Virology **372:**372-383.

75. **Meng, X., C. Jiang, J. Arsenio, K. Dick, J. Cao, and Y. Xiang.** 2009. Vaccinia virus K1L and C7L inhibit antiviral activities induced by type I interferons. Journal of virology **83:**10627-10636.

76. **Moss, B.** 2001. *In* Fields Virology. D. M. Knipe and P. M. Howley (ed.). Lippincott Williams & Wilkins, Philidephia.

77. **Moss, B.** 2006. Poxvirus entry and membrane fusion. Virology **344:**48-54.

78. **Moss, B., and P. L. Earl.** 2001. Overview of the vaccinia virus expression system. Current protocols in protein science / editorial board, John E. Coligan ... [et al.] **Chapter 5:**Unit5 11.

79. **Myskiw, C., J. Arsenio, R. van Bruggen, Y. Deschambault, and J. Cao.** 2009. Vaccinia virus E3 suppresses expression of diverse cytokines through inhibition of the PKR, NF-kappaB, and IRF3 pathways. Journal of virology **83:**6757-6768.

80. **Najera, J. L., C. E. Gomez, J. Garcia-Arriaza, C. O. Sorzano, and M. Esteban.** 2010. Insertion of vaccinia virus C7L host range gene into NYVAC-B genome potentiates immune responses against HIV-1 antigens. PloS one **5:**e11406.

81. **Nguyen, T. L., H. Abdelbary, M. Arguello, C. Breitbach, S. Leveille, J. S. Diallo, A. Yasmeen, T. A. Bismar, D. Kirn, T. Falls, V. E. Snoulten, B. C. Vanderhyden, J. Werier, H. Atkins, M. J. Vaha-Koskela, D. F. Stojdl, J. C. Bell, and J. Hiscott.** 2008. Chemical targeting of the innate antiviral response by histone deacetylase inhibitors renders refractory cancers sensitive to viral oncolysis. Proceedings of the National Academy of Sciences of the United States of America **105:**14981-14986.

82. **Oguiura, N., D. Spehner, and R. Drillien.** 1993. Detection of a protein encoded by the vaccinia virus C7L open reading frame and study of its effect on virus multiplication in different cell lines. The Journal of general virology **74 (Pt 7):**1409-1413.

83. **Ottolino-Perry, K., J. S. Diallo, B. D. Lichty, J. C. Bell, and J. A. McCart.** 2010. Intelligent design: combination therapy with oncolytic viruses. Molecular therapy : the journal of the American Society of Gene Therapy **18:**251-263.

84. **Parato, K. A., C. J. Breitbach, F. Le Boeuf, J. Wang, C. Storbeck, C. Ilkow, J. S. Diallo, T. Falls, J. Burns, V. Garcia, F. Kanji, L. Evgin, K. Hu, F. Paradis, S. Knowles, T. H. Hwang, B. C. Vanderhyden, R. Auer, D. H. Kirn, and J. C. Bell.** 2012. The oncolytic poxvirus JX-594 selectively replicates in and destroys cancer cells driven by genetic pathways commonly activated in cancers. Molecular therapy : the journal of the American Society of Gene Therapy **20:**749-758.

85. **Parato, K. A., D. Senger, P. A. Forsyth, and J. C. Bell.** 2005. Recent progress in the battle between oncolytic viruses and tumours. Nature reviews. Cancer **5:**965-976.

86. **Park, B. H., T. Hwang, T. C. Liu, D. Y. Sze, J. S. Kim, H. C. Kwon, S. Y. Oh, S. Y. Han, J. H. Yoon, S. H. Hong, A. Moon, K. Speth, C. Park, Y. J. Ahn, M. Daneshmand, B. G. Rhee, H. M. Pinedo, J. C. Bell, and D. H. Kirn.** 2008. Use of a targeted oncolytic poxvirus, JX-594, in patients with refractory primary or metastatic liver cancer: a phase I trial. The lancet oncology **9:**533-542.

87. **Perkus, M. E., S. J. Goebel, S. W. Davis, G. P. Johnson, K. Limbach, E. K. Norton, and E. Paoletti.** 1990. Vaccinia virus host range genes. Virology **179:**276-286.

88. **Perkus, M. E., K. Limbach, and E. Paoletti.** 1989. Cloning and expression of foreign genes in vaccinia virus, using a host range selection system. Journal of virology **63:**3829-3836.

89. **Pol, J. G., J. Resseguier, and B. L. Lichty.** 2012. Oncolytic viruses: a step into cancer immunotherapy. Virus Adaptation and Treatment **4:**1-21.

90. **Power, A. T., and J. C. Bell.** 2008. Taming the Trojan horse: optimizing dynamic carrier cell/oncolytic virus systems for cancer biotherapy. Gene therapy **15:**772-779.

91. **Power, A. T., J. Wang, T. J. Falls, J. M. Paterson, K. A. Parato, B. D. Lichty, D. F. Stojdl, P. A. Forsyth, H. Atkins, and J. C. Bell.** 2007. Carrier cell-based delivery of an oncolytic virus circumvents antiviral immunity. Molecular therapy : the journal of the American Society of Gene Therapy **15:**123-130.

92. **Puhlmann, M., C. K. Brown, M. Gnant, J. Huang, S. K. Libutti, H. R. Alexander, and D. L. Bartlett.** 2000. Vaccinia as a vector for tumor-directed gene therapy: biodistribution of a thymidine kinase-deleted mutant. Cancer gene therapy **7:**66-73.

93. **Reed, L. J., and H. Muench.** 1938. A simple method of estimating fifty percent endpoints. American Journal of Hygiene **27:**493-497.

94. **Reynolds, L. P., A. T. Grazul-Bilska, and D. A. Redmer.** 2000. Angiogenesis in the corpus luteum. Endocrine **12:**1-9.

95. **Rice, A. D., P. C. Turner, J. E. Embury, L. L. Moldawer, H. V. Baker, and R. W. Moyer.** 2011. Roles of vaccinia virus genes E3L and K3L and host genes PKR and RNase L during intratracheal infection of C57BL/6 mice. Journal of virology **85:**550-567.

96. **Rintoul, J. L., C. G. Lemay, L. H. Tai, M. M. Stanford, T. J. Falls, C. T. de Souza, B. W. Bridle, M. Daneshmand, P. S. Ohashi, Y. Wan, B. D. Lichty, A. A. Mercer, R. C. Auer, H. L. Atkins, and J. C. Bell.** 2012. ORFV: A Novel Oncolytic and Immune Stimulating Parapoxvirus Therapeutic. Molecular therapy : the journal of the American Society of Gene Therapy.

97. **Romano, P. R., F. Zhang, S. L. Tan, M. T. Garcia-Barrio, M. G. Katze, T. E. Dever, and A. G. Hinnebusch.** 1998. Inhibition of double-stranded RNA-dependent protein kinase PKR by vaccinia virus E3: role of complex formation and the E3 N-terminal domain. Molecular and cellular biology **18:**7304-7316.

98. **Savory, L. J., S. A. Stacker, S. B. Fleming, B. E. Niven, and A. A. Mercer.** 2000. Viral vascular endothelial growth factor plays a critical role in orf virus infection. Journal of virology **74:**10699-10706.

99. **Sharp, T. V., F. Moonan, A. Romashko, B. Joshi, G. N. Barber, and R. Jagus.** 1998. The vaccinia virus E3L gene product interacts with both the regulatory and the substrate binding regions of PKR: implications for PKR autoregulation. Virology **250:**302-315.

100. **Shisler, J. L., and X. L. Jin.** 2004. The vaccinia virus K1L gene product inhibits host NF-kappaB activation by preventing IkappaBalpha degradation. Journal of virology **78:**3553-3560.

101. **Smith, G. L., and M. Law.** 2004. The exit of vaccinia virus from infected cells. Virus research **106:**189-197.

102. **Smith, G. L., B. J. Murphy, and M. Law.** 2003. Vaccinia virus motility. Annual review of microbiology **57:**323-342.

103. **Smith, G. L., A. Vanderplasschen, and M. Law.** 2002. The formation and function of extracellular enveloped vaccinia virus. The Journal of general virology **83:**2915-2931.

104. **Stanford, M. M., M. Shaban, J. W. Barrett, S. J. Werden, P. A. Gilbert, J. Bondy-Denomy, L. Mackenzie, K. C. Graham, A. F. Chambers, and G. McFadden.** 2008. Myxoma virus oncolysis of primary and metastatic B16F10 mouse tumors in vivo. Molecular therapy : the journal of the American Society of Gene Therapy **16:**52-59.

105. **Stojdl, D. F., B. Lichty, S. Knowles, R. Marius, H. Atkins, N. Sonenberg, and J. C. Bell.** 2000. Exploiting tumor-specific defects in the interferon pathway with a previously unknown oncolytic virus. Nature medicine **6:**821-825.

106. **Sullivan, J. T., A. A. Mercer, S. B. Fleming, and A. J. Robinson.** 1994. Identification and characterization of an orf virus homologue of the vaccinia virus gene encoding the major envelope antigen p37K. Virology **202:**968-973.

107. **Sutter, G., A. Ramsey-Ewing, R. Rosales, and B. Moss.** 1994. Stable expression of the vaccinia virus K1L gene in rabbit cells complements the host range defect of a vaccinia virus mutant. Journal of virology **68:**4109-4116.

108. **Symons, J. A., A. Alcami, and G. L. Smith.** 1995. Vaccinia virus encodes a soluble type I interferon receptor of novel structure and broad species specificity. Cell **81:**551-560.

109. **Thorne, S. H., T. H. Hwang, W. E. O'Gorman, D. L. Bartlett, S. Sei, F. Kanji, C. Brown, J. Werier, J. H. Cho, D. E. Lee, Y. Wang, J. Bell, and D. H. Kirn.** 2007. Rational strain selection and engineering creates a broad-spectrum, systemically effective oncolytic poxvirus, JX-963. The Journal of clinical investigation **117:**3350-3358.

110. **Vaha-Koskela, M. J., J. E. Heikkila, and A. E. Hinkkanen.** 2007. Oncolytic viruses in cancer therapy. Cancer letters **254:**178-216.

111. **Vanderplasschen, A., and G. L. Smith.** 1997. A novel virus binding assay using confocal microscopy: demonstration that the intracellular and extracellular vaccinia virions bind to different cellular receptors. Journal of virology **71:**4032-4041.

112. **Vijaysri, S., G. Jentarra, M. C. Heck, A. A. Mercer, C. J. McInnes, and B. L. Jacobs.** 2008. Vaccinia viruses with mutations in the E3L gene as potential replication-competent, attenuated vaccines: intra-nasal vaccination. Vaccine **26:**664-676.

113. **Vijaysri, S., L. Talasela, A. A. Mercer, C. J. McInnes, B. L. Jacobs, and J. O. Langland.** 2003. The Orf virus E3L homologue is able to complement deletion of the vaccinia virus E3L gene in vitro but not in vivo. Virology **314:**305-314.

114. **Weber, O., A. Siegling, A. Friebe, A. Limmer, T. Schlapp, P. Knolle, A. Mercer, H. Schaller, and H. D. Volk.** 2003. Inactivated parapoxvirus ovis (Orf virus) has antiviral activity against hepatitis B virus and herpes simplex virus. The Journal of general virology **84:**1843-1852.

115. **White, S. D., and B. L. Jacobs.** 2012. The amino terminus of the vaccinia virus e3 protein is necessary to inhibit the interferon response. Journal of virology **86:**5895-5904.

116. **Willis, K. L., J. O. Langland, and J. L. Shisler.** 2011. Viral double-stranded RNAs from vaccinia virus early or intermediate gene transcripts possess PKR activating function, resulting in NF-kappaB activation, when the K1 protein is absent or mutated. The Journal of biological chemistry **286:**7765-7778.

117. **Wittek, R.** 2006. Vaccinia immune globulin: current policies, preparedness, and product safety and efficacy. International journal of infectious diseases : IJID : official publication of the International Society for Infectious Diseases **10:**193-201.

118. **Zhang, P., B. L. Jacobs, and C. E. Samuel.** 2008. Loss of protein kinase PKR expression in human HeLa cells complements the vaccinia virus E3L deletion mutant phenotype by restoration of viral protein synthesis. Journal of virology **82:**840-848.

Contributions of Collaborators

Drs. Bertram Jacobs and James Jancovich provided the initial stock of VV-E3L^{OrfV}.

Anti-C7L antibody used in Figure 3 and Appendix II was provided by Dr. Gerd Sutter.

Anti-E3L antibody used in Figure 3 was provided by Dr. Stuart Isaacs.

Initial stocks provided of WRΔTK and WRΔVGF were cloned and rescued by Drs. Jiahu Wang and Chris Storbek.

Initial stock provided of VVdd-mCherry was made by Dr. Fabrice Le Bouef.

Aimee Laporte cloned and created pcDNA-E3L^{VV} and pcDNA-K3L^{VV} used in Figure 3 and helped with generating the data for Figure 12.

Theresa Falls performed all intravenous and intratumoral animal injections.

Appendices

Appendix I. Vaccinia Virus host-range C7L (A), E3L (B), K1L (C) and K3L (D) gene sequences. Start sequences are in bold, while stop sequences are underlined. Sequences were obtained from http://www.poxvirus.org (September 9, 2010).

A

ATGGGTATACAGCACGAATTCGACATCATTATTAATGGAGATATCGCGTTGAGA-
AATTTCAGTTACATAAAGGGGATAACTACGGATGCAAACTAAAAATTATTTCGAA
TGATTACAAGAAATTAAAGTTTAGATTCATTATACGCCCAGATTGGTCGGAAATC
GACGAGGTCAAAGGATTAACCGTATTTGCAAACAACTATGCGGTGAAAGTTAAT
AAGGTAGATGACACGTTCTATTACGTAATATATGAGGCTGTAATACATCTGTATAA
CAAAAAAACAGAGATATTGATTTATTCTGATGATGAGAACGAGCTCTTCAAACA
CTATTACCCATACATCAGTCTAAATATGATTAGTAAAAAGTATAAAGTTAAAGAA
GAGAACTACTCATCCCCGTATATAGAACATCCGTTAATCCCGTATA GAGATTATGA
GTCCATGGAT TAA

B

ATGTCTAAAATCTATATCGACGAGCGTTCTAACGCAGAGATTGTGTGTGAGAG-
GAAGAAGGAGCTACTGCTGCACAACTAACTAGACAACTTAATATGGAGAAGCG
AGAAGTTAATAAAGCTCTGTACGATCTTCAACGTAGTGCTATGGTGTACAGCTCC
GACGATATTCCTCCTCGTTGGTTTATGACAACGGAGGCGGATAAGCCGGATGCT
GATGCTATGGCTGACGTCATAATAGATGATGTATCCCGCGAAAAATCAATGAGAG
AGGATCATAAGTCTTTTGATGATGTTATTCCGGCTAAAAAAATTATTGATTGGAA
AGGTGCTAACCCTGTCACCGTTATTAATGAGTACTGCCAAATTACTAGGAGAGAT
TGGTCTTTTCGTATTGAATCAGTGGGGCCTAGTAACTCTCCTACATTTTATGCCTG
TGTAGACATCGACGGAAGAGTATTCGATAAGGCAGATGGAAAATCTAAACGAGA
TGCTAAAAATAATGCAGCTAAATTGGCAGTAGATAAACTTCTTGGTTACGTCATC
ATTAGATTCTGA

C

ATGGATCTGTCACGAATTAATACTTGGAAGTCTAAGCAGCTGAAAAGCTT
TCTCTCTAGTAAAGATACATTTAAGGCGGATGTCCATGGACATAGTGCCTTGTAT-
TATGCAATAGCTGATAATAACGTGCGTCTAGTATGTACGTTGTTGAACGCTGGAG
CATTGAAAAATCTTCTAGAGAATGAATTTCCATTACATCAGGCAGCCACA
TTAGAAGATACCAAAATAGTAAAGATTTTGCTATTCAGTGGAATGATATTCAAAT-
GACAAAGGAAACACCGCATTGTATTATGCGGTTGATAGTGGTAACATGCAAACG
GTGAAACTGTTTGTTAAGAAAAATTGGAGACTGATGTTCTATGGGAAAACTGGA
TGGAAAACTTCATTTTATCATGCCGTCATGCTTAATGATGTAAGTATTGTATCATA
CTTTCTTTCAGAAATACCATCTACTTTTGATCTGGCTATTCTCCTTAGTTGTATTCA
CACCACTATAAAAAATGGACACGTGGATATGATGATTCTCTTGCTCGACTATATG
ACGTCGACAAACACCAATAATTCCCTTCTCTTCATTCCGGACATTAAATTGGCTA
TAGATAATAAAGACATTGAGATGTTACAGGCTCTGTTCAAATACGACATTAATAT
CTACTCTGTTAATCTGGAAAATGTACTATTGGATGATGCCGAAATAACTAAGATG
ATTATAGAAAAGCATGTTGAATACAAGTCTGACTCCTATACAAAAGATCTCGATA
TCGTCAAGAATAATAAATTGGATGAAATAATTAGCAAAAACAAGGAACTCAGAC
TCATGTACGTCAATTGTGTAAAGAAAA ACTAA

D

ATGCTTGCATTTTGTTATTCGTTGCCCAATGCGGGTGATGTAATAAGGGCAGAG-
TAGAAGGATTATGCTCTATATATTTATCTTTTTGACTATCCTCACTTTGAAGCTATC
TTGGCAGAGAGTGTTAAGATGCATATGGATAGATATGTTGAATATAGGGATAAAC
TGGTAGGGAAAACTGTAAAAGTTAAAGTGATTAGAGTTGATTATACAAAAGGAT
ATATAGATGTCAATTACAAAAGGATGTGTAGACATCAATAA

Appendix II. Confirmation of C7L^{VV} insertion in OrfV. DNA from round 5 recombinant plaques was collected alongside OrfV-C7LVV virus purification. PCR was performed using C7LVV primers listed in Table 1 alongside a VV-COP positive control (A). Expression of C7LVV was confirmed by western blotting of transiently transfected/infected cell lysates, with OrfV and VV-COP serving as negative and positive controls, respectively. Amido black staining serves as a loading control (B).

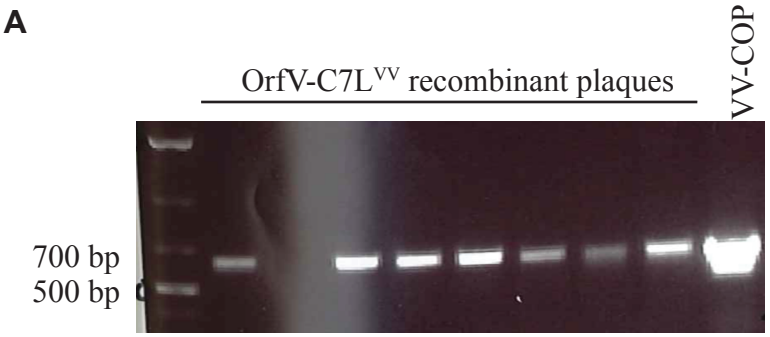
A
OrfV-C7L^{VV} recombinant plaques
VV-COP
700 bp
500 bp

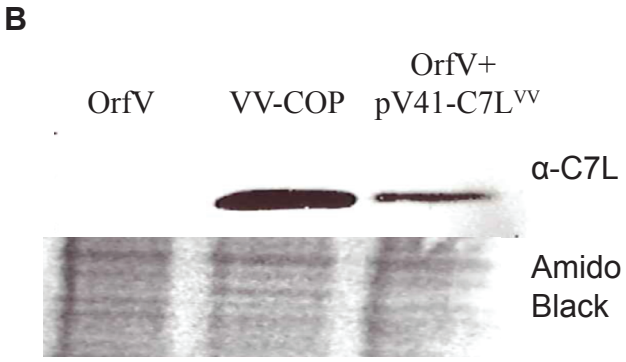
B
OrfV
VV-COP
OrfV+
pV41-C7L^{VV}
α-C7L
Amido
Black

Appendix III. VSe1 and TSA are unable to increase VV-E3LOrfV yields. HeLa cells were pretreated with either complete media or 2-fold dilutions of VSe1 (A) or TSA (B) for 4 hours. VV-E3LOrfV at MOI 0.01 was then added directly into the wells. 72 hours post infection cytotoxicity was assessed using alamarBlue (i; n=6) and replicates were pooled for titering (ii). To assess if VSe1 enhanced viral yields of VV-E3L^{OrfV}, HeLa cells were either pretreated with complete media or VSe1 at 19.5 μM for 4 hours. VV-E3L^{OrfV} at MOI 0.01 was directly added into the media. Cell lysates and supernatants were harvested separately, to mirror the process of virus stock production and titered (Aiii; n=3).

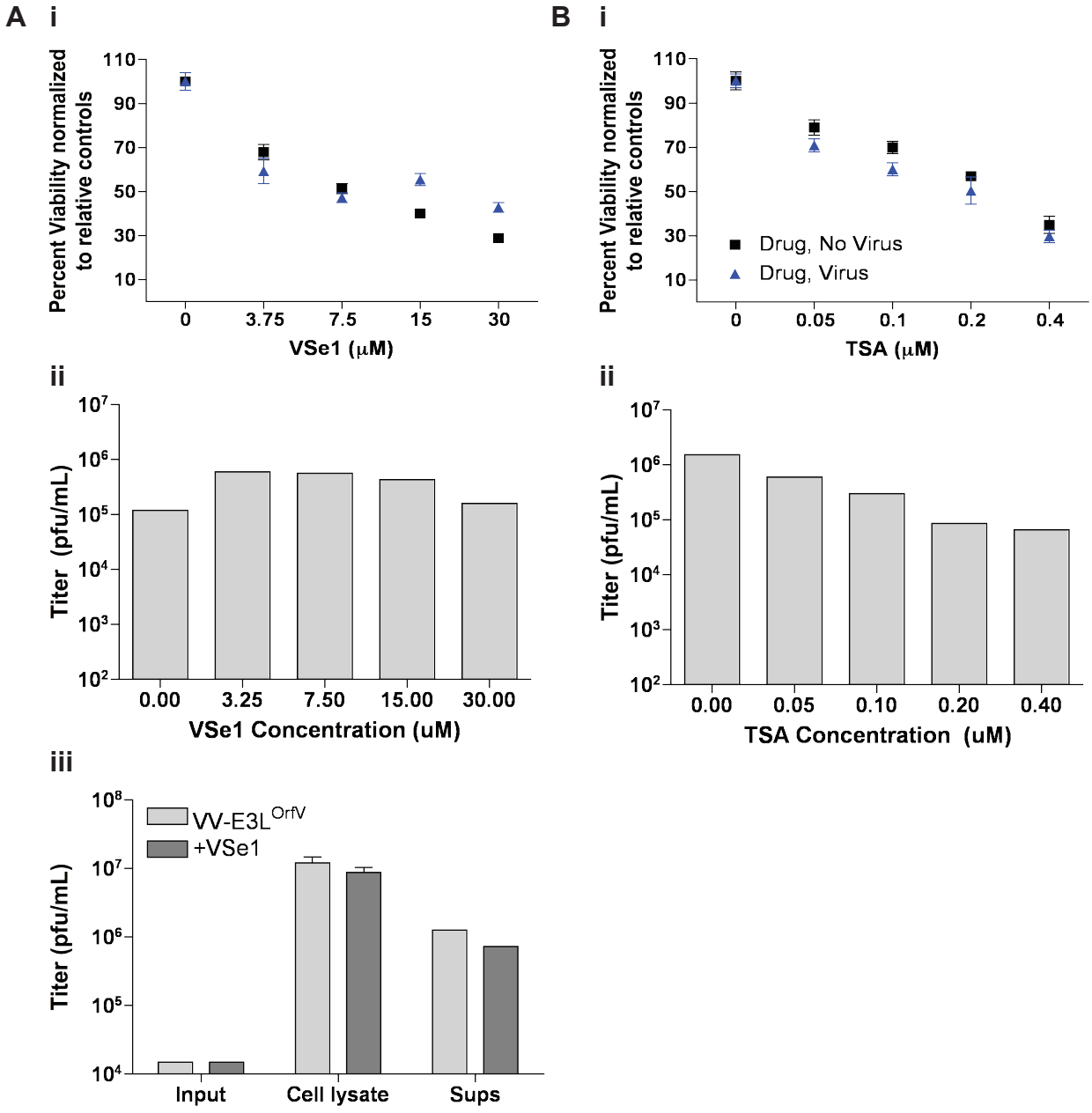
A
i
Percent Viability normalized to relative controls
110
90
70
50
30
10
0
3.75
7.5
15
30
VSe1 (μM)
ii
Titer (pfu/mL)
10^7
10^6
10^5
10^4
10^3
10^2
0.00
3.25
7.50
15.00
30.00
VSe1 Concentration (uM)
iii
Titer (pfu/mL)
10^8
10^7
10^6
10^5
10^4
VV-E3L^OrfV
+VSe1
Input
Cell lysate
Sups
B
i
Percent Viability normalized to relative controls
110
90
70
50
30
10
Drug, No Virus
Drug, Virus
0
0.05
0.1
0.2
0.4
TSA (μM)
ii
Titer (pfu/mL)
10^7
10^6
10^5
10^4
10^3
10^2
0.00
0.05
0.10
0.20
0.40
TSA Concentration (uM)

Curriculum Vitae

Education

2010-2012 **Master's of Science degree in Biochemistry**
University of Ottawa, Ottawa, Ontario

2006-2010 **Honor's Bachelor of Science, Cell and Developmental Biology**
The University of Western Ontario, London, Ontario
Related Courses: Cell Biology Laboratory, Advanced Cell Biology, Advanced Immunology, Advanced Developmental Biology, Developmental Genetics, Cell Biology Seminar, Honor's Research Thesis

Research Experience

2010-present **M.Sc. Student**, Department of Biochemistry, Microbiology and Immunology, University of Ottawa, Ottawa, ON
Thesis: *Potentiating the oncolytic efficacy of poxviruses*

2009-2010 **Honor's Student**, Department of Biology, University of Western Ontario
Thesis: *Investigating Myxoma virus-mediated oncolysis in metastatic epithelial ovarian cancer using patient ascites-derived cells*

Summer 2009 **Research Associate**, Translational Ovarian Cancer Research Program, London Regional Cancer Program

Summer 2008 **Summer Student**, Centre for Cancer Therapeutics, Ottawa Hospital Research Institute

Summer 2007 **Summer Student,** Centre for Cancer Therapeutics, Ottawa Hospital Research Institute

Academic Awards and Accomplishments

2011 **OICR Ontario Trainee Travel Award for Canadian Cancer Research Conference**, Ontario Institute for Cancer Research
2010-2012 **Admission Scholarship** ($15,000/2 years), University of Ottawa
2010 **Western Gold Medal**, The University of Western Ontario
2007-2010 **Dean's Honor Roll**, The University of Western Ontario

Skills

- Excellent communication abilities in presenting results in written and oral presentations
- Many years experience working in small and large research groups
- Laboratory techniques: Tissue culture, western blotting, cloning, phase-contrast and fluorescent microscopy, animal models of cancer
- Microsoft Office (Word, Excel, Powerpoint), Prism Graphpad, Adobe (Photoshop, Illustrator)

Publications

Correa, R.J.M., **Komar, M.**, Tong, J.G.K., Sivapragasam, M., Rahman, M.M., McFadden, G., DiMattia, G.E., Shepherd, T.G. (2012). *Myxoma virus-mediated oncolysis of ascites-derived human ovarian cancer cells and spheroids is impacted by differential AKT activity. Gynecol Oncol* **125**(2): 441-50.

Presentations

Komar M.H.*, Rintoul J.L., Falls T.J. and Bell J.C. (2012, June). VV-E3L^{OrfV}, an interferon sensitive oncolytic virus candidate. Poster presented at: XIX International Poxvirus, Asfarvirus and Iridovirus Conference; Salamanca, Spain. [International Conference]

Komar, M.H* and Bell, J.C. (2012, March). *VV-mE3L as a novel oncolytic virus candidate.* Oral presentation presented at: University of Ottawa, Department of Biochemistry, Microbiology and Immunology (BMI) Seminar Day; Ottawa, ON. [Institutional Conference]

Komar M.H.*, Rintoul J.L., Laporte A.N., Falls T. and Bell J.C. (2011, November). *VV-mE3L as a novel oncolytic virus candidate.* Poster presented at: Canadian Cancer Research Conference; Toronto, ON. [International Conference]

Komar M.H.*, Rintoul J.L., Laporte A.N., Falls T. and Bell J.C. (2011, November). *VV-mE3L as a novel oncolytic virus candidate.* Poster Session presented at: 11th annual Ottawa Hospital Research Institute (OHRI) Research Day; Ottawa, ON. [Institutional Conference]

Komar, M.H.*, Rintoul, J.L. and Bell, J.C. (2011, May). *Increasing the oncolytic efficiency of Orf virus using Vaccinia virus host-range genes C7L and K1L.* Poster Session presented at: University of Ottawa, Department of Biochemistry, Microbiology and Immunology (BMI) Poster Day; Ottawa, ON. [Institutional Conference]

Komar, M.H.*, Rintoul, J.L. and Bell, J.C. (2011, March). *Increasing the oncolytic efficiency of Orf virus using Vaccinia virus host-range genes C7L and K1L.* Abstract submitted: The 6th International Conference on Oncolytic Viruses As Cancer Therapeutics; Las Vegas, NV, USA. [International Conference]

Komar M*, Rintoul J, Bell JC. (2010, November). *Testing the oncolytic potential of a new mutant E3L Vaccinia virus*. Poster Session presented at: 10th annual Ottawa Hospital Research Institute (OHRI) Research Day; Ottawa, ON. [Institutional Conference]

Komar M, Correa RJM,, Bertrand M, Sugimoto A, Préfontaine M, McFadden G, DiMattia GE, Shepherd TG*. (2010, June). *Activated Akt signalling is required for Myxoma virus-mediated oncolysis of ascites-derived human epithelial ovarian cancer cells and spheroids.* Poster session presented at: 5th annual Canadian Conference on Ovarian Cancer Research; Toronto, ON. [National Conference]

Komar M*, Correa RJM,, Bertrand M, Sugimoto A, Préfontaine M, McFadden G, DiMattia GE, Shepherd TG. (2010, March). *Investigating Myxoma virus-mediated oncolysis in metastatic epithelial ovarian cancer using patient-ascites derived cells.* Oral presentation presented at: Ontario Biology Day York University; Toronto, ON. [Local Conference]

Shepherd TG, Correa RJM, **Komar M***, Bertrand M, Sugimoto A, Préfontaine M, Lanvin D, McFadden G, DiMattia GE. (2009, June). *Investigating Myxoma virus-mediated oncolysis of metastatic epithelial ovarian cancer using patient ascites-derived cells.* Poster session presented at: The CIHR—STP in Cancer Research & Technology Transfer and the Department of Oncology Department Annual Research & Education Day; London, ON. [Institutional conference]

Patents

Bell, John; Rintoul, Julia; Laporte, Aimee, Nicole; **Komar, Monica**. (Patent filed March 2012). *Oncolytic Parapoxviruses*. PAT 6738-0 US

Professional Development

2012 **Foundations in Project Management I,** MITACS Step
2012 **Radiation Safety Training,** The Ottawa Hospital, Ottawa, ON
2011 **Palliative Care Course**, Roger's House, Ottawa ON
2011 **Effective Networking**, MITACS Step
2011 **The Art of Powerful Conversation**, MITACS Step
2007 **National Institutional Animal User Training (NIAUT)**, University of Ottawa, Ottawa, ON

Extracurricular Activities

2011-present **Family Support Volunteer**, Roger's House, Ottawa, ON
2010-present **Science Outreach Volunteer**, Let's Talk Science
2009-2010 **Department of Biology Exam Proctor**, University of Western Ontario,